Regulation of Store-Operated Channel Molecules ORAI and STIM by Oxidative Stress in Blood Vessels

Nikoleta Daskoulidou

Submitted in accordance with the requirements for the degree of

Doctor of Philosophy

The University of Hull and The University of York

Hull York Medical School

March 2013

Dedicated to my parents, Sofia and Eleftherios Daskoulidis

"First, have a definite, clear practical ideal; a goal, an objective. Second, have the necessary means to achieve your ends; wisdom, money, materials, and methods. Third, adjust all your means to that end."

Aristotle, 384 BC – 322 BC

Abstract

ORAI and STIM genes are recently identified store-operated calcium channel molecules that play important roles in human physiology. In this thesis, the effects of oxidative stress conditions including high glucose, homocysteine and H_2O_2 on the expression of ORAI and STIM, Ca^{2+} influx, ORAI channel activity and potential underlying mechanisms were investigated using cell models and *in vivo* tissue samples from diabetic patients and mice.

ORAI1-3 and STIM1-2 were detected in vascular endothelial cells and smooth muscle cells using RT-PCR, western blotting and immunostaining. Their expression was upregulated by chronic treatment with high glucose in cell models. The upregulation was also observed in human aorta from Type 2 diabetic patients and kidney tissues from streptozotocin-induced and Akita Type 1 diabetic mouse models. The high glucose-induced gene upregulation was prevented by the calcineurin inhibitor cyclosporin A and store-operated channel blocker diethylstilbestrol. H_2O_2 also upregulated ORAI1-3 and STIM1-2, however, homocysteine increased STIM1-2 expression, but downregulated ORAI1-3.

Ca^{2+} influx and ORAI channel activity were investigated using Ca^{2+} imaging and whole-cell patch clamp. Chronic treatment with high glucose enhanced store-operated Ca^{2+} influx in endothelial cells, but there was no effect if treated acutely. In HEK-293 cells overexpressing STIM1/ORAI1-3, high glucose had no acute effect on ORAI1-3 currents, but homocysteine decreased the currents. The cytosolic STIM1 movement was monitored by live-cell fluorescence imaging. Oxidative stress did not change STIM1-EYFP translocation and clustering after Ca^{2+} store-depletion.

The effect of hyperosmolarity on STIM and ORAI expression and channel activity was also investigated. Hyperosmolarity inhibited ORAI1-3 currents and downregulated ORAI1-3 and STIM1-2 gene expression, but did not alter cytosolic STIM1-EYFP translocation.

It is concluded that store-operated channel molecules, STIMs and ORAIs, are new proteins regulated by oxidative stress, especially in diabetes, which may provide a novel concept for the abnormality of Ca^{2+} homeostasis in blood vessels from patients with diabetes.

Table of Contents

Abstract ..... **iv**
Table of Contents ..... **v**
List of Abbreviations ..... **x**
List of Figures ..... **xiv**
List of Tables ..... **xvii**
List of Digital Video Materials ..... **xvii**
Acknowledgements ..... **xviii**
Author's Declaration ..... **xx**

Chapter 1 General Introduction **1**
1.1 Introduction 2
1.2 Oxidative stress 3
1.3 Oxidative stress and diabetes 4
1.4 Diabetic vascular injury 5
1.5 Calcium signalling in blood vessels 6
1.6 Store-operated Ca^{2+} entry 9
1.7 Molecular basis of store-operated Ca^{2+} entry 10
1.7.1 Stromal-interacting molecules 10
1.7.1.1 STIMs and SOCE 12
1.7.2 ORAIs 13
1.7.2.1 ORAIs and SOCE 15
1.7.3 Transient receptor potential channels as SOCs 16
1.7.4 Mechanism of ORAI store-operated channel activation 17
1.7.5 Pharmacology of ORAI and STIM channels 21
1.7.6 Pathophysiology of ORAI and STIM channels 22
1.7.6.1 ORAI and STIM in the immune system 22
1.7.6.2 ORAI and STIM in the cardiovascular system 23
1.7.6.3 ORAI and STIM in cancer 24
1.8 Oxidative stress and Ca^{2+} signalling 25
1.9 Aims of the research project 26

Chapter 2 Materials and Methods 27
2.1 Materials 28
2.1.1 Chemicals and reagents 28
2.1.2 Solutions 29
2.1.3 Antibodies 30
2.1.4 Primers 30
2.1.5 Small interfering RNA 32
2.2 Methods 33
2.2.1 Human blood vessels 33
2.2.2 Culture of blood vessel segments 33
2.2.3 Diabetic mice samples 33
2.2.4 Cell culture 34
2.2.5 Reverse-transcriptase polymerase chain reaction (RT-PCR) 35
2.2.5.1 Total RNA isolation 35
2.2.5.2 Reverse transcription 36
2.2.5.3 Polymerase chain reaction 36
2.2.5.4 Real-time PCR 36
2.2.5.5 Analysis of real-time PCR data 37
2.2.5.6 Agarose gel electrophoresis 39
2.2.6 Western blotting 39
2.2.7 Immunohistochemistry 41
2.2.8 Molecular cloning of full length ORAI1-3 and plasmid construction 41
2.2.9 Transfection of ORAI and STIM plasmids into HEK-293 cells 43
2.2.10 Small interfering RNA transfection 44
2.2.11 Ca^{2+} imaging and live-cell fluorescence imaging 45
2.2.12 Whole-cell patch clamp recordings 45
2.2.13 Cell proliferation assay 46
2.2.14 Interleukin-6 ELISA 46
2.2.15 Cell migration and tube formation assays 47
2.2.16 Statistics 48

Chapter 3 Expression of Store-Operated Ca^{2+} Channel Molecules ORAI and STIM and the Regulation by Oxidative Stress 49

3.1 Introduction 50

3.2 Expression of ORAI and STIM in human blood vessels 52

3.3 Regulation of ORAI and STIM expression by high glucose in *in vitro* models 58

3.3.1 Effect of high glucose on the expression of ORAIs and STIMs in endothelial cells 58

3.3.2 Effect of high glucose on the expression of ORAIs and STIMs in smooth muscle cells 60

3.3.3 Effect of high glucose on the expression of ORAIs and STIMs in human blood vessels 62

3.4 Regulation of ORAI and STIM expression in diabetes 64

3.4.1 Human aorta samples from patients with Type 2 diabetes 64

3.4.2 Type 1 diabetic mouse models 66

3.5 Upregulation of ORAI and STIM by high glucose is mediated by calcineurin/ NFAT signalling pathway 70

3.6 ORAI and STIM expression regulated by homocysteine 74

3.7 ORAI and STIM regulated by H_2O_2 78

3.8 Discussion 80

3.9 Summary 85

Chapter 4 Effects of Oxidative Stress on Ca^{2+} Influx, the Activity of ORAI Channels and the Role of Cytosolic STIM1 Movement 86

4.1 Introduction 87

4.2 Ca^{2+} influx enhanced by high glucose in endothelial cells 89

4.2.1 Effect of acute application of high glucose on Ca^{2+} influx 89

4.2.2 Effect of chronic treatment with high glucose on Ca^{2+} influx 91

4.3 Functional expression of ORAI and STIM in HEK293 cells 94

4.3.1 Molecular cloning of full length ORAI1-3 94

4.3.2 Expression of ORAI and STIM in HEK293 cells 96

4.3.3 Characterization of ORAI channels overexpressed in HEK293 cells 98

4.4 ORAI channel activity regulated by oxidative stress 100

4.4.1 Direct effect of high glucose on ORAI channel activity 100

4.4.2 Direct effect of homocysteine on ORAI channel activity.....105
4.5 STIM1 translocation and clustering regulated by oxidative stress.....108
4.5.1 STIM1 translocation regulated by high glucose.....108
4.5.2 STIM1 translocation regulated by homocysteine.....111
4.5.3 STIM1 translocation regulated by H_2O_2.....114
4.6 Endothelial function regulated by oxidative stress and the involvement of ORAI channels.....117
4.6.1 Effect of high glucose on endothelial cell migration and tube formation.....117
4.6.2 Involvement of ORAI channels in IL-6 secretion in endothelial cells.....119
4.6.3 Involvement of homocysteine in endothelial cell proliferation and IL-6 secretion.....121
4.7 Discussion.....123
4.8 Summary.....126

Chapter 5 Osmolarity Sensitivity of ORAI Channels.....128
5.1 Introduction.....129
5.2 Effect of hyperosmolarity on endothelial cell migration.....131
5.3 Ca^{2+} entry decreased by hyperosmolarity in vascular endothelial cells.....133
5.4 ORAI and STIM expression downregulated by hyperosmolarity.....135
5.5 Inhibition of ORAI channels by hyperosmolarity.....137
5.6 Effect of hyperosmolarity on STIM1 clustering and translocation.....139
5.7 Discussion.....141
5.8 Summary.....142

Chapter 6 General Discussion.....143
6.1 Main results and significance of the study.....144
6.2 Mechanism of high glucose-induced upregulation of SOCE.....144
6.3 Limitations of the study.....147
6.4 Future directions.....147
6.5 Conclusion.....148

References **149**
List of Publications **200**
Appendix I pcDNA4/TO vector map **202**
Appendix II Example sequencing for full length ORAI2 ..... **203**
Appendix III Alignment of ORAI1 to the plasmid mCherry-ORAI1 sequence **204**

List of Abbreviations

2-APB	2-aminoethoxydiphenyl borate
ANOVA	Analysis of variance
BAPTA	1,2-bis(o-aminophenoxy)ethane- N,N,N',N' -tetracetic acid
BLAST	Basic local alignment search tool
BMI	Body mass index
bp	Base pairs
BSA	Albumin from bovine serum
Ca^{2+}	Calcium ion
cDNA	Complementary DNA
CMD	CRAC modulatory domain
CRAC	Ca^{2+} release-activated channels
CsA	Cyclosporin A
CVD	Cardiovascular disease
Cys	Cysteine
DAG	Diacylglycerol
DES	Diethylstilbestrol
dH_2O	Distilled water
DM	Diabetes mellitus
DMSO	Dimethyl sulfoxide
DMEM	Dulbecco's modified eagle medium
DNA	Deoxyribonucleic acid
DNase	Deoxyribonuclease

dNTP	Deoxyribonucleotide triphosphate
ECL	Enhanced chemiluminescence
EDTA	Ethylenediaminetetraacetic acid
EGTA	Ethylene glycol tetraacetic acid
ELISA	Enzyme-linked immunosorbent assay
ER/SR	Endoplasmic/ sarcoplasmic reticulum
EYFP	Enhanced yellow fluorescent protein
FCCP	Carbonyl cyanide 4-(trifluoromethoxy)phenylhydrazone
FCS	Fetal calf serum
GFP	Green fluorescent protein
GPCR	G protein-coupled receptor
H_2O_2	Hydrogen peroxide
HAEC	Human aortic endothelial cells
HBSS	Hank's balanced salt solution
Hcy	Homocysteine
HEK293	Human embryonic kidney cells
HEPES	4-(2-Hydroxyethyl)piperazine-1-ethanesulfonic acid
HG	High glucose
HHS	Hyperosmolar hyperglycaemic state
HUVEC	Human umbilical vein endothelial cells
I_{CRAC}	Ca^{2+} release-activated Ca^{2+} current
IgG	Immunoglobulin G
IL-6	Interleukin-6
IP_3	Inositol 1, 4, 5-triphosphate

IP_3R	IP_3 receptor
LIMA	Left internal mammary artery
M-MLV	Moloney murine leukaemia virus
mCFP	Monomeric cyan fluorescent protein
MEM	Minimum essential medium
NFAT	Nuclear factor of activated T-cells
NOS	Nitric oxide synthase
OAG	1-oleoyl-2-acetyl-sn-glycerol
OD	Optical density
PAGE	Polyacrylamide gel electrophoresis
PBS	Phosphate buffers saline
PCR	Polymerase chain reaction
PM	Plasma membrane
PMCA	Plasma membrane Ca^{2+} ATPase
RBL	Rat basophilic leukemia
RIPA	Radio-immunoprecipitation assay
RNA	Ribonucleic acid
RNase	Ribonuclease
RNS	Reactive nitrogen species
ROI	Region of interest
ROS	Reactive oxygen species
RTK	Receptor tyrosine kinase
RyR	Ryanodine receptor
SAM	Sterile-alpha motif

SCID	Severe combined immunodeficiency
SDS	Sodium dodecyl sulphate
SEM	Standard error of the mean
SERCA	Sarcoplasmic reticulum Ca^{2+} ATPase
siRNA	Small interfering RNA
SMC	Smooth muscle cell
SOAR	STIM-ORAI activating region
SOC	Store-operated channel
SOCE	Store-operated Ca^{2+} entry
STIM	Stromal-interacting molecule
STZ	Streptozotocin
TBST	Tris-buffered saline tween-20
TEMED	Tetramethylethylenediamine
TG	Thapsigargin
TM	Transmembrane domain
TPEN	*N*,*N*,*N* ',*N* '-tetrakis(2-pyridylmethyl)ethylenediamine
TRPC	Transient receptor potential canonical
TRPM	Transient receptor potential melastatin
TRPV	Transient receptor potential vanilloid
VEGF	Vascular endothelial growth factor
VOC	Voltage-operated channels

List of Figures

		Page
Figure 1-1	Ca^{2+} permeable channels and pumps in the PM and ER	8
Figure 1-2	STIM1 functional domains	11
Figure 1-3	ORAI channel domains	14
Figure 1-4	Mechanism of store-operated ORAI channel activation by STIM	19
Figure 2-1	Example of real-time PCR amplification plots and analysis	38
Figure 3-1	Detection of ORAI and STIM mRNAs in human blood vessels and cells	53
Figure 3-2	ORAI and STIM proteins detected by western blotting	55
Figure 3-3	Localization of ORAIs and STIMs in human left internal mammary arteries	57
Figure 3-4	Upregulation of ORAI and STIM expression by high glucose	59
Figure 3-5	ORAI and STIM expression regulated by high glucose in smooth muscle cells	61
Figure 3-6	Regulation of ORAI and STIM expression by high glucose in organ-cultured human left internal mammary artery	63
Figure 3-7	ORAI and STIM expression in human aorta	65
Figure 3-8	ORAI and STIM expression in the kidney from streptozotocin-induced Type 1 diabetic mice	67
Figure 3-9	ORAI and STIM mRNA expression in the kidney tissues from Akita Type 1 diabetic mice	69
Figure 3-10	Inhibition of high glucose-induced upregulation of ORAI and STIM expression by cyclosporin A	71
Figure 3-11	Regulation of ORAI and STIM expression by diethylstilbestrol	73
Figure 3-12	Regulation of ORAI and STIM mRNA expression by homocysteine	75
Figure 3-13	Regulation of ORAI and STIM protein expression by homocysteine	77

Figure 3-14	Regulation of ORAI and STIM mRNA expression by H_2O_2	79
Figure 4-1	Effect of acute high glucose application on Ca^{2+} influx in vascular endothelial cells	90
Figure 4-2	Ca^{2+} influx enhanced by chronic treatment with high glucose in store-depleted and non-store-depleted vascular endothelial cells	92
Figure 4-3	Ca^{2+} release and Ca^{2+} influx enhanced by chronic treatment with high glucose in vascular endothelial cells	93
Figure 4-4	Detection of full length ORAI1-3	95
Figure 4-5	Example for the PCR screening of ORAI colonies	95
Figure 4-6	Expression pattern for STIM1-EYFP, STIM1-EYFP/TO-mCherry-ORAI1, STIM1-EYFP/TO-mCherry-ORAI2 and STIM1-EYFP/TO-mCFP-ORAI3 in HEK293 cells	97
Figure 4-7	Representative *IV* relationships of ORAI1-3 overexpressed in HEK293 T-REx cells	99
Figure 4-8	ORAI1 channel current not affected by high glucose	101
Figure 4-9	ORAI2 channel current not affected by high glucose	102
Figure 4-10	ORAI3 channel current not affected by high glucose	103
Figure 4-11	No significant current induced by TG in the non-transfected HEK293 T-REx cells and the effect of high glucose	104
Figure 4-12	ORAI1-3 channel currents inhibited by homocysteine	107
Figure 4-13	STIM1 translocation and clustering not affected by acute application of high glucose in the stable transfected STIM1–EYFP cells	109
Figure 4-14	STIM1 translocation and clustering not affected by chronic treatment with high glucose in the stable transfected STIM1–EYFP cells	110
Figure 4-15	No effect of acute application of homocysteine on STIM1 movement in the stable transfected STIM1–EYFP cells	112
Figure 4-16	No effect of chronic treatment with homocysteine on STIM1 translocation and clustering in the stable transfected STIM1–EYFP cells	113
Figure 4-17	STIM1 translocation and clustering not affected by acute	115

	application of H_2O_2 in the stable transfected STIM1–EYFP cells	
Figure 4-18	STIM1 translocation and clustering not affected by chronic treatment with H_2O_2 in the stable transfected STIM1–EYFP cells	116
Figure 4-19	Migration and tube formation of endothelial cells inhibited by high glucose	118
Figure 4-20	IL-6 secretion increased after ORAI silencing in HAEC	120
Figure 4-21	HAEC proliferation and IL-6 secretion inhibited by homocysteine	122
Figure 5-1	Effect of hyperosmolarity on endothelial cell migration	132
Figure 5-2	Ca^{2+} influx inhibited by mannitol in EA.hy926 cells	134
Figure 5-3	Downregulation of ORAI and STIM expression by hyperosmolarity	136
Figure 5-4	Effect of mannitol on ORAI1-3 channel activity	138
Figure 5-5	Effect of hyperosmolarity on STIM1 translocation and clustering	140
Figure 6-1	Mechanism of store-operated Ca^{2+} entry regulated by high glucose	146

List of Tables

		Page
Table 2-1	Solutions	29
Table 2-2	Primers for RT-PCR	31
Table 2-3	Tagged primers for the PCR amplification of full length ORAI and GFP	32
Table 2-4	Sequences of small interfering RNAs for ORAI genes	32
Table 3-1	Blood glucose level and body weight in streptozotocin-induced Type 1 diabetic model	66
Table 3-2	Blood glucose level and body weight in Akita Type 1 diabetic model	68

List of Digital Video Materials

The following digital video data are enclosed in the CD attached to this thesis:

Video 1	Effect of thapsigargin on STIM1 translocation and clustering
Video 2	Effect of high glucose on STIM1 translocation and clustering
Video 3	Effect of high glucose on thapsigargin-induced STIM1 translocation and clustering

Acknowledgements

Completing a PhD is a creative and enjoyable journey, which I would not have been able to complete without the support of some people over the last three years. First and foremost I would like to express my special appreciation and thanks to my supervisor, Dr Shang-Zhong Xu. I am appreciative of all his contributions of time, ideas, and funding to make my PhD experience productive and stimulating. The motivation, thorough eye, immense knowledge and enthusiasm he has for his research was contagious and motivational for me. His guidance provided refreshing insight and critical questions that were exhilarating. His advice on both research as well as on my career have been invaluable. I would like to thank Sam for encouraging my research, allowing me to grow as a research scientist and serving as a role model to me as a junior member of academia.

Besides my supervisor, I am also grateful to my Thesis Advisory Panel members, Prof Stephen L. Atkin and Dr Thozhukat Sathyapalan, for serving as my committee members and for their encouragement. Our discussions were inspirational and stimulating and provided me with valuable and insightful comments and suggestions during my graduate career. I would like to thank Prof Atkin for his time and interest in my research and for his constructive criticism on this thesis.

I am appreciative of my fellow lab members Bo, Hongni, Gui-Lan and James for great teamwork and for making my time at Hull York Medical School a more enjoyable experience. I wish to thank my fellow PhD student, Bo Zeng for the significant contributions to ORAI/STIM overexpression experiments. I would also like to acknowledge honorary group member Dr Hongni Jiang. We worked together on the endothelial cell migration and tube formation experiments, and I very much appreciated her enthusiasm, intensity and willingness to work with me.

I am also grateful to all the people in Dr Maria's Gomez group at Lund University in Sweden for providing the kidney tissues from diabetic mouse models and Prof AV Tepikin (University of Liverpool) for providing the STIM1-EYFP cDNA. In regards to the clinical samples collected for my doctorial study, I would especially like to thank Dr Steve Griffin (Castle Hill hospital, Hull and East Yorkshire NHS trust) for providing me with human blood vessel samples.

I gratefully acknowledge the funding sources that made my PhD work possible and especially the University of Hull for offering me the 80th Anniversary PhD Scholarship. I also thank the Centre for Cardiovascular and Metabolic Research, the Graduate School and the American Physiological Society for funding my oral presentation in the international meeting of Experimental Biology 2012 in San Diego, California.

I owe my deepest gratitude to my family. Words cannot express how grateful I am to my father, Eleftherios Daskoulidis, and my mother, Sofia Daskoulidou, for all the sacrifices they have made on my behalf and for all their unwavering love and encouragement that was my driving force. They raised me with a love of science and supported me in all my pursuits. I would also like to thank my beloved siblings, Konstantinos Daskoulidis and Melina Daskoulidou for supporting me and encouraging me throughout this experience. Thank you all for always believing in me at every single step of my life.

Nikoleta Daskoulidou
Hull York Medical School
March 2013

Author's Declaration

I confirm that this work is original and that if any passage(s) or diagram(s) have been copied from academic papers, books, the internet or any other sources, these are clearly identified by the use of quotation marks and the reference(s) is fully cited. I certify that, other than where indicated, this is my own work and does not breach the regulations of HYMS, the University of Hull or the University of York regarding plagiarism or academic conduct in examinations. I have read the HYMS Code of Practice on Academic Misconduct, and state that this piece of work is my own and does not contain any unacknowledged work from any other sources. I confirm that any patient information obtained to produce this piece of work has been appropriately anonymised.

Chapter 1

General Introduction

1.1 Introduction

Although there has been a reduction in cardiovascular disease (CVD) mortality that has occurred over the last 40 years in Western countries, patients with diabetes have experienced less decline in CVD mortality than those without diabetes, with a two to four-fold increased risk of cardiovascular events (Fox *et al.*, 2004; Roger *et al.*, 2012). The UK is facing a huge increase in the number of people with diabetes. During the last 16 years, the number of people diagnosed with the disease has increased from 1.4 to 2.9 million. If the current trends continue, this number is estimated to further increase to 5 million by 2025 (Hex *et al.*, 2012).

CVD is one of the major complications that cause mortality in people diagnosed with diabetes. Around half of people diagnosed with diabetes (44% for Type 1 diabetes and 52% for Type 2 diabetes) die due to the vascular complications of the disease (Williamson *et al.*, 2000; Morrish *et al.*, 2001). The increased risk in diabetes is mainly due to the adverse effects of hyperglycemia and oxidative stress, the two main factors causing vascular endothelial damage and subsequently leading to the development of atherosclerosis (Kirpichnikov & Sowers, 2001; Avogaro *et al.*, 2011).

Apart from the health issue, diabetes and the associated complications have a significant economic impact on government health system with the direct medical cost related to the disease diagnosis and treatment and the indirect cost related to the decreased productivity and homecare (Hex *et al.*, 2012). Around 10 per cent (~£10 billion) of the National Health Service budget is estimated to be spent on diabetes with 80 per cent of the cost spent on the diabetic complications (Hex *et al.*, 2012). The total cost including the indirect cost is estimated around £23.7 billion and will increase to £39.8 billion by 2035/6 (Hex *et al.*, 2012). All these numbers indicate that diabetes and its complications are a leading health challenge and have become a global economic health burden.

1.2 Oxidative stress

Oxidative stress is termed as excess formation and/or insufficient removal of highly reactive molecules such as reactive oxygen species (ROS) and reactive nitrogen species (RNS) (Turko *et al.*, 2001; Maritim *et al.*, 2003). Free radicals such as superoxide ($\cdot O_2^-$), hydroxyl ($\cdot OH$), peroxyl, hydroperoxyl as well as nonradical species such as hydrogen peroxide (H_2O_2) and hydrochlorous acid are ROS, whereas free radicals such as nitric oxide ($\cdot NO$) and nitrogen dioxide ($\cdot NO_2^-$), as well as nonradicals like peroxynitrite ($ONOO^-$) and nitrous oxide are RNS. Both ROS and RNS are produced in all cells as derivatives of oxygen metabolism (Turko *et al.*, 2001; Evans *et al.*, 2002).

ROS and RNS within a physiological range are necessary for cell functions including the regulation of cell proliferation, differentiation and apoptosis (Bae *et al.*, 1997; Ghosh & Myers, 1998; Lee *et al.*, 1998; Sauer *et al.*, 2001), the removal of aged cellular components (Griendling *et al.*, 2000; Droge, 2002; Chiarugi & Cirri, 2003), and the immune function against microorganisms (Tohyama *et al.*, 2004; Valko *et al.*, 2007). ROS at low concentrations function as signalling molecules in regulating vascular smooth muscle cell contraction, relaxation and growth, such as superoxide and H_2O_2 (Rao & Berk, 1992; Cosentino *et al.*, 1994; Zafari *et al.*, 1998; Touyz & Schiffrin, 1999). However, excess production of ROS/RNS, i.e., oxidative stress condition, can damage cell structure through the modifications of cellular proteins, lipids, and DNA, and thus lead to the loss of normal cell function (Valko *et al.*, 2007; Xu *et al.*, 2009).

Oxidative stress is involved in many diseases including diabetes (Perez-Matute *et al.*, 2009); cardiovascular diseases such as atherosclerosis (Podrez *et al.*, 2000), heart failure (Givertz & Colucci, 1998), and myocardial infarction (Ansley & Wang, 2013); neurological disorders such as Alzheimer disease (Butterfield *et al.*, 2002), Parkinson disease (Tretter *et al.*, 2004) and Schizophrenia (Zhang *et al.*, 2013); obesity (Keaney *et al.*, 2003); chronic kidney diseases (Siddharth *et al.*, 2012); breast cancer (Wang *et al.*, 1996); fragile X syndrome (de Diego-Otero *et al.*, 2008); and chronic fatigue syndrome (Shungu *et al.*, 2012). However, some studies have demonstrated that short-term oxidative stress may have beneficial effects, such as the

potential prevention of aging by a cellular process called stress-response hormesis (Cypser & Johnson, 2002; Gems & Partridge, 2008).

1.3 Oxidative stress and diabetes

Diabetes mellitus (DM) is a group of metabolic disorders characterized by hyperglycemia resulting from insufficiency of secretion or action of endogenous insulin (Alberti & Zimmet, 1998). It is often accompanied by glycosuria, polydipsia, and polyuria. Type 1 DM is characterized by loss of the insulin-producing beta cells of the islets of Langerhans in the pancreas that leads to insulin deficiency, whereas Type 2 DM is characterized by insulin resistance (American Diabetes Association, 2005). The major aetiology of diabetes is hyperglycemia as a result of decreased glucose uptake into muscle and adipose tissue. The high mortality of diabetes is due to diabetic complications, especially the high risk of vascular complications (Alberti & Zimmet, 1998). The microvascular complications of diabetes include retinopathy, nephropathy and neuropathy; and macrovascular complications include coronary artery disease, cerebrovascular disease, and peripheral vascular disease due to atherosclerosis (Brownlee & Cerami, 1981).

Oxidative stress has been implicated in the development and progression of the diabetic complications (Kirpichnikov & Sowers, 2001). Large-scale studies have demonstrated that the initiating cause leading to the tissue damage in diabetes is hyperglycemia (The Diabetes Control and Complications Trial Research Group, 1993; UK Prospective Diabetes Study Group, 1998). Hyperglycemia triggers the overproduction of ROS from various sources including oxidative phosphorylation, glucose autooxidation, NADPH oxidase, lipooxygenase, cytochrome P450 monooxygenases, and nitric oxide synthase (NOS) (Baynes, 1991; Young *et al.*, 1995; Baynes & Thorpe, 1999; Lipinski, 2001; Ceriello, 2003; Maritim *et al.*, 2003). Impaired antioxidant defence mechanisms via glutathione, catalase, superoxide dismutase and thioredoxin in diabetic conditions also lead to increased ROS level (Halliwell *et al.*, 1990; McLennan *et al.*, 1991; Saxena *et al.*, 1993; Lipinski, 2001; Maritim *et al.*, 2003; Perez-Matute *et al.*, 2009). The level of antioxidants such as vitamin C, vitamin E and lipoic acid have been linked to the development of diabetic

complications as their role is to eliminate the production of critical radicals such as H_2O_2 and superoxide (Lipinski, 2001; Perez-Matute *et al.*, 2009; Golbidi *et al.*, 2011). Moreover, genetic background affecting insulin resistance or insulin production and some other independent factors such as hypertension and hyperlipidemia are also linked to the progress of tissue damage triggered in diabetic conditions (Kulkarni *et al.*, 2003; Zeggini *et al.*, 2008; Dermitzakis & Clark, 2009; Manolio *et al.*, 2009).

1.4 Diabetic vascular injury

The imbalance between production of ROS and antioxidant defences leads to dysfunction of cells and consequently tissue injury. It has been demonstrated that hyperglycemia-induced oxidative stress is a risk factor for CVD, such as coronary artery disease, cerebrovascular disease and peripheral vascular disease, which have been reported as diabetic macrovascular complications responsible for the high mortality of people diagnosed with DM (Pyorala *et al.*, 1987; The Diabetes Control and Complications Trial Research Group, 1993; Laakso, 1999; Johansen *et al.*, 2005). The pathophysiological processes leading to vascular damage in CVD when ROS are produced at high levels include the dysfunction of endothelial cells, the increased contractility, abnormal growth and apoptosis of smooth muscle cells, monocyte migration, lipid peroxidation, inflammation, and increased deposition of extracellular matrix proteins (Rao & Berk, 1992; Harrison, 1997).

The generation of superoxide induced by hyperglycemia at the mitochondrial level was found to be the initial step of oxidative stress in diabetes (Nishikawa *et al.*, 2000; Brownlee, 2001). Increased level of glucose and other sugars, such as fructose and glyceraldehyde-3-phopshate, induces the mitochondrial overproduction of ROS and RNS that result in the increased intracellular formation of advanced glycated end products, increased expression of the receptor for advanced glycated end products (a member of the immunoglobulin superfamily of receptors), activation of protein kinase C, or the increased activity of the hexosamine pathway, which are underlying mechanisms that induce endothelial tissue damage (Brownlee, 2005; Goldin *et al.*, 2006).

1.5 Calcium signalling in blood vessels

Calcium ion (Ca^{2+}) is a second messenger in all eukaryotic cells. It differentially regulates diverse cellular phenomena via spatiotemporal partitioning of Ca^{2+} levels. The intracellular Ca^{2+} concentrations are regulated by external and internal stimuli, such as membrane depolarization, stretch, extracellular agonists, intracellular messengers or the depletion of intracellular stores. Ca^{2+} itself can directly or indirectly affect many protein functions, such as enzymes, channels and transporters, and thus regulate many cellular processes as a second messenger such as exocytosis, contraction, metabolism, transcription, fertilization, proliferation, and immune response (Berridge *et al.*, 2003). Ca^{2+} not only controls short-term cell response, such as contraction and secretion, but also regulates longer-term cell function, such as cell growth and cell division (Berridge *et al.*, 1998; Venkatachalam *et al.*, 2002). Substantial evidence has demonstrated that even small disturbance in Ca^{2+} homeostasis can provoke serious dysfunction of fundamental cellular processes and cause several diseases (Berridge, 2012).

There are two ways to control cytoplasmic Ca^{2+} concentration in eukaryotic cells, i.e., Ca^{2+} release from intracellular Ca^{2+} stores and Ca^{2+} influx into the cell. Up to date, extensive research has been done in revealing the organelles that function as Ca^{2+} stores and the mechanisms involved (Berridge *et al.*, 2003). The endoplasmic/ sarcoplasmic reticulum (ER/SR) has been found to be of great importance for Ca^{2+} storage and release (Pozzan *et al.*, 1994). Other organelles like mitochondria, Golgi apparatus, lysosomes, nuclear envelope, and some secretory granules have also been reported to contribute to intracellular Ca^{2+} storage (Pozzan *et al.*, 1994; Sorrentino & Rizzuto, 2001; Carafoli, 2002).

The major families of Ca^{2+}-permeable ion channels located on the plasma membrane (PM) and the ER are presented in Figure 1-1. Intracellular Ca^{2+} dynamics is controlled by the opening or closing of these Ca^{2+} permeable ion channels. Receptor-operated channels are activated by neurotransmitters or hormones via G-protein-coupled receptors (GPCRs). Voltage-operated channels (VOCs) are activated by membrane depolarization and are found in the excitable cells like neurons, muscles and glial cells. Store-operated channels (SOCs) are found to be widely expressed in

all eukaryotes and activated by the depletion of the Ca^{2+} stores within the ER (Partiseti *et al.*, 1994; Locke *et al.*, 2000). Ligand-gated channels are opened or closed in response to the binding of chemical messengers, whereas stretch-activated ion channels are activated or deactivated in response to membrane tension. Another pathway for Ca^{2+} entry is Na^{+}-Ca^{2+} exchanger, which functions in reverse mode after membrane depolarization (Philipson & Nicoll, 2000). Ca^{2+} pumps, like the plasma membrane Ca^{2+} ATPase (PMCA) and the sarcoplasmic reticulum Ca^{2+} ATPase (SERCA) are important regulators for cytosolic Ca^{2+} concentrations, as they pump Ca^{2+} out of the cells or into the ER, respectively, and maintain the cellular Ca^{2+} homeostasis (Carafoli, 1991; Periasamy & Kalyanasundaram, 2007). ER store depletion leading to activation of SOCs can also be mediated by activation of ryanodine receptors (RyRs) (Fill & Copello, 2002). Cellular functions are mediated by particular Ca^{2+} channels depending on the biophysical kinetics of channel activation and the sensitivity to the stimuli, such as rapid events like exocytosis and contraction are mediated by the rapidly activated VOC and RyR channels, whereas the long-term functions like gene transcription are regulated by the slow activated SOC channels (Soboloff *et al.*, 2012).

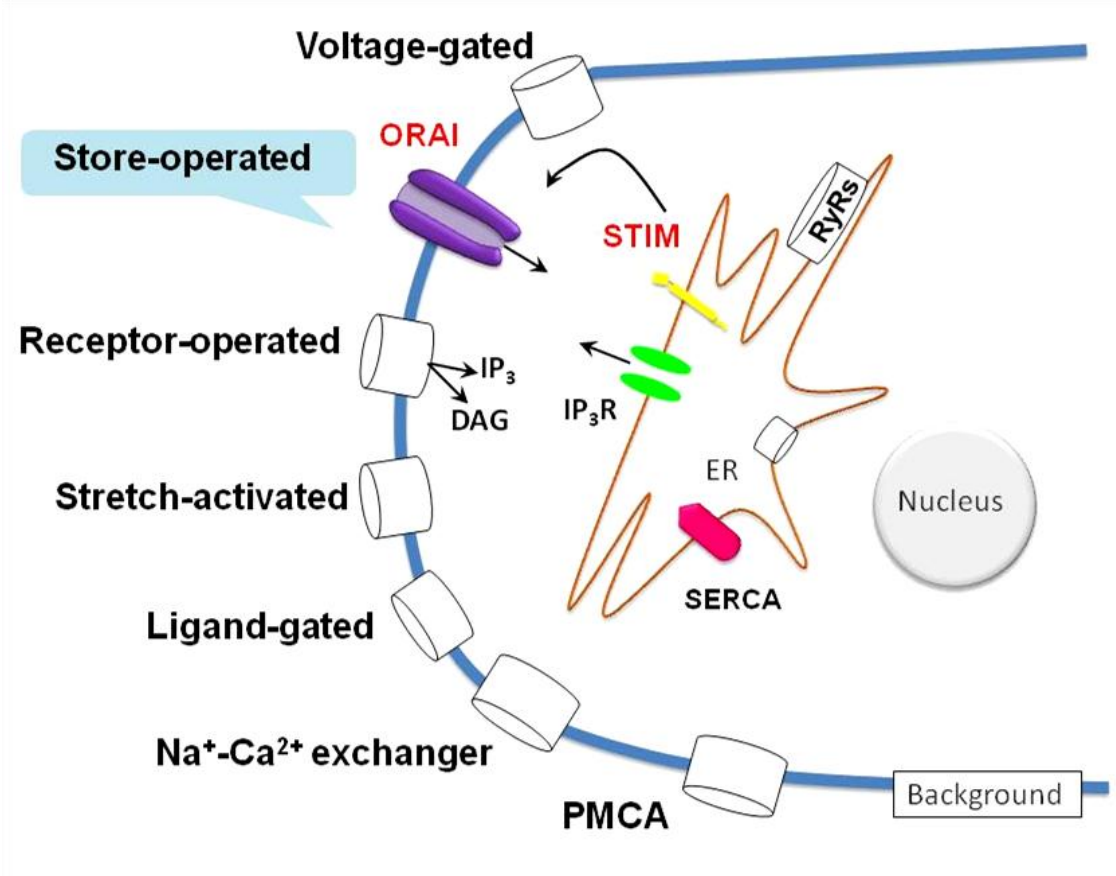

Figure 1-1 Ca^{2+} permeable channels and pumps in the PM and ER. PMCA; plasma membrane Ca^{2+} ATPase, SERCA; sarcoplasmic reticulum Ca^{2+} ATPase, RyRs; ryanodine receptors, DAG; diacylglycerol, IP_3; inositol 1, 4, 5-triphosphate, IP_3R; IP_3 receptors.

1.6 Store-operated Ca^{2+} entry

Store-operated Ca^{2+} entry (SOCE), also called capacitative Ca^{2+} entry, is the process in which depletion of Ca^{2+} stores in the ER induces Ca^{2+} influx from the extracellular space into the cytosol through the activation of PM-localized Ca^{2+}-permeable channels, i.e., SOCs or Ca^{2+} release-activated channels (CRACs) (Parekh & Penner, 1997; Parekh & Putney, 2005). Activation of GPCRs or receptor tyrosine kinases (RTKs) by various growth factors, hormones, or neurotransmitters, can generate the second messengers inositol 1, 4, 5-triphosphate (IP_3) and diacylglycerol (DAG). In the first phase, IP_3 functions as a chemical message that diffuses rapidly within the cytosol and interacts with IP_3 receptors (IP_3R) located on the ER. Ca^{2+} in the ER is then released from the ER lumen and results in cytoplasmic Ca^{2+} elevation (Berridge *et al.*, 1998; Berridge *et al.*, 2000; Clapham, 2007). In the second phase, the depletion of ER Ca^{2+} activates PM-localized SOCs and triggers the influx of extracellular Ca^{2+} into the cell (Parekh & Putney, 2005). DAG, the other product of phospholipase C activation, can induce Ca^{2+} influx into a cell via a receptor-operated pathway (Hofmann *et al.*, 1999; Harteneck *et al.*, 2000; Hofmann *et al.*, 2000).

The concept of SOCE was first proposed in 1986 (Putney, 1986) and evidenced by the experiments in parotid acinar cells using a Ca^{2+} dye (Takemura *et al.*, 1989; Takemura & Putney, 1989). The electrophysiological studies provided direct evidences that store depletion can activate a Ca^{2+}-selective current. In 1992, the store-operated current was first recorded in rat basophilic leukemia (RBL) mast cells (Hoth & Penner, 1992), called Ca^{2+} release-activated Ca^{2+} current or I_{CRAC}, which shed light on the understanding of SOCE (Hoth & Penner, 1992; Hoth & Penner, 1993). I_{CRAC} is the best characterized store-operated current in RBL mast cells and Jurkat T cells with non-voltage activated, inwardly rectifying, and highly Ca^{2+}-selective properties, and a tiny single-channel conductance of < 30 fS (femto-Siemens) (Hoth & Penner, 1992).

1.7 Molecular basis of store-operated Ca^{2+} entry

Many genes have been claimed to code the SOCs (Winslow *et al.*, 2003; Prakriya *et al.*, 2006). The transient receptor potential canonical (TRPC) subfamily was suggested as the molecular basis of SOCs (Parekh & Putney, 2005; Worley *et al.*, 2007), especially the TRPC1 (Xu & Beech, 2001). Recently, the discovery of STIM1 and ORAI1 shed light on the molecular identity of the I_{CRAC} with the higher Ca^{2+} selectivity and inward rectification (Huang *et al.*, 2006; Yeromin *et al.*, 2006). STIM1 acts as a sensor of Ca^{2+} content in the ER, while ORAI1 may form the CRAC channel itself (Gwack *et al.*, 2007; Mignen *et al.*, 2007; Putney, 2007).

1.7.1 Stromal-interacting molecules

The stromal-interacting molecules (STIMs) were identified prior to the discovery of their involvement in Ca^{2+} entry (Oritani & Kincade, 1996; Williams *et al.*, 2001). STIM1 was originally identified in a search for cell surface proteins on stromal cells and was reported to be involved in pre-B cell survival and tumour suppression (Oritani & Kincade, 1996; Williams *et al.*, 2001). In 2005, STIM1 was identified as a component of SOCE using an RNA interference screen in Drosophila S2 cells and in STIM1-overexpressed HeLa cells (Liou *et al.*, 2005; Roos *et al.*, 2005).

STIM is identified as a type-I (single-spanning) membrane protein with the N-terminus in the ER lumen and the C-terminus in the cytosol (Manji *et al.*, 2000; Spassova *et al.*, 2006; Hogan *et al.*, 2010) (Figure 1-2). STIM contains an N-terminus, a single transmembrane region and a C-terminus. The N-terminal region contains a canonical EF-hand domain which is a Ca^{2+}-binding motif that serves as the Ca^{2+} sensor to detect changes in $[Ca^{2+}]_i$, a 'hidden' EF-hand domain, and a sterile-alpha motif (SAM) that is used for protein-protein interactions (Stathopulos *et al.*, 2006; Stathopulos *et al.*, 2008). A single-pass transmembrane motif separates the N-terminal from the C-terminal region that contains three coiled-coil domains, CC1, CC2 and CC3, that mediate interactions between STIM proteins allowing them to oligomerize upon activation, a proline-rich motif and a lysine-rich tail (Williams *et al.*, 2001; Williams *et al.*, 2002; Kim & Bowie, 2003; Li *et al.*, 2007; Zheng *et al.*, 2008).

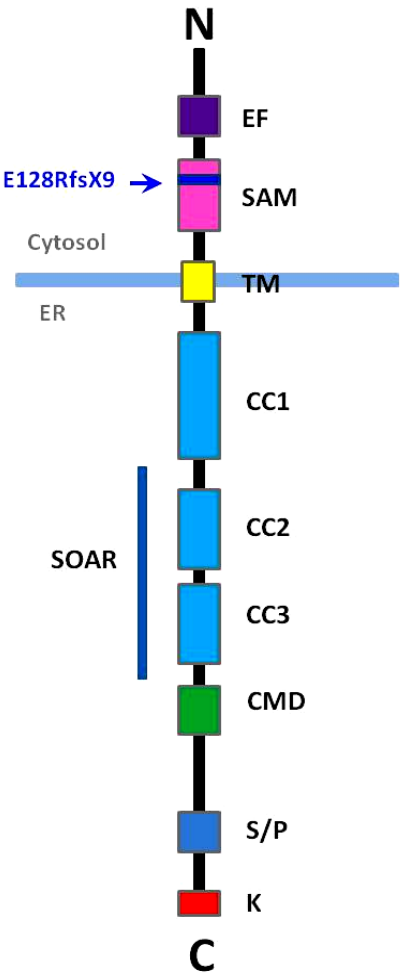

Figure 1-2 STIM1 functional domains. EF, canonical/hidden EF-hand motif; SAM, sterile alpha motif; TM, transmembrane domain; CC1/CC2/CC3, coiled-coil domains 1–3; CMD, CRAC modulatory domain; S/P, serine/proline-rich region; K, polybasic cluster; SOAR, STIM-ORAI activating region. E128RfsX9 is a mutation identified in patients with immunodeficiency (indicated by the arrow).

It has been reported that a highly conserved domain with 98 amino-acids in STIM1, named STIM-ORAI activating region (SOAR), is necessary and sufficient to fully activate ORAI channels after direct coupling to them (Yuan *et al.*, 2009b). This segment is similar to the reported CRAC modulatory domain (CMD) and ORAI1-activating small fragment (Muik *et al.*, 2009; Park *et al.*, 2009; Yuan *et al.*, 2009b). The same region mediates the strong suppression of voltage-gated Cav1.2 calcium channel when STIM1 is activated by store depletion or mutational modification (Wang *et al.*, 2010).

There are two isoforms for STIM in vertebrates, i.e. STIM1 and STIM2. The two isoforms are widely expressed in mammalian cells. Human STIM1 gene was mapped to human chromosome 11p15.5 (Stathopulos *et al.*, 2006) and STIM2 to 4p15.1 (Wissenbach *et al.*, 2007). Human STIM1 has 65% amino acid identity to STIM2. STIM1 is mainly located in the ER, but also to a limited extent in the PM, whereas STIM2 protein is expressed only intracellularly (Soboloff *et al.*, 2006a; Soboloff *et al.*, 2006b; Spassova *et al.*, 2006; Hogan *et al.*, 2010). STIM1 and STIM2 have almost identical EF-hand-containing N-terminal domains, transmembrane region and coiled-coil regions in the C-terminal domain. Their sequences deviate toward a short segment at the N-terminus and a longer one near the C-terminus (Soboloff *et al.*, 2006b; Dziadek & Johnstone, 2007; Deng *et al.*, 2009).

1.7.1.1 STIMs and SOCE

A number of studies have demonstrated that STIM1 is required for store-operated Ca^{2+} entry. STIM1 has a dual role in a cell, which functions as a sensor of Ca^{2+} concentration in the ER and a messenger coupling the store depletion information to the PM to trigger ORAI channel opening (Liou *et al.*, 2005; Roos *et al.*, 2005; Spassova *et al.*, 2006).

Despite sharing close structural homology with STIM2, it was found that STIM1 is a stronger activator of ORAI channels than STIM2 (Bird *et al.*, 2009). However, STIM2 is a more potent sensor for Ca^{2+} concentration in the ER, as it can be activated at higher Ca^{2+} concentrations after a mild reduction in ER Ca^{2+} level as well as the basal Ca^{2+} levels, suggesting STIM2 is an important regulator for basal

activity (Brandman *et al.*, 2007). In addition, STIM2 showed a slower activation of ORAI1 compared to that by STIM1 (Parvez *et al.*, 2008; Zhou *et al.*, 2009). Nevertheless, STIM1 overexpressed alone led to a moderate increase in CRAC current, suggesting the channel complex formation of STIM1/ORAI1 is crucial for the size of CRAC current (Liou *et al.*, 2005; Roos *et al.*, 2005). On the contrary, when STIM2 was overexpressed, endogenous SOCE mediated by STIM1 was strongly inhibited (Soboloff *et al.*, 2006b; Brandman *et al.*, 2007). The physiological difference of STIM1 and STIM2 is still unclear, but STIM1 appears to be an obligatory mediator of SOC activation, while the STIM2 protein may function as a regulator in the store-operated signalling pathway (Brandman *et al.*, 2007; Parvez *et al.*, 2008; Stathopulos *et al.*, 2009).

1.7.2 ORAIs

ORAI has been identified as the component of CRAC channel in 2006 (Feske *et al.*, 2006; Prakriya *et al.*, 2006). The "Orai" stands for the keepers of the gates of heaven in Greek mythology. The Orai means hours in Greek and there are three Hours: Eunomia (Order or Harmony), Dike (Justice) and Eirene (Peace). According to this, the three homolog genes were designated as Orai1, Orai2 and Orai3, which encode ORAI1, ORAI2 and ORAI3 channel proteins (Feske *et al.*, 2006). They are regarded as highly Ca^{2+}-selective ion channels in the PM and share no homology with other ion channel family (DeHaven *et al.*, 2007). Each isoform has an intracellular N-terminus and C-terminus and one transmembrane region with four domains (Lis *et al.*, 2007; Maruyama *et al.*, 2009) (Figure 1-3). Cross-linking studies have demonstrated that ORAI proteins form dimers at the resting state, whereas they function as tetramers to form the CRAC channel pore (Gwack *et al.*, 2007; Ji *et al.*, 2008; Mignen *et al.*, 2008; Penna *et al.*, 2008).

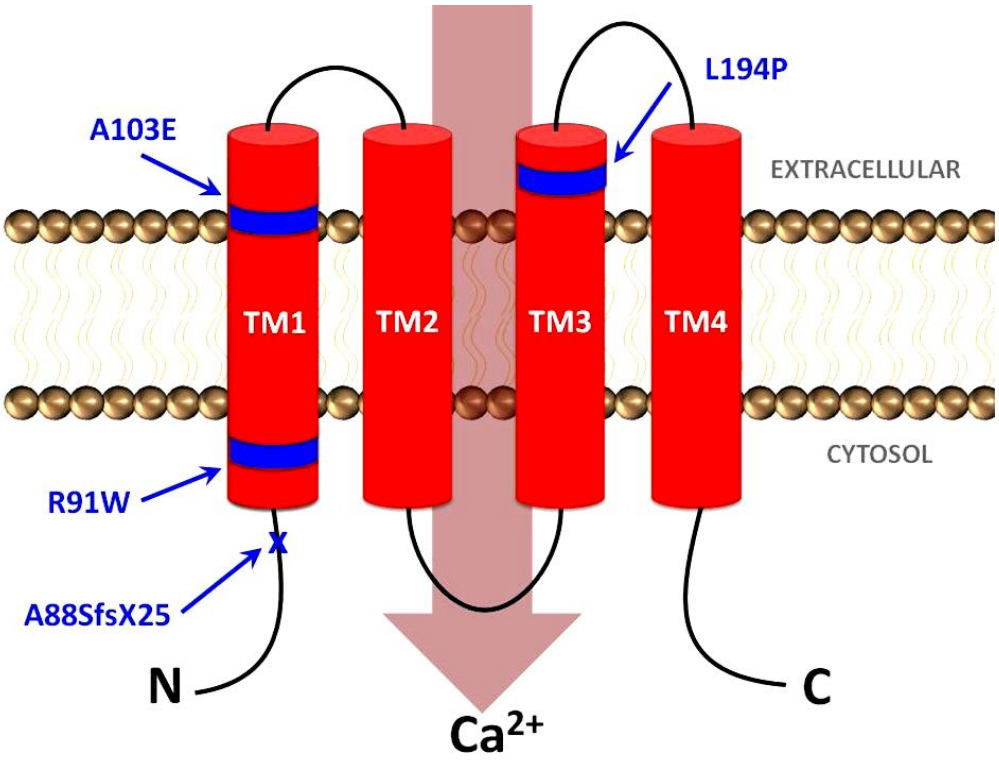

Figure 1-3 ORAI channel domains. TM1-4, transmembrane domains 1-4. A103E, L194P, R91W and A88SfsX25 are the mutations in patients indicated by the arrows.

Just one year after the discovery of STIM1 as the component of SOC, ORAI1 was identified by Feske *et αl*. as a channel protein responsible for Ca^{2+} entry following ER Ca^{2+} store depletion with two approaches (Feske *et al.*, 2006). The first approach was tracking the molecular basis of T cell receptor function loss in patients with one form of hereditary severe combined immunodeficiency (SCID) syndrome, who are defective in SOCE and CRAC channel function. After positional cloning of the mutant locus, the ORAI1 gene was identified. SOCE was fully restored by expression of the wild-type ORAI1 in the T cells from patients with SCID. The second approach utilized RNA interference to functionally suppress ORAI1 in Drosophila S2 cells, and revealed that ORAI1 is a key element of CRAC channel. In the same period of time, similar genes were identified in Drosophila by two other groups using genome-wide RNA interference screens and their orthologous genes in human (Vig *et al.*, 2006; Zhang *et al.*, 2006).

1.7.2.1 ORAIs and SOCE

ORAI1 is an essential molecule for SOCE. SOC or CRAC channel is reconstituted by ORAI1 in most mammalian cell types (Mercer *et al.*, 2006; Prakriya *et al.*, 2006; Gwack *et al.*, 2007). It has been demonstrated that mutations within the pore region of ORAI1 are capable of changing the biophysical properties of SOCE (Feske *et al.*, 2006; Yeromin *et al.*, 2006; Guo & Huang, 2008). Based on the ion permeability studies with different point mutations of ORAI1 in the transmembrane region 1 and 3, it was suggested that these regions form the pore of CRAC channel (Prakriya *et al.*, 2006; Yeromin *et al.*, 2006). Furthermore, several studies have revealed that ORAI1 co-expressed with STIM1 in human embryonic kidney 293 (HEK293) cells resulted in a big increase of SOCE compared to the cells expressing STIM1 alone (Mercer *et al.*, 2006; Peinelt *et al.*, 2006; Prakriya *et al.*, 2006; Hewavitharana *et al.*, 2007; Takahashi *et al.*, 2007; Varnai *et al.*, 2009).

ORAI2 has been reported to exhibit properties similar to ORAI1 as overexpression of ORAI2 alone also resulted in inhibition of SOCE in HEK293 cells, whereas its co-expression with STIM1 resulted in markedly increased Ca^{2+} entry. The magnitude of the currents with ORAI2 was less than that with ORAI1 though (Mercer *et al.*,

2006). ORAI3, however, did not synergistically increase Ca^{2+} entry when co-expressed with STIM1 (Mercer *et al.*, 2006; Gross *et al.*, 2007). In contrast, it was shown that ORAI3 is able to restore Ca^{2+} entry in cells in which the endogenous ORAI1 was silenced by RNA interference and the Ca^{2+} entry was reduced (Gwack *et al.*, 2007; Guo & Huang, 2008).

In expression experiments, ORAI1 was reported to have higher Ca^{2+} influx efficacy that ORAI2 and ORAI2 a higher efficacy than ORAI3 (Mercer *et al.*, 2006), and an N-terminal tail region was found to determine this order (Takahashi *et al.*, 2007). This region appeared to play an important role in the formation of the pore of the channel, whereas the C-terminus region was reported to participate in the activation process between ORAI1, but not ORAI2 or ORAI3, and STIM1 (Takahashi *et al.*, 2007; Frischauf *et al.*, 2009).

1.7.3 Transient receptor potential channels as SOCs

The canonical subfamily of TRP channels (TRPCs) are Ca^{2+}-permeable cationic channels. There are seven members in the TRPC subfamily, i.e., TRPC1-7. According to their amino acid similarities, the seven members can be grouped as TRPC1, TRPC2 (a pseudogene in human), TRPC3 and TRPC6-7, and TRPC4-5 (Xu & Beech, 2001; Clapham, 2003; Putney, 2005; Xu *et al.*, 2008a; Beech *et al.*, 2009). The common structure of TRPC family contains four N-terminal ankyrin repeats, six transmembrane-spanning domains and a putative pore region located between transmembrane domains 5 and 6 (Hofmann *et al.*, 2002). TRPC channels mediate the non-selective Ca^{2+}-permeable cationic current with outward rectification (Xu *et al.*, 2006a; Xu *et al.*, 2006b), which are different from that of the I_{CRAC}.

TRPC channels have been proposed to act as SOCs as they were found to be activated by store depletion in HEK293 cells overexpressing TRPC genes (Salido *et al.*, 2009). For instance, the SOCE was increased in HEK293 cells overexpressing TRPC1, whereas it was decreased in the cells co-expressing a dominant-negative form of TRPC1 (Ohba *et al.*, 2007). In addition, the SOCE in vascular endothelial cells from knockout TRPC4 mice was also decreased (Freichel *et al.*, 2001). Moreover, TRPC1 blocking antibody (T1E3) specifically inhibited SOCE in smooth

muscle cells (Xu & Beech, 2001). These studies suggest some members of TRPCs are components of SOCs, although some TRPC isoforms are controversial, such as TRPC3 and TRPC6 appear not to function as SOCs (Putney, 2004; Parekh & Putney, 2005; Yuan *et al.*, 2009a).

A direct activation of TRPCs by STIM1 has been demonstrated by several research groups (Huang *et al.*, 2006; Kim *et al.*, 2009; Pani *et al.*, 2009; Lee *et al.*, 2010), however, there are some opposing evidences reported by others which indicated that TRPC channel activity is independent of STIM1 (Varga-Szabo *et al.*, 2008a; DeHaven *et al.*, 2009; Wang *et al.*, 2010). Despite this controversy, recent studies have revealed that the insertion of TRPC1 in the PM was induced by Ca^{2+} entry via ORAI1, suggesting that there is a close connection between these channels (Cheng *et al.*, 2011; Soboloff *et al.*, 2012).

Biochemical assembly of STIM1-ORAI1-TRPCs complexes and functional interaction between TRPC channels and ORAI1 has also been reported by several studies (Ambudkar *et al.*, 2007; Liao *et al.*, 2007; Ong *et al.*, 2007; Jardin *et al.*, 2008; Kim *et al.*, 2009). The channel function of both TRPCs and ORAI1 channels appeared to be required for TRPC1 and STIM1-dependent SOCE at physiological low expression levels (Cheng *et al.*, 2008; Kim *et al.*, 2009), however, both channels could function independently when TRPC and ORAI genes were expressed at high levels in same cells (Zeng *et al.*, 2008).

1.7.4 Mechanism of ORAI store-operated channel activation

STIM1 clustering and translocation to the subplasmalemmal space near PM has been suggested to be the mechanism that communicates the Ca^{2+} store depletion in the ER to the SOCs located in the PM (Liou *et al.*, 2005; Zhang, 2005) (Figure 1-4). The reduction of the Ca^{2+} concentration in the ER results in the activation of STIM molecules, the sensors of the Ca^{2+} concentration in the ER. It has been found that the ER-luminal domain of STIM1 is the responsible domain for sensing Ca^{2+}. Depletion of Ca^{2+} concentration in ER leads to dissociation of Ca^{2+} from the EF-hand domain of STIM1, and results in STIM1 clustering (oligomerization) and redistribution of

STIM1 clusters, or called puncta, to the location of ER juxtaposed to the PM (translocation) (Smyth *et al.*, 2008; Hogan *et al.*, 2010). The process of STIM1 clustering then triggers ORAI channels in the PM via binding to the C-terminus of ORAI and causes ORAI channel opening and thus Ca^{2+} entry from the extracellular space to the cell (Penna *et al.*, 2008; Hogan *et al.*, 2010). It has been demonstrated that STIM1 redistribution is a reversible process providing that the ER Ca^{2+} stores are refilled through SOCs or other Ca^{2+}-permeable pathways (Liou *et al.*, 2005; Varnai *et al.*, 2007; Smyth *et al.*, 2008).

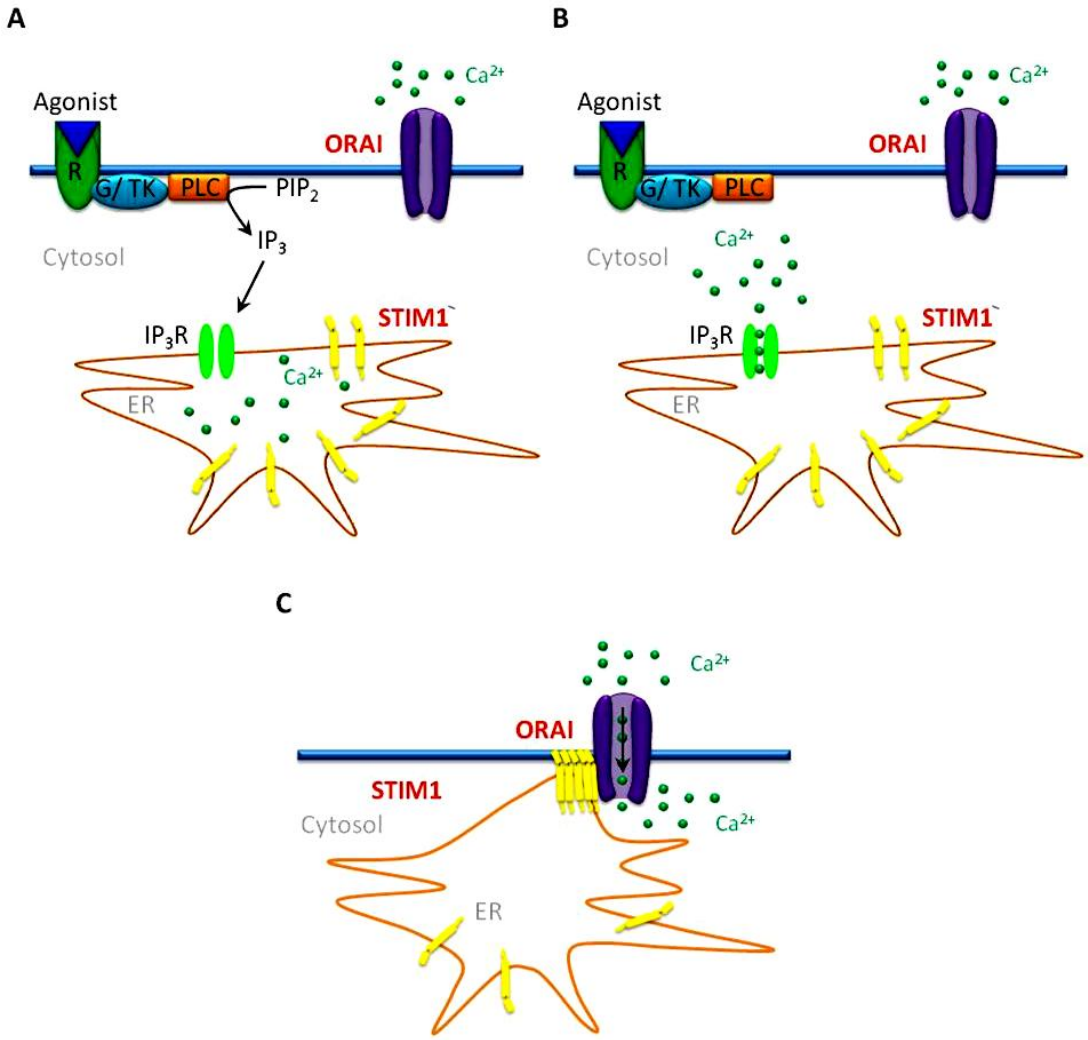

Figure 1-4 Mechanism of store-operated ORAI channel activation by STIM. A, Activation of GPCRs or RTKs by agonists (growth factors, hormones, and neurotransmitters) generates the second messengers inositol 1, 4, 5-triphosphate (IP_3) and diacylglycerol (DAG). IP_3 functions as a chemical message that diffuses rapidly within the cytosol and interacts with IP_3 receptors (IP_3R). **B,** Activation of IP_3R located on the ER causes Ca^{2+} release from ER store. **C,** The reduction of the Ca^{2+} concentration in the ER results in the aggregation of the Ca^{2+} sensors STIM1. The STIM molecules form clusters (puncta) and translocate to the sections of ER juxtaposed to the PM, where they activate PM-localized ORAI channels and result in Ca^{2+} influx.

Apart from ER Ca^{2+} store depletion, STIM1 clustering and translocation could also be triggered by other conditions, for example, the modification of Cys^{56} in the N-terminus of STIM1 by ROS-induced S-glutathionylation. Such modification may reduce the Ca^{2+} binding to the EF-hand domain, although the ER stores are still replete (Hawkins *et al.*, 2010). In addition, STIM1 could also sense temperature as it can be activated by small increases in temperature from 37 ºC to 41 ºC; however, higher temperatures cause STIM1-ORAI1 uncoupling, but this process is reversible after cooling the temperature (Mancarella *et al.*, 2011b; Xiao *et al.*, 2011). STIM1 could also be activated under hypoxic conditions and the underlying mechanisms are unknown (Mancarella *et al.*, 2011a). Finally, an ER Ca^{2+} store-independent mechanism for STIM1 clustering has been recently demonstrated by our group using pharmacological regulators and stable transfected HEK-293 cells overexpressing STIM1-EYFP, suggesting a new alternative mechanism for regulating cytosolic STIM1 movement may exist (Zeng *et al.*, 2012).

Physiological IP_3R activation is not the only mechanism for SOCE activation. Any procedure or signal that leads to reduction or depletion of ER Ca^{2+} stores will trigger the activation of SOCE. There are two experimental approaches to deplete the ER Ca^{2+} stores, i.e., active store depletion and passive store depletion (Zeng *et al.*, 2012).

Active store depletion: The application of GPCR agonists to activate IP_3Rs or the activation of RyRs to cause Ca^{2+} release are active store depletion procedures, such as the use of physiological agonists like hormones, neurotransmitters and nucleotides (Parekh & Putney, 2005). Patch clamp recording techniques have been used to characterize and measure I_{CRAC}. During whole-cell patch clamp recording, the contents of the cell cytoplasm slowly exchange with the pipette contents. The cytosol can be dialyzed with IP_3 or related analogues and thimerosal can be used to sensitize IP_3R to resting IP_3 levels (Parekh & Penner, 1995).

Passive store depletion: The store depletion by inhibition of SERCA pump or causing membrane leakage belongs to passive store depletion procedures. Exposure of the cells to SERCA pump inhibitors such as thapsigargin (TG), cyclopiazonic acid and di-tert-butylhydroquinone prevent store refilling; the Ca^{2+} ionophore ionomycin can be applied to make the ER membrane permeable; high concentrations of Ca^{2+}

chelators such as ethylene glycol tetraacetic acid (EGTA) or 1,2-bis(o-aminophenoxy)ethane- N,N,N',N' -tetracetic acid (BAPTA) chelate Ca^{2+} that leaks from the stores and thus prevent store refilling (Parekh & Penner, 1997; Lewis, 1999). Direct application of membrane-permeable metal Ca^{2+} chelators like *N*,*N*,*N*',*N*'-tetrakis(2-pyridylmethyl)ethylenediamine (TPEN) into the stores is another method that is used to chelate free Ca^{2+} into the ER lumen without affecting the total Ca^{2+} stored (Hofer *et al.*, 1998).

1.7.5 Pharmacology of ORAI and STIM channels

Despite the importance of ORAI and STIM channels in physiological and pathological conditions, there are just few inhibitors reported, such as 2-aminoethoxydiphenyl borate (2-APB). Some of inhibitors have been demonstrated to inhibit SOCE in native cells, but the effect on ORAI channels are unknown, such as diethylstilbestrol (DES), BTP2, SKF-96365, and divalent and trivalent cations (Putney, 2001; Sweeney *et al.*, 2009; Varnai *et al.*, 2009; Roberts-Thomson *et al.*, 2010). The specificity of these inhibitors is unclear and needs to be further investigated.

2-APB is a SOC inhibitor, however, it has non-selective inhibition on other cationic channels (Wang *et al.*, 2002; Xu *et al.*, 2005). 2-APB inhibits ORAI1 and ORAI2 channels, but activates ORAI3 channels. The difference is related to the ORAI channel gating property change, rather than the coupling process of STIM1 to ORAI during channel activation (DeHaven *et al.*, 2008; Peinelt *et al.*, 2008; Penna *et al.*, 2008; Schindl *et al.*, 2008), because 2-APB showed similar effect on STIM1 clustering and translocation in the HEK293 cells co-expressing STIM1-EYFP and ORAI1 or ORAI2 or ORAI3 channels (Zeng *et al.*, 2012).

DES is a synthetic non-steroidal estrogen. DES potently inhibits SOCs and I_{CRAC} in RBL cells, smooth muscle cells, and human platelets (Zakharov *et al.*, 2004; Hopson *et al.*, 2011), however, the effect on STIM1 or ORAI channels are unknown.

BTP2, a 3,5-bistrifluoromethyl pyrazole derivative, was reported to inhibit nuclear factor of activated T-cells (NFAT) activation, T-cell cytokine secretion, SOCE and

I_{CRAC} (Trevillyan *et al.*, 2001; Chen *et al.*, 2002; Ishikawa *et al.*, 2003; Zitt *et al.*, 2004). It also inhibited some TRPC channels (He *et al.*, 2005), but the effect on ORAI channels are unclear.

In early studies, divalent cations, such as Sr^{2+} (strontium), and trivalent lanthanides, such as La^{3+} and Gd^{3+}, have been used at specific and narrow concentration range to block SOCE, but these cations are nonspecific and affect other Ca^{2+} channels (Broad *et al.*, 1999; Trebak *et al.*, 2002; Peinelt *et al.*, 2006; Yeromin *et al.*, 2006; Bird *et al.*, 2008). On the other hand, lanthanides (Gd^{3+} and La^{3+}) are unique channel activators for TRPC4 and TRPC5 (Xu *et al.*, 2005; Xu *et al.*, 2012).

SKF-96365, an imidazole compound, was found to inhibit SOCE and I_{CRAC} in several cells, such as mast cells, Jurkat and RBL cells (Franzius *et al.*, 1994; Kozak *et al.*, 2002; Prakriya & Lewis, 2002) and in cells expressing a constitutively active (EF-hand mutant) STIM1 (Huang *et al.*, 2006). However, it has been demonstrated that SKF-96365 blocks other channels, such as VOCs (Merritt *et al.*, 1990) and TRPCs (Xu *et al.*, 2012).

1.7.6 Pathophysiology of ORAI and STIM channels

It has been established that SOCE is central to the physiology of eukaryotic cells. SOCE serves as the main Ca^{2+} entry mechanism in a variety of non-excitable cells and plays an important role in cellular Ca^{2+} signalling and cellular processes ranging from proliferation to apoptosis (Lam *et al.*, 1994; Golovina *et al.*, 2001; Wu *et al.*, 2004). Replenishment of Ca^{2+} stores in the ER by SOCE ascertains that principal functions which are carried out in the ER, such as protein folding, and other cellular functions that require Ca^{2+} release from the ER are maintained (Parekh, 2003; Laporte *et al.*, 2004).

1.7.6.1 ORAI and STIM in the immune system

Early studies before the discovery of ORAI channels have linked SOCE with immune cell function (Prakriya & Lewis, 2003). Mutations in ORAI1 from three unrelated families diagnosed with SCID have been reported to affect ORAI1

expression and consequently SOCE (Feske, 2010). In the first case, a missense mutation in exon 1 of Orai1 resulted in replacement of a highly conserved arginine with tryptophan at position 91 (R91W) of ORAI channel protein in the patients. The ORAI1 mutant (R91W) was expressed in the PM, but showed no functional CRAC channel activity or SOCE. Expression of wild-type ORAI1 in T cells from the patient restored SOCE (Feske *et al.*, 2006). In the second case, an insertion mutation (A88EfsX25) was identified, which caused premature termination of ORAI1 at the end of the first transmembrane domain. The ORAI1 channel protein was not expressed in the PM and subsequently there was no channel function and SOCE (McCarl *et al.*, 2009). In a third family, two missense mutations in exon 2 of ORAI1 were found. One led to substitution of an alanine with a glutamate (A103E) in the first transmembrane domain and the other to substitution of a leucine with a proline (L194P) in the third transmembrane domain (Le Deist *et al.*, 1995; McCarl *et al.*, 2009). The ORAI1 protein expression was inhibited in both cases. In addition, the mutation (E128RfsX9) of STIM1 has also been identified in patients with SCID and the premature termination of STIM1 led to reduced levels of STIM1 expression and defective SOCE, but ORAI expression was not affected. Expression of STIM1 was able to restore SOCE (Picard *et al.*, 2009). The positions of the mutations are demonstrated in Figure 1-2 and Figure 1-3. These genetic and functional studies suggest the ORAI1 channel and STIM1 are essential for immune response.

The clinical phenotypes associated with ORAI and STIM deficiency in patients are similar and characterized by immunodeficiency leading to repeated severe infections including pneumonia, meningitis, and gastroenteritis (Partiseti *et al.*, 1994; Le Deist, 1995; Feske, 1996; Feske, 2009; McCarl *et al.*, 2009; Picard *et al.*, 2009). Apart from immunodeficiency, these patients face other disorders, like myopathy, defective dental enamel formation and impaired sweat production or anhidrosis (McCarl *et al.*, 2009; Picard *et al.*, 2009).

1.7.6.2 ORAI and STIM in the cardiovascular system

The pathophysiological importance in the cardiovascular system has also been demonstrated. Ca^{2+} influx was significantly impaired in platelets from ORAI1 and STIM1 knockout mice and mutant ORAI1 (R93W) mice, which affects SOCE and

platelet aggregation, and then thrombus formation (Varga-Szabo *et al.*, 2008b; Bergmeier *et al.*, 2009; Braun *et al.*, 2009). The same mice were found to be protected against severe ischemic brain infraction compared to the wild-type mice (Varga-Szabo *et al.*, 2008b; Braun *et al.*, 2009).

It has also been demonstrated that knockdown of ORAI1 and STIM1 expression inhibited I_{CRAC}, proliferation, migration and angiogenesis in vascular endothelial cells and smooth muscle cells (Abdullaev *et al.*, 2008; Potier *et al.*, 2009; Li *et al.*, 2011). Moreover, high levels of ORAI1 and STIM1 mRNA and protein have been found in aortas of hypertensive rats suggesting that ORAI and STIM could be upregulated in hypertension (Giachini *et al.*, 2009a). Upregulation of ORAI1 and STIM1 expression has also been reported in platelets isolated from Type 2 diabetic patients (Zbidi *et al.*, 2009), which is in agreement with a previous study reporting that SOCE is enhanced in platelets from Type 2 diabetic patients (Saavedra *et al.*, 2004).

1.7.6.3 ORAI and STIM in cancer

ORAI1 and STIM1 have also been linked to cancer, as inhibition of these channels by RNA interference led to decreased breast tumour cell migration and invasiveness *in vitro* and metastasis *in vivo* (Yang *et al.*, 2009). STIM1 was originally identified as a potential tumour suppressor gene in melanoma and rhabdoid tumour cells (Sabbioni *et al.*, 1997), but overexpressed STIM1 with ORAI1 was reported to promote the invasiveness of non-tumorigenic breast cells (Yang *et al.*, 2009), suggesting that the role of STIM1 in cancer development is more complicated and could be cell specific. Moreover, expression of ORAI3 was increased in breast cancer tissues and cell line MCF-7 (Motiani *et al.*, 2010). The cancer cell proliferation was inhibited after the transfection with ORAI3 small interfering RNA (siRNA) (Faouzi *et al.*, 2010).

1.8 Oxidative stress and Ca^{2+} signalling

Several Ca^{2+} influx or efflux pathways or events are regulated by ROS, such as VOCs, intracellular Ca^{2+} release channels, Ca^{2+} pumps, and Ca^{2+} sparks (Cheng *et al.*, 1993; Droge, 2002; Yan *et al.*, 2006; Bogeski *et al.*, 2011). TRP and SOC channels have been reported to be regulated by ROS (Droge, 2002; Yan *et al.*, 2006; Hidalgo & Donoso, 2008; Xu *et al.*, 2008a; Bogeski *et al.*, 2011). Superoxide and H_2O_2 increase Ca^{2+} concentration in vascular smooth muscle cells and endothelial cells (Lounsbury *et al.*, 2000). These effects have been attributed to redox-dependent inositol trisphosphate-induced Ca^{2+} mobilization, increased Ca^{2+} influx, and decreased Ca^{2+}-ATPase activation (Lounsbury *et al.*, 2000; Ermak & Davies, 2002). Plasma membrane K^+ channels that control hyperpolarization-elicited relaxation of vascular smooth muscle cells are opened by mechanisms associated with thiol oxidation by ROS (Touyz & Schiffrin, 2000; Droge, 2002; Ermak & Davies, 2002).

The involvement of SOC channels in oxidative stress has been suggested. For instance, ORAI1 channel current was inhibited by H_2O_2 in human T lymphocytes (Bogeski *et al.*, 2010). In diabetic conditions, upregulation of TRPC1 and TRPC6 expression was demonstrated in the Goto-Kakizaki Type 2 diabetic rats (Mita *et al.*, 2010); the reduced TRPC6 expression was reported in cultured mesangial cells and in the glomeruli isolated from streptozotocin-induced diabetic rats (Graham *et al.*, 2007); and increased expression of TRPC4 was reported in diabetic human saphenous vein (Chung *et al.*, 2009). Although there are some reports addressing the regulation of oxidative stress on Ca^{2+} influx or TRPC channels in diabetes, the expression and function of ORAI and STIM in vascular endothelial cells and their regulation under diabetic conditions are still unknown.

1.9 Aims of the research project

The aim of this project is to understand the expression of store-operated Ca^{2+} channel molecules ORAI and STIM in blood vessels and their regulation by oxidative stress. To achieve this, the following experiments have been designed:

1. To detect the mRNA and protein expression of ORAI1-3 and STIM1-2 in human vascular endothelial cells and blood vessels and investigate the regulation by oxidative stress conditions using *in vitro* cell culture models. The oxidative stress is mimicked by incubation with high glucose, homocysteine and hydrogen peroxide. The expression of ORAI and STIM in samples from *in vivo* diabetic animal models and diabetic patients will also be used. Moreover, the underlying mechanism for Ca^{2+} signalling related gene regulation will be explored.

2. To study the effect of oxidative stress on SOCE in vascular endothelial cells using Ca^{2+} imaging. The functional contribution of ORAI channels to endothelial cell function will also be investigated using siRNA transfection.

3. Using whole-cell patch clamp recordings, the effect of oxidative stress on heterogeneously expressed ORAIs/STIM1 channels in HEK293 cells will be investigated. The effect of SOC blockers on ORAI isoforms will be examined.

4. The effect of oxidative stress on the mechanisms of store-operated channel activation by STIM1 clustering and intracellular movement will be studied using live-cell fluorescence imaging.

5. The role of hyperosmolarity on ORAI and STIM channel expression and activity.

Chapter 2

Materials and Methods

2.1 Materials

2.1.1 Chemicals and reagents

General salts and following chemicals and reagents were purchased from Sigma–Aldrich (Poole, UK) including TG, D-glucose, α-mannitol, 2-APB, DES, sodium azide, H_2O_2, $CaCl_2$, homocysteine (Hcy), cyclosporin A (CsA), Fura-PE3/AM, BAPTA, fetal calf serum (FCS), EGTA, trypsin, bromophenol blue, ammonium persulfate, albumin from bovine serum (BSA), acrylamide, ethidium bromide, glycerol, glycine, 4-(2-hydroxyethyl)-1-piperazineethanesulfonic acid (HEPES), paraformaldehyde, *N*,*N*,*N'*,*N'*- Tetramethylethylenediamine (TEMED), dimethyl sulfoxide (DMSO), tween-20, sodium dodecyl sulfate (SDS), vascular endothelial growth factor (VEGF), KODAK processing chemicals for autoradiography films (developer and fixer) and Tris base. Moloney murine leukaemia virus (M-MLV) reverse transcriptase, T4 DNA ligase, GoTaq®Green master mix, dNTP mix, blue/ orange 6× loading dye and DNA ladder 100 bp were purchased from Promega (Southampton, UK). SYBR®Green PCR master mix (2×) was purchased from Applied Biosystems (Paisley, UK), NucleoSpin® RNA II isolation kit from Macherey- Nagel (Duren, Germany), and PageRuler™Plus prestained protein ladder from Fermentas Life Sciences (Cambridge, UK). Random primers, ribonuclease (RNase) inhibitor, Lipofectamine™ 2000, UltraPure™ agarose and pcDNA/TO vector were purchased from Invitrogen (Paisley, UK), and nitrocellulose membrane (Amersham™ Hybond™-ECL) and enhanced chemiluminescence (ECL) western blotting detection system (Hyperfilm ECL Amersham™ ECL Plus) were purchased from GE Healthcare (Buckinghamshire, UK). VECTASTAIN® ABC kit was purchased from Vector Laboratories (Peterborough, UK), cell proliferation reagent WST-1 from Roche Diagnostics Ltd (West Sussex, UK), AssayMax Human Interleukin-6 (IL-6) ELISA (enzyme-linked immunosorbent assay) Kit from ASSAYPRO (Cambridge, UK) and Phusion High-Fidelity DNA polymerase from New England BioLabs (Hitchin, UK). QIAquick PCR Purification Kit, QIAquick Gel Extraction Kit and QIAprep Spin Miniprep Kit were purchased from QIAGEN (Crawley, UK).

2.1.2 Solutions

Ponceau S staining solution, radio-immunoprecipitation assay (RIPA) buffer concentrate and bovine skin collagen solution were purchased from Sigma–Aldrich. Hank's balanced salt solution (HBSS), phosphate buffered saline (PBS) solution, standard bath solution, Ca^{2+}-free standard bath solution and pipette solution were prepared in the lab and the components are given in Table 2-1.

Table 2-1 Solutions

Solution	Components (in mM)
HBSS	NaCl 137; KCl 5.4; NaH_2PO_4 0.34; K_2HPO_4 0.44; $CaCl_2$ 0.01; HEPES 10; D-glucose 8; pH adjusted to 7.4 using NaOH
PBS	NaCl 137; KCl 2.7; $Na_2HPO_4.12H_2O$ 10; KH_2PO_4 2; pH adjusted to 7.4 using HCl
Standard bath solution	NaCl 130; KCl 5; $MgCl_2$ 1.2; $CaCl_2$ 1.5; HEPES 10; D-glucose 8; pH adjusted to 7.4 using NaOH
Ca^{2+}-free standard bath solution	NaCl 130; KCl 5; $MgCl_2$ 1.2; EGTA 0.4; HEPES 10; D-glucose 8; pH adjusted to 7.4 using NaOH
Pipette solution	BAPTA 10; $MgCl_2$ 8; HEPES 10; Cs-methanesulfonate 145; pH adjusted to 7.2 using CsOH

2.1.3 Antibodies

Anti-human ORAI1, ORAI2, STIM1 and STIM2 were purchased from Alomone Labs (Jerusalem, Israel), anti-human ORAI3 from ProSci Inc (Poway, CA, USA), rabbit anti-β-actin from Santa Cruz Biotechnology Inc (Santa Cruz, CA, USA), and goat anti-rabbit immunoglobulin G (IgG)-horseradish peroxidase-secondary antibody was purchased from Sigma-Aldrich.

2.1.4 Primers

The primer sets for ORAI1, ORAI2, ORAI3, STIM1 and STIM2 were designed across introns to avoid the genomic DNA contamination and custom synthesized by Sigma-Genosys (Sigma-Aldrich). The sequence specificity for each primer was confirmed by BLAST (basic local alignment search tool) searching in the GenBank. The sequences are given in Table 2-2. Full-length ORAI1, ORAI2, ORAI3 and green fluorescent protein (GFP) coding regions were amplified using the primers given in Table 2-3.

Table 2-2 Primers for RT-PCR

Gene	Species	Accession No	F/R	Primer sequence (5' to 3')	T_m (°C)	Location	Size (bp)
β-actin	Human	NM_001101.3	F	ACAGAGCCTCGCCTTTGC	65.7	30-47	211
	Human	NM_001101.3	R	GGAATCCTTCTGACCCATGC	65.7	240-221	
	Mouse	NM_007393.3	F	TGTTACCAACTGGGACGACA	60	304-324	165
	Mouse	NM_007393.3	R	GGGGTGTTGAAGGTCTCAAA	59.94	468-449	
ORAI1	Human	NM_032790	F	AGGTGATGAGCCTCAACGAG	70.1	378-397	238
	Human	NM_032790	R	CTGATCATGAGCGCAAACAG	69.5	615-596	
	Rat	NM_001013982	R	CTGATCATGAGGGCGAACAG	65.8	491-510	
ORAI2	Human	NM_001126340	F	CATAAGGGCATGGATTACCG	66.7	296-315	210
	Human	NM_001126340	R	CGGGTACTGGTACTGCGTCT	67.8	505-486	
	Mouse	NM_178751.3	F	CACAAGGGCATGGATTACCG	67.3	193-212	210
	Mouse	NM_178751.3	R	AGGGTACTGGTACTTGGTCT	56.6	402-383	
ORAI3	Human	NM_152288.2	F	GGCTACCTGGACCTCATGG	58.9	306-324	176
	Human	NM_152288.2	R	GGTGGGTACTCGTGGTCACT	58.3	462-481	
	Mouse	NM_198424	F	GGCTACCTGGACCTTATGG	60.9	274-292	176
	Mouse	NM_198424	R	GGTGGGTATTCATGATCGTT	61.1	449-430	
	Rat	NM_001014024	F	GGCTACCTCGACCTTATGG	61.1	253-271	176
	Rat	NM_001014024	R	GGTGGGTATTCATGATCGCT	63.7	409-428	
STIM1	Human	NM_003156	F	TGTGGAGCTGCCTCAGTATG	58.41	995 -1014	183
	Human	NM_003156	R	AAGAGAGGAGGCCCAAAGAG	58.47	1177 - 1158	
	Mouse	NM_009287	F	TGTGGAGCTGCCACAGTATG	65.1	1024-1042	182
	Mouse	NM_009287	R	AAGAGAGGAGGCCCAAACAG	64.5	1205-1186	
STIM2	Human	NM_020860	F	CAGCCATCTGCACAGAGAAG	58.12	857 - 876	202
	Human	NM_020860	R	AGGTTCGTGCACTGCTATCC	58.75	1058 - 1039	
	Mouse	NM_001081103	F	TAGTCACCTGCACAGAGAAG	58.2	688-707	202
	Mouse	NM_001081103	R	AGTTTCATGAACTGCTATCC	55.8	889-870	

Table 2-3 Tagged primers for the PCR amplification of full length ORAI and GFP

Primer name	Sequence (5' to 3')
HindIII-GFP-F	TTTTAAGCTTCGCCACCATGGTGAGCAAGG
BamHI-GFP-R	TAGGATCCCTTGTACAGCTCGTCCATGC
BglII-ORAI1-F	AATAGATCTGCGGCGTGCTCCATGCATCC
EcoRI-ORAI1-R	ATGAATTCGGGCCTAGGCATAGTGGCTG
BglII-ORAI2-F	AGTAGATCTCCCACCATGAGTGCTGAGCTT
EcoRI-ORAI2-R	TAGAATTCCCTCACAAGACCTGCAGGCT
BamHI-ORAI3-F	TAGGATCCAGGATGAAGGGCGGCGAG
EcoRI-ORAI3-R	TATGAATTCTCACACAGCCTGCAGCTCC

2.1.5 Small interfering RNA

ORAI1 or ORAI2 or ORAI3 siRNAs were designed using the Ambion software (Invitrogen). The sequences are given in Table 2-4. Scrambled siRNA was purchased from Sigma–Aldrich.

Table 2-4 Sequences of small interfering RNAs for ORAI genes

siRNA	Strand	Sequence (5' to 3')
siORAI1	Sense	CGAGCACUCCAUGCAGGCGtt
	Antisense	CGCCUGCAUGGAGUGCUCGtt
siORAI2	Sense	CGUGCCUAUCGACCCCUCUtt
	Antisense	AGAGGGGUCGAUAGGCACGtt
siORAI3	Sense	AGCUUCCAGCCGCACGUCUtt
	Antisense	AGACGUGCGGCUGGAAGCUtt

2.2 Methods

2.2.1 Human blood vessels

Human aorta, left internal mammary artery (LIMA) and aorta samples were obtained from patients undergoing cardiac bypass surgery or renal surgery in East Yorkshire NHS Trust Hospitals. Ethical approval was obtained from Hull and East Yorkshire local ethical committee and patients gave informed consent in accordance with the Declaration of Helsinki. The samples were collected in cold HBSS and transported into the lab immediately. The connective tissue around blood vessels was carefully removed. Blood vessels were then cut into approximately 3 mm long segments with a sharp blade for RNA isolation or organ culture.

2.2.2 Culture of blood vessel segments

Human LIMA segments (see 2.2.1) were cultured in 35-mm culture dishes with DMEM/F-12+GlutaMax™-I (Invitrogen) containing 10% (v/v) FCS, 100 units/ml penicillin and 100 μg/ml streptomycin, with or without addition of the drugs, and kept in an incubator at 37 °C under 95% air and 5% CO_2 in a humidified atmosphere.

2.2.3 Diabetic mice samples

The streptozotocin (STZ)-induced Type 1 diabetic mice and Akita mice were maintained in Lund University and the use of the animal for research was approved by the Malmo/Lund Animal Care and Use Committee. Blood glucose level and body weight were measured at the start and the end of the experiment. The normal and diabetic kidney samples were collected and stored in a -80 °C freezer for RT-PCR or western blotting.

2.2.4 Cell culture

Endothelial cell culture: Human aortic endothelial cells (HAEC) were purchased from PromoCell (Heidelberg, Germany) and the human vascular endothelial cell line EA.hy926 was purchased from American Type Culture Collection (ATCC, Middlesex, UK). The cells were cultured in Endothelial Cell Basal Medium (PromoCell) supplemented with 10% FCS, 0.1 ng/ml recombinant human epidermal growth factor, and 1 ng/ml basic fibroblast growth factor.

Smooth muscle cell isolation and culture: Smooth muscle cells (SMCs) isolated from rat aorta and human saphenous vein were cultured in Minimum Essential Medium with nucleosides (GIBCO, Invitrogen) supplemented with 10% FCS and 100 units/ml penicillin and 100 μg/ml streptomycin. Eight-week-old male rats were killed by inhalation of CO_2 in accordance with the Schedule 1 in the Code of Practice of UK Animals Scientific Procedures Act 1986. The thoracic aorta was dissected out and the adventitia was carefully removed. The endothelium was removed by gently rubbing the luminal surface with a curved forceps. The smooth muscle layer was cut into 0.5 mm^2 segments and cultured in DMEM/F-12+GlutaMax™-I medium supplemented with 10% FCS, 100 units/ml penicillin and 100 mg/ml streptomycin for cell expansion. Smooth muscle cells were isolated from saphenous vein samples obtained from patients undergoing cardiac bypass surgery in East Yorkshire NHS Trust Hospitals. The medial layer was cut into small pieces (~2×3 mm) and incubated at 37 °C for 1 hour in HBSS containing 2 mg/ml collagenase and 4 mg/ml papain. After 3 washes in HBSS, the mixture was mechanically agitated with a fire-polished glass Pasteur pipette to release cells, which were then cultured in DMEM/F-12+GlutaMax™-I medium supplemented with 10% FCS, 100 units/ml penicillin and 100 mg/ml streptomycin for cell expansion (Xu *et al.*, 2006b).

Human Embryonic Kidney (HEK) cell culture: HEK293 T-REx cells (Invitrogen) were cultured in DMEM/F-12+GlutaMax™-I medium supplemented with 10% FCS, 100 units/ml penicillin and 100 mg/ml streptomycin.

All cells were maintained at 37 °C under 95% air and 5% CO_2 in a humidified atmosphere. The culture medium was first changed after 24 hours and then every 48 hours until the cells reached the desired confluence. The primary cultured endothelial cells and smooth muscle cells at 2-5 passages were used for experiments.

2.2.5 Reverse-transcriptase polymerase chain reaction (RT-PCR)

2.2.5.1 Total RNA isolation

Total RNA was extracted from both cells and tissues using the NucleoSpin RNA II kit. Cells were trypsinized and centifuged at 1,000 × g for 5 minutes. Cell pellet was used for total RNA isolation according to the manufacturer's protocol. Briefly, cell pellet was lysed by adding 350 µl lysis buffer and 3.5 µl β-mercaptoethanol. For tissue samples, tissue was cut into approximately 1 mm^3 pieces using sterile surgical scissors at 4 °C and the lysis buffer was added in a tube containing the pieces of tissue. The cell or tissue lysate was then filtered through a NucleoSpin® Filter after centrifugation at 11,000 × g for 1 minute and the homogenized lysate was mixed with 350 µl 70% (v/v) ethanol, loaded onto the NucleoSpin® RNA II column and centrifuged at 11,000 × g for 30 seconds. The silica membrane was desalted by addition of 350 µl membrane desalting buffer, followed by centrifugation at 11,000 × g for 1 minute and incubation with 95 µl rDNase reaction mixture at room temperature for 15 minutes. Then, the column was washed three times and RNA was eluted in 30 µl RNase-free H_2O after centrifugation at 11,000 × g for 1 minute.

The concentration of the extracted RNA was measured using a NanoPhotometer (IMPLEN, Munich, Germany). The purity of RNA was determined by the absorbance (optical density, OD) measured at 230 nm, 260 nm and 280 nm. The ratio of the OD at 260 nm and 280 nm and the one of the OD at 260 nm and 230 nm were used to assess the RNA purity. A value of 1.8- 2.0 for the 260/280 ratio and a value >2 for the 260/230 ratio indicated that the RNA is pure. Total RNA was aliquoted and stored at -80 °C for further use.

2.2.5.2 Reverse transcription

The RNA isolated from the samples was reverse transcribed with the M-MLV reverse transcriptase using random primers. The amount of 0.5 µg RNA was used for the reverse transcription (RT) reactions. The RT reaction tube contained 1 µl 10 mM random primers, 0.5 µg or 1 µg RNA and nuclease-free H_2O up to the volume of 13.5 µl. The mixture was placed at the thermocycler (Applied Biosystems) at 70 °C for 5 minutes and then rapidly on ice for 5 minutes. A volume of 5 µl 5× RT buffer, 5 µl 10 mM dNTP mix, 1 µl M-MLV reverse transcriptase and 0.5 µl RNase inhibitor were added to each RT reaction tube. The final reaction volume was 25 µl and the mixture was placed at the thermocycler at 37 °C for 1 hour incubation. The cDNA was stored at -20 °C for PCR analysis.

2.2.5.3 Polymerase chain reaction

Polymerase chain reaction (PCR) amplification was run on the thermocycler. Each reaction volume was 20 µl, which contained 10 µl GoTaq® Green Master Mix, 4.5 µl 1 pmol/µl forward primer, 4.5 µl 1 pmol/µl reverse primer (Table 2-2) and 1 µl cDNA (RT product). The PCR cycle consisted of an initial denaturation step of 95 °C for 5 minutes followed by 40 repeated cycles of 95 °C for 15 seconds denaturation, 59.5 °C for 30 seconds annealing and primer extension at 72 °C for 30 seconds, then final extension at 72 °C for 7 minutes. The housekeeping gene, β-actin, was detected as endogenous control, water was used as a non-template control and non-reverse transcribed samples were run in parallel to confirm that positive results were not due to amplification of genomic DNA.

2.2.5.4 Real-time PCR

Real-time PCR quantification was performed using the StepOne™ Real-Time PCR System (Applied Biosystems). The SYBR green method was used (Zipper *et al.*, 2004). The primer sequences are given in Table 2-2. Each reaction volume contained 5 µl of SYBR® green PCR master mix, 1 µl of 1 pmol/µl forward primer, 2 µl of 1 pmol/ µl reverse primer, 1 µl cDNA and 2.5 µl H_2O. The total reaction volume was 10 µl. The reactions in real-time PCR tubes or plates were sealed with stripped caps

or adhesive films. The PCR cycles consisted of an initial denaturation step of 94 °C for 5 minutes followed by 45 repeated cycles of 94 °C for 30 seconds denaturation, 54 °C for 45 seconds annealing and primer extension at 72 °C for 45 seconds, and a final extension step at 72 °C for 10 minutes. The melt curve analysis was performed for quality control and consisted of three steps; 95 °C for 15 seconds, 60 °C for 1 minute and 95 °C for 15 seconds. All the samples were examined in triplicates. The housekeeping gene, β-actin, was measured in parallel as an internal standard. Water was used as a non-template control and non-reverse transcribed samples were run in parallel to exclude the possibility of genomic DNA contamination.

2.2.5.5 Analysis of real-time PCR data

The $\Delta\Delta C_T$ method, also referred as comparative C_T method, is used for relative quantification for the real-time PCR results (Livak & Schmittgen, 2001). This method relates the signal of the target gene in a treatment group to that in the untreated/ control sample. Changes in expression of the target gene in a treated group compared to an untreated one, are measured relative to a reference gene in both treated and control group. A housekeeping gene, which is assumed to be uniformly and constantly expressed in all samples, is used as reference gene.

The SYBR green method was used in this study to measure the expression of the genes of interest in real-time. The fluorescence increase is measured in real time as the SYBR green dye binds to the increasing amount of DNA in the reaction tube. The fractional cycle number at which the amount of amplified target reaches a fixed threshold is known as the threshold cycle (C_T value) (Figure 2-1). The ΔC_T values of the treated and the untreated samples are calculated: $\Delta C_T = C_T$ (target gene) $- C_T$ (reference gene). The $\Delta\Delta C_T$ value is calculated: $\Delta\Delta C_T = \Delta C_T$ (treated sample) $- \Delta C_T$ (control/untreated sample). The amount of target, presented as the fold change in gene expression normalized to an endogenous reference gene and relative to the untreated control, is calculated using $2^{-\Delta\Delta C_T}$. The relative expression was analyzed using StepOne Software v2.0 (Applied Biosystems) and the threshold was set manually (Figure 2-1).

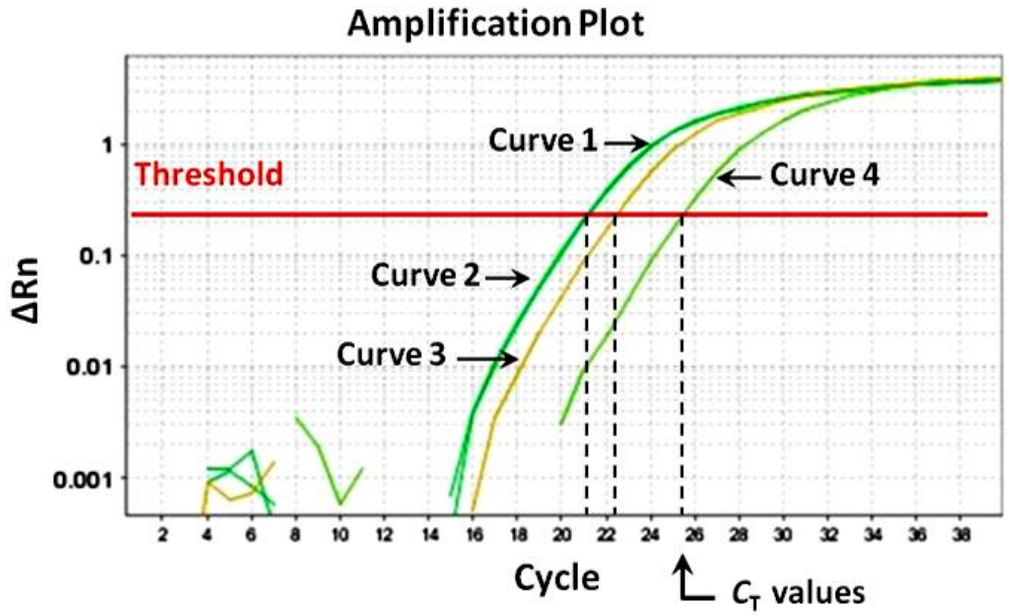

Figure 2-1 Example of real-time PCR amplification plots and analysis. The example data plot was exported from StepOne Software v2.0. The threshold cycle, called C_T value, is the cycle number at which the amount of amplified target reaches a fixed threshold. Δ*R*n is the magnitude of the fluorescence signal generated during the PCR at each cycle. The amplification plot curve 1 is the control gene (β-actin) in the untreated sample; curve 2 is the control gene (β-actin) in the treated sample; curve 3 is the target gene in the untreated sample, and curve 4 is the target gene in the treated sample. The expression of the control gene is similar in the treated and untreated samples. $C_{T\,1}$ = 21.92, $C_{T\,2}$ = 21.95, $C_{T\,3}$= 23.15, and $C_{T\,4}$ = 26.99. So, $\Delta C_{T\,(\text{treated sample})} = C_{T\,(\text{target gene})} - C_{T\,(\text{reference gene})} = 26.99 - 21.95 = 5.04$; $\Delta C_{T\,(\text{untreated sample})} = C_{T\,(\text{target gene})} - \Delta C_{T\,(\text{reference gene})} = 23.15 - 21.92 = 1.23$; $\Delta\Delta\, C_{T\,(\text{target})} = \Delta\, C_{T\,(\text{treated sample})} - \Delta\, C_{T(\text{untreated sample})} = 5.04 - 1.23 = 3.81$; and $\Delta\Delta\, C_{T\,(\text{control})} = \Delta\, C_{T\,(\text{untreated sample})} - \Delta\, C_{T(\text{untreated sample})} = 1.23 - 1.23 = 0$. The expression of the target gene, presented as the fold change in gene expression normalized to an endogenous reference gene and relative to the untreated control, is: $2^{-\Delta\Delta C_{T\,(\text{target})}} = 2^{-3.81} = 0.0713$ ($2^{-\Delta\Delta C_{T\,(\text{control})}} = 1$ always), suggesting that the target gene is downregulated after treatment by 0.9287 fold.

2.2.5.6 Agarose gel electrophoresis

The PCR products were checked for their quality through 1, 1.5 or 2% agarose gels containing 0.5 μg/ml ethidium bromide. The PCR products were mixed with blue/orange 6× loading dye that helps to track how far the DNA sample has run and also sediments it in the gel well. The PCR gel was photographed by a gel documentation system (UVP, Cambridge, UK).

2.2.6 Western blotting

All cells and tissues were lysed with RIPA buffer and the extracted protein lysates were run under dodecyl sulfate polyacrylamide gel electrophoresis (SDS-PAGE). Polyacrylamide gels comprising 4% acrylamide stacking gels (800 μl acrylamide 30%, 3.74 ml Tris 0.5 M pH 6.8, 50 μl SDS 10%, 3.74 ml dH_2O, 15 μl TEMED, 50 μl ammonium persulfate 10%) overlying 10% acrylamide resolving gels (6.7 ml acrylamide 30%, 5 ml Tris 1.5 M pH 8.8, 200 μl SDS 10%, 7.1 ml dH_2O, 32 μl TEMED, 72 μl ammonium persulfate 10%) were prepared to separate proteins. Protein soluble (15 μl) was loaded into each well, after cell lysates were heated at 95 °C in SDS sample buffer (4% SDS, 20% glycerol, 10% (v/v) β-mercaptoethanol, 50 mM Tris base, 0.012% bromophenol blue, pH 6.8) to linearise the proteins for 5 minutes. A volume of 3 μl of prestained protein ladder 10 kDa to 250 kDa was also loaded. SDS-PAGE running buffer (25 mM Tris base, 192 mM glycine, 0.1% SDS, pH 8.3) was added to a tank chamber and SDS-PAGE gels were then separated by electrophoresis at a constant voltage (90 V) for 15 minutes followed by 180 V for about 45 minutes to separate the protein bands.

The separated proteins in the SDS-PAGE gel were transferred onto a nitrocellulose membrane at constant voltage (15 V) for 45 minutes. The procedure involved the arrangement of a transfer cassette that included a piece of nitrocellulose membrane at a size of 5 × 7 cm, two fibre pads and the SDS-PAGE gel, all soaked in transfer buffer (25g Tris base, 192 mM glycine, 20% (v/v) methanol, pH 8.3). A pad was

placed on the apparatus suitable for the transfer and then the gel, the membrane and a second pad were placed sequentially.

For immunodetection, the transfer sandwich was disassembled and the nitrocellulose membrane was cut into the approximate dimensions of the gel. The uniformity and overall effectiveness of transfer of proteins from the gel to the membrane was checked by staining the membrane with 1% Ponceau S dye. The membrane was washed with Tris-buffered saline with tween-20 (TBST, 20 mM Tris base, 150 mM NaCl, 0.1% (v/v) tween-20, pH 7.4) for 5 minutes and then incubated in TBST containing 10% milk for 30 minutes at room temperature to block the non-specific binding sites. The membrane was then washed for 15 minutes with TBST.

Anti-human ORAI1-3 and STIM1-2 primary antibodies raised in rabbit were diluted 1:200 (0.2 μg/ml) in TBST buffer containing 1% BSA and 0.05% sodium azide. The blot was incubated with primary antibodies overnight at 4 °C, washed with TBST buffer twice at 15 minutes intervals and incubated with a goat anti-rabbit IgG-horseradish peroxidase-secondary antibody (1:2000 in TBST buffer containing 1% milk) for 1 hour at room temperature followed by three washings with TBST buffer at 10 minutes intervals.

Visualization was carried out using Amersham^{TM} ECL Plus western blotting detection system and exposure to X-ray films developed using KODAK processing chemicals. To develop the nitrocellulose membrane, ECL solutions were mixed and added to the membrane which was then shaken in the dark at room temperature for 5 minutes. Excess ECL solution was removed and the membrane was wrapped in cling film and placed in a developing cassette. In a dark room, a Hyperfilm ECL was exposed to the nitrocellulose membrane for an appropriate length of time depending on the amount of detected protein on the membrane. The exposed Hyperfilm ECL was then placed into a tray containing the developer (1:5) for 1 minute, rinsed into water, transferred to another tray containing the fixer (1:4) and rinsed again into water. The density of protein band in the blot was quantified using ImageJ software (National Institutes of Health, USA).

To detect β-actin protein as an internal standard for protein quantification, the membrane was washed twice with TBST buffer at 15 minutes intervals, then blocked

with TBST containing 10% milk for 30 minutes at room temperature, and finally incubated with 1:400 rabbit anti-β-actin in TBST containing 1% BSA and 0.1% sodium azide for 1 hour at room temperature. The antibody was removed and the membrane was washed with TBST buffer twice at 15 minutes intervals. The membrane was then incubated with the secondary antibody for 1 hour and developed as described in the previous paragraph. Rabbit antibodies were used for the detection of both target proteins (ORAI1-3, STIM1-2) and β-actin since the proteins could be distinguished on the blot by their different molecular weights.

2.2.7 Immunohistochemistry

Paraffin-embedded LIMA sections with a thickness of 5 μm were immunostained with rabbit anti-ORAI1-3 and anti-STIM1-2 antibodies using VECTASTAIN® ABC kit. All sections underwent deparaffinisation using xylene and endogenous peroxidase blocking using 3% (v/v) H_2O_2 in PBS for 20 minutes, along with blocking in non-specific serum to ensure the staining was specific (Bhandari *et al.*, 2008). ORAI1-3 and STIM1-2 primary antibodies at 1:250 dilutions were used and the tissue sections were incubated at 4 °C overnight followed by biotinylated anti-rabbit immunoglobulins at 1:1000 for 20 min. Incubation with antigen pre-absorbed antibodies or without primary antibody was used as a negative control. The sections were then incubated with the secondary antibody from the VECTASTAIN® ABC kit for 30 minutes, followed by peroxidase substrate solution until desired stain intensity develops. Some slides were counterstained with hematoxylin.

2.2.8 Molecular cloning of full length ORAI1-3 and plasmid construction

Full-length ORAI1, ORAI2 and ORAI3 coding regions were amplified by RT-PCR using the total RNA isolated from HAEC. The specific primers designed with restriction enzyme site were used. The primer sequences are given in Table 2-3. The PCR reaction contained 1× Phusion High-Fidelity buffer, 200 μM dNTPs (50 μM each), 0.5 μM of each primer, 10 ng/μl cDNA, and 0.02 units/μl Phusion High-Fidelity DNA polymerase. The PCR cycles consisted of an initial denaturation step

of 98 °C for 30 seconds, followed by 35 repeated cycles of 98 °C for 10 seconds denaturation, 68 °C for 30 seconds annealing and primer extension at 72 °C for 1 minute, and a final extension step at 72 °C for 5 minutes. The PCR products for ORAI1-3 were purified from the 1.5% agarose gel after electrophoresis. ORAI1 and ORAI2 were digested with BglII and EcoRI and cloned into pcDNA4/TO-mCherry vector cut by BamHI and EcoRI, and ORAI3 was digested with BamHI and EcoRI and cloned into pcDNA4/TO-mCFP vector. The ligated products were transformed into DH5α E. coli competent cells (Invitrogen, Paisley, UK). Colonies were screened by PCR using specific primers for ORAI1, ORAI2 and ORAI3. The positive colonies were selected and grown for plasmid cDNA isolation.

The coding sequences of enhanced yellow fluorescent protein (EYFP), monomeric red fluorescent protein (mCherry, RFP) and monomeric cyan fluorescent protein (mCFP) were amplified with the primers HindIII-GFP-forward and BamHI-GFP-reverse from the vectors pIRES-EYFP, RFP-C1 and mCFP-C3, respectively. Each PCR reaction tube contained 1× Phusion High-Fidelity buffer, 200 µM dNTPs (50 µM each), 0.5 µM forward primers, 0.5 µM reverse primers, 40 pg/µl template DNA, and 0.02 units/µl Phusion High-Fidelity DNA polymerase. The PCR cycles consisted of an initial denaturation of 98 °C for 30 seconds, followed by 35 repeated cycles of 98 °C for 10 seconds and 72 °C for 1 minute, and a final extension at 72 °C for 5 minutes. PCR products were analysed by electrophoreses on 1.5% agarose gel containing 0.5 µg/ml ethidium bromide and expected bands were purified using a QIAquick PCR Purification Kit.

The EYFP, mCherry and mCFP-encoding DNA fragments were ligated into the digested pcDNA4/TO plasmids with T4 DNA ligase at room temperature for 4 hours. The ligation mixtures were gently added to JM109 *E. coli* competent cells (Promega, Southampton, UK), the cells were then placed on ice for 30 minutes, heat-shocked at 42 °C for 1 minute, transferred into SOC medium (Invitrogen, Paisley, UK) and cultured at 37 °C for 1 hour in a shaking incubator (300 rpm). The cells were spread on LB agar plates containing 100 µg/ml ampicillin and incubated at 37 °C overnight. On the next day the bacterial colonies were picked into LB medium (Invitrogen, Paisley, UK) and cultured at 37 °C for 2 hours. Positive colonies were characterized by PCR using cell suspensions as templates. The PCR reaction volume

contained 1 µl cell suspension, 0.5 µM HindIII-GFP-forward and BamHI-GFP-reverse primers, and 1x GoTaq®Green master mix. The PCR cycles consisted of an initial denaturation of 95 °C for 30 seconds, followed by 30 repeated cycles of 94 °C for 30 seconds, 65 °C for 30 seconds and 72 °C for 45 seconds, and a final extension at 72 °C for 5 minutes. The colonies showing a 733-bp band in the PCR products were inoculated into 5 ml lysogeny broth medium containing 100 µg/ml ampicillin and cultured at 37 °C overnight in a shaking incubator (200 rpm). The plasmids were extracted using a QIAprep Spin Miniprep Kit. Small amount of cell suspensions were mixed into LB medium containing 20% glycerol and stored at -80 °C. The primer sequences are given in Table 2-3 and the pcDNA4/TO vector map is presented at Appendix I.

2.2.9 Transfection of ORAI and STIM plasmids into HEK-293 cells

HEK293 T-REx cells were seeded in a 35-mm culture dish and grown for 24 hours to reach 90% confluency. The plasmid cDNAs (STIM1-EYFP in pEYFP-N1 vector, mCherry-ORAI1, mCherry-ORAI2 and mCFP-ORAI3 plasmids in pcDNA4 vectors) were transfected into the cells using Lipofectamine™ 2000. The STIM1–EYFP plasmids in pEYFP-N1 vector were kindly provided by Prof AV Tepikin (University of Liverpool). Each plasmid cDNA (3 µg) and 5 µl Lipofectamine™ 2000 transfection reagent were separately mixed with 250 µl Opti-MEM (minimum essential medium) I Reduced Serum Medium (Invitrogen, Paisley, UK), and kept at room temperature for 5 minutes. The two mixtures were merged into one tube, shaken vigorously and then incubated at room temperature for 20 minutes to allow the mixture of plasmid cDNA and Lipofectamine™ 2000 to form complexes. During incubation, the DMEM/F-12+GlutaMax™-I medium was removed from the cell culture dish and replaced by 1 ml Opti-MEM medium. The plasmid-lipofectamine mixture was then gently dropped into the dish. The dish was rocked 2-3 times and moved into the incubator. The Opti-MEM medium was changed back to DMEM/F-12+GlutaMax™-I medium 6 hours later.

G418 was added into the cell culture dish to a final concentration of 400 µg/ml 24 hours after transfection. The cells were maintained for 1 week under G418 selection

and the medium was changed on every day for six days to remove dead cells. The survived cells were trypsinized and seeded into 60-mm culture dishes at a density of 500 cells/dish. Cells were cultured in medium without G418 and grew into clumps after 5-7 days.

After inspecting STIM1-EYFP expression under a Nikon Eclipse Ti-E inverted fluorescence microscope, cell clumps showing EYFP fluorescence (excitation/ emission wavelengths of 500/535 nm) were manually picked out from the dishes by 200-µl tips mounted on a pipette. These cells (in approximately 20 µl medium) were carefully transferred into 50 µl 0.05% trypsin/EDTA (ethylenediaminetetraacetic acid) solution and kept at room temperature for 3 minutes. Then the cells were mixed into DMEM/F-12+GlutaMax™-I medium and cultured as usual. The cells were stored in medium containing 10% (v/v) DMSO in liquid nitrogen when it is necessary.

Plasmids encoding mCherry-ORAI1, mCherry-ORAI2 and mCFP-ORAI3 were transfected into STIM1–EYFP cells and the expression of these genes was induced with 1 mg/ml tetracycline in the culture medium. The transfection and selection procedures were similar to these used for the generation of STIM1–EYFP cells.

2.2.10 Small interfering RNA transfection

ORAI1, ORAI2 or ORAI3 siRNA (Table 2-4) was transfected into HAEC using Lipofectamine™ 2000. For each transfection, 20 µM siRNA were diluted into 250 µl Opti-MEM I Reduced Serum Medium, and 5 µl of Lipofectamine™ 2000 were diluted into 250 µl Opti-MEM medium and the solutions were kept at room temperature for 5 minutes. The diluted siRNA was gently mixed with the diluted Lipofectamine™ 2000 and incubated for 20 minutes at room temperature to allow DNA-Lipofectamine™ 2000 complexes to form. The final concentration of siRNA was 20 pmol/µl. DNA-Lipofectamine™ 2000 complexes were then added to the dishes containing the cells and mixed gently. The dishes were shaken evenly after 3 hours and medium was changed after 6 hours incubation with the transfectants at 37 °C under 95% air and 5% CO_2 in a humidified atmosphere. The culture dishes with

scrambled siRNA were set as controls in parallel. Cell culture media (200 µl) were collected at the time points of 0 and 12 hours and stored at -20°C for IL-6 ELISA.

2.2.11 Ca^{2+} imaging and live-cell fluorescence imaging

For Ca^{2+} imaging experiments, EA.hy926 cells on coverslips were loaded with 1 µM Fura-PE3/AM for 30 min at 37 °C in standard bath solution, followed by 5 minutes wash in Ca^{2+}-free standard bath solution (Table 2-1) at room temperature. Cells were excited alternately by 340 and 380 nm light and emission was collected via a 510 nm filter. Images were sampled every 5 seconds in pairs for the two excitation wavelengths by an ORCA-R2 CCD camera (Hamamatsu, Japan). The ratio F_{340}/F_{380} of Ca^{2+} dye fluorescence, measured by a Nikon Ti-E system with NIS-Element Ca^{2+} imaging software, was used to represent the intracellular Ca^{2+} level. All experiments were performed at room temperature.

For live-cell fluorescence imaging, the stably transfected STIM1-EYFP cells were seeded on 13 mm diameter glass coverslips and cultured for 24–72 hours. Live cell images for EYFP/ mCherry/ mCFP fluorescence were captured using the microscope equipped with a Nikon Plan Fluor 100×/1.30 oil objective. The puncta around the PM with 1 mm thickness area (about one punctum) was counted as PM puncta. The fluorescence intensity of STIM1–EYFP was monitored by NIS-Elements software (Version 3.2, Nikon, Tokyo, Japan) and the regions of interest (ROIs) were drawn manually as the previous report (Zeng *et al.*, 2012). All experiments were performed at room temperature.

2.2.12 Whole-cell patch clamp recordings

Whole-cell patch-clamp recordings were performed on HEK293 T-REx cells expressing different ORAI cultured on 6-mm coverslips (Xu *et al.*, 2006b; Xu *et al.*, 2012). Patch pipettes were made from borosilicate glass capillaries and the resistance of the pipettes was 5-7 MΩ. The recording chamber had a volume of 150 µl and was perfused at a rate of about 2 ml/min. To deplete the internal Ca^{2+} store, TG at 1 µM

was added in the pipette solution (Table 2-1). The ORAI1 and ORAI2 channels were activated in standard bath solution (Table 2-1) containing 1 μM TG and ORAI3 channels were activated in bath solution containing 100 μM 2-APB. Membrane currents were measured using an Axopatch 200B patch clamp amplifier (Molecular devices, Union City, CA, USA). The data were acquired by Clampex 10.2 and analysed in Clampfit 10.2 (Molecular devices). A 1-s ramp voltage protocol from –100 mV to 100 mV was applied at a frequency of 0.1 Hz from a holding potential of –60 mV. Signals were sampled at 3 kHz and filtered at 1 kHz. The salt-agar bridge was used to connect the ground wire (Ag-AgCl) in the bath chamber. All the experiments were performed at room temperature (22-26°C).

2.2.13 Cell proliferation assay

Cell proliferation reagent WST-1, a salt tetrazolium that can be cleaved by cellular enzymes, was used in the cell proliferation studies. The assay reflects the metabolic activity of the cells. The overall metabolic activity measured by optical absorption correlates well with the viable cell number as determined by cell counting. Cells were cultured in 96-well plates containing 100 μl media and treated with drugs when they reached 30% confluency. After 48 hours of incubation with drugs, media were removed, cells were washed with DMEM/F-12+GlutaMax™-I media without phenol red and 100 μl WST-1/no phenol red containing media mixture was added to each well. WST-1 was finally added to each well. The absorbance was read on a microplate reader (BMG Labtech, Aylesbury, UK) at wavelengths of 450 nm and 605 nm after 2 hours of incubation with WST-1. The baseline was subtracted for each study and set at the time point that the drug was added.

2.2.14 Interleukin-6 ELISA

AssayMax Human IL-6 ELISA Kit was used for the detection of IL-6 secretion in cell culture media. This assay employs a quantitative sandwich enzyme immunoassay technique that measures IL-6. Each well was loaded with 50 μl of sample and the plate was covered and incubated for 2 hours, followed by 5 washing

steps with 200 µl of wash buffer. The plate was inverted and tapped dry on absorbent paper towel at each step. A volume of 50 µl biotinylated IL-6 antibody was added to each well and incubated for 2 hours. Five washings with 200 µl of wash buffer followed as above and 50 µl of streptavidin-peroxidase conjugate were then added to each well and incubated for 30 minutes. Five washings with 200 µl of wash buffer took place as above and 50 µl of chromogen substrate were then added to each well and incubated for approximately 12 minutes or till the optimal blue colour density developed. The absorbance was measured using a microplate reader at a wavelength of 405 nm.

2.2.15 Cell migration and tube formation assays

For cell migration assay, EA.hy926 cells were grown to confluence in 24-well plates in endothelial cell medium supplemented with 1% FCS. Base medium (10 ml) with any additives (high glucose or mannitol) was prepared, filtered, placed in sterile 15 ml falcon tubes and stored at 4 °C. Four separate wounds (2 horizontal and 2 vertical) were scratched through the cells in each well, using a sterile 200 µl pipette tip, resulting in a linear scrape of ~0.3 mm width through the pipette tip and cells. The cells were then rinsed carefully with PBS and cultured in 1.5 ml of warmed up endothelial cell medium containing 1% FCS with or without any additives. After 24 hours culture, the cells were fixed with 4% paraformaldehyde, photographed using an inverted microscope with a 10× objective, and the number of cells moving across the edge of the wound were counted.

For tube formation assay, bovine skin collagen was used and diluted into 1.5 mg/ml with extracellular matrix under 2-8 °C as working solution. The pH and osmolarity was adjusted by 1 M NaOH and 10× PBS, respectively. Human VEGF was added to a final concentration of 20 ng/ml to promote the proliferation and angiogenesis of vascular endothelial cells (Hoeben *et al.*, 2004). The collagen working solution at a volume of 120 µl was added to each well of 48-well plate, and allowed to gelatinize for 30 minutes at 37 °C. EA.hy926 cells were resuspended in extracellular matrix solution and added to each well at a volume of 300 µl (~3×10^4 cells/well) and incubated at 37 °C for 30 minutes under 95% air and 5% CO_2. Then, the cells were

treated with high glucose or vehicle. After 24 hours culture, cells were fixed with 4% paraformaldehyde, stained with 0.025% crystal violet, and photographed using an inverted microscope with a 20× objective. Four images per well were recorded. The angiogenic score was calculated for each image by a semi-quantitative method using the following formula as described in the report (Aranda & Owen, 2009):

$$\text{Angiogenic score} = \frac{[(\text{No.of sprouting cells})\times 1 + (\text{No.of connected cells})\times 2 + (\text{No.of polygons})\times 3]}{\text{Total No. of cells}} + (0, 1 \text{ or } 2).$$

This formula was designed to accurately emulate the degree of in vitro angiogenesis by taking into account the different steps observed during the procedure. A score of 1 point is given to each cell that shows projections which do not result in contact with other cells (sprouting). When two or more cells join by projections or direct cell contact, a score of 2 points is awarded to each cell involved in this process, and the formation of a polygon (enclosed structures) is given a score of 3 points. The total number of the cells present within the optical field is referred to as the 'total number of cells'. Score of 1 or 2 is added to the total value when luminal structures consisting of walls of two to three cells thick or walls of 4 or more cells thick are present, respectively. Absence of these structures is given no score (0).

2.2.16 Statistics

All data are presented as mean ± SEM (standard error of the mean) and *n* is the number of individual experiments. Data sets were compared using paired or unpaired Student's *t*-tests for two groups, and ANOVA (analysis of variance) Dunnett's post-hoc analysis was used for multiple group comparisons with significance indicated by * if $P < 0.05$, ** if $P < 0.01$ and *** if $P < 0.001$. The western blotting or PCR experiments are representative of at least 3 independent experiments.

Chapter 3

Expression of Store-Operated Ca^{2+} Channel Molecules ORAI and STIM and the Regulation by Oxidative Stress

3.1 Introduction

ORAIs and STIMs are recently identified store-operated Ca^{2+} channel molecules, which play essential roles in cell functions from gene expression to cell growth (Zhang, 2005; Prakriya *et al.*, 2006). ORAI channels are ubiquitously expressed in the body, but the expression level may vary depending on cell type. Dysfunction of ORAI channels is related to some diseases, such as the mutation of ORAI1 channel and STIM1 have been reported to cause severe combined immune deficiency syndrome due to the loss of I_{CRAC} or SOC in the T-cells (Picard *et al.*, 2009; Feske, 2011). The ORAI1 knockout mice showed resistance to pathological thrombus formation due to the malfunction of platelet without SOC (Braun *et al.*, 2009).

Oxidative stress is an important pathophysiological mechanism for endothelium dysfunction in diabetes. Hyperglycemia and hyperhomocysteinemia are two common cardiovascular risk conditions related to oxidative stress or the overproduction of ROS, which triggers a range of pathophysiological responses in the vascular endothelial cells and ultimately lead to the vascular injury and atherosclerosis (Ma, 2010).

Hyperglycemia is a common uncontrolled disease condition that causes overproduction of ROS that play a central role in the onset, progression, and pathological consequences of Type 1 and Type 2 diabetes or diabetic complications (Mene *et al.*, 1997; Zhang *et al.*, 2007). The role of Ca^{2+}-permeable channels in the pathophysiology of diabetes or hyperglycemia has been described (Kimura *et al.*, 1998a; Kimura *et al.*, 1998b; Pieper & Dondlinger, 1998; Tamareille *et al.*, 2006). For instance, TRPC1 expression was increased by high glucose in bovine aorta endothelial cells (Bishara & Ding, 2010), but TRPC6 expression was decreased in the cultured mesangial cells (Graham *et al.*, 2007). The regulation of transient receptor potential melastatin 6 (TRPM6) and TRPM7 by high glucose has been reported in human monocytes (Wuensch *et al.*, 2010). However, the regulation of high glucose or hyperglycemia on the expression of ORAIs and STIMs is not fully understood.

Hyperhomocysteinemia is another oxidative stress-related pathophysiological condition. High level of Hcy has been implicated in endothelial dysfunction and

atherosclerosis, which has been regarded as an independent risk factor for CVDs (Boushey *et al.*, 1995; Mayer *et al.*, 1996; Mangiagalli *et al.*, 2004). Hyperhomocysteinemia occurring in diabetes and Hcy level in the blood were decreased after glycemic control was improved in Type 2 diabetic patients (Passaro *et al.*, 2003). The mechanism of Hcy-induced oxidative stress is still unclear, but the increased ROS production through the regulation of redox system in the body, such as NADPH oxidase and thioredoxin system, has been suggested (Tyagi *et al.*, 2005). Store-operated Ca^{2+} entry was inhibited by high concentrations of Hcy in human umbilical vein endothelial cells (HUVECs) (Zhang *et al.*, 2005), but the effects of Hcy on the expression of ORAIs and STIMs and the channel activity of ORAI1-3 are still unknown.

H_2O_2 is a typical ROS in a cell. ORAI1 current was inhibited by H_2O_2, but ORAI3 current was not affected (Bogeski *et al.*, 2010). The differential sensitivity could be due to the extracellular cysteine (Cys^{195}) in ORAI1, which acts as the target for oxidation, but ORAI3 has no such cysteine in the region. Moreover, Ca^{2+} influx may be increased by H_2O_2 through TRPM2 (Grupe *et al.*, 2010) or TRPC3 and TRPC4 channels (Poteser *et al.*, 2006). These observations suggest that several Ca^{2+}-permeable channels are regulated by H_2O_2, and thus the oxidative stress-induced Ca^{2+} influx could have multiple mechanisms.

In this chapter, I aimed to investigate: 1) the gene expression of ORAI1-3 and STIM1-2 in human vascular tissues or cells including endothelial cells, smooth muscle cells, and blood vessel samples (aorta, LIMA and saphenous vein) from patients; 2) the regulation on the expression of ORAIs and STIMs by oxidative stress conditions including high glucose, Hcy and H_2O_2 using *in vitro* cell or organ culture models and *in vivo* tissue samples from patients and diabetic mice; 3) the potential underlying mechanism for ORAI and STIM gene regulation.

3.2 Expression of ORAI and STIM in human blood vessels

The mRNAs of ORAI1, ORAI2, ORAI3, STIM1 and STIM2 were detected by RT-PCR in human blood vessels including LIMA, saphenous vein and aorta, and primary cultured HAECs, vascular endothelial cell line EA.hy926, and primary cultured smooth muscle cells from human saphenous vein using the primers given in Table 2-2. The β-actin was used as positive control and the reaction without reverse transcriptase (no RT) was set as negative control (Figure 3-1).

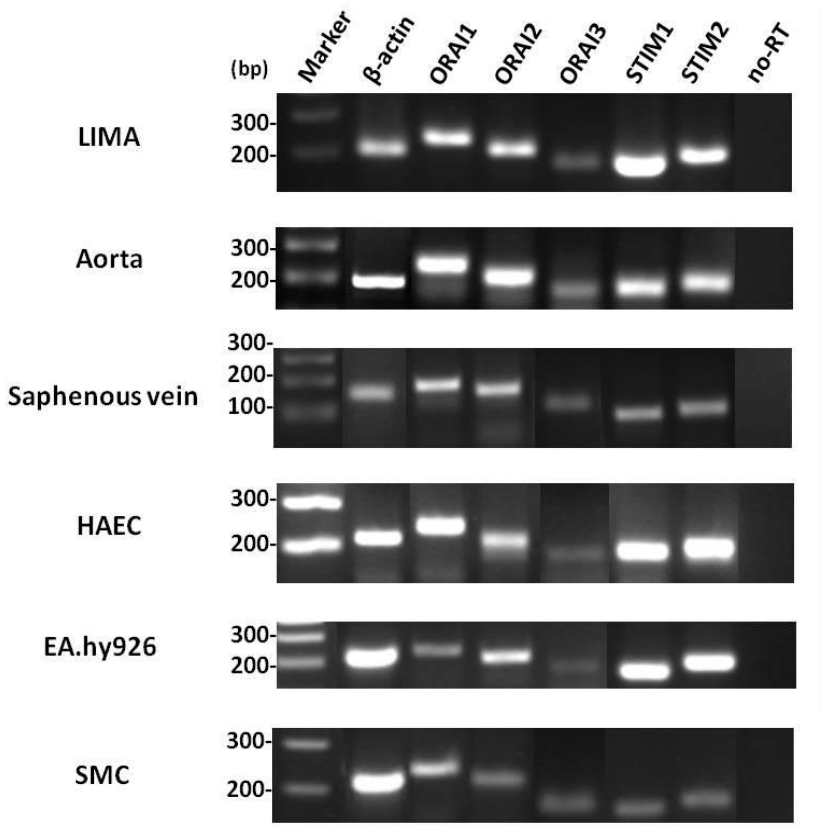

Figure 3-1 Detection of ORAI and STIM mRNAs in human blood vessels and cells. PCR products were shown in the 2% agarose gel stained with ethidium bromide. The expected size of PCR amplicons is 238 bp for ORAI1, 210 bp for ORAI2, 176 bp for ORAI3, 183 bp for STIM1, 202 bp for STIM2 and 211 bp for β-actin. No product was detected in the reaction without reverse-transcriptase (no-RT). LIMA; Left internal mammary artery, HAEC; Human aortic endothelial cells, SMC; Smooth muscle cells isolated from human saphenous vein.

ORAI and STIM proteins in the lysates of HAEC, EA.hy926 cells and human LIMA were examined by western blotting (Figure 3-2). The protein bands for ORAI1 (~33 kDa), ORAI2 (~29 kDa), ORAI3 (~31 kDa), STIM1 (~75 kDa) and STIM2 (~100 kDa) were detected (Figure 3-2A). The β-actin (~43 kDa) was used as positive control and the specificity of the antibodies used in this study was confirmed by using the lysates from HEK293 cells overexpressing ORAI1 and ORAI2 channels tagged with fluorescent protein mCherry, and the cells overexpressing STIM1 tagged with EYFP (Figure 3-2B).

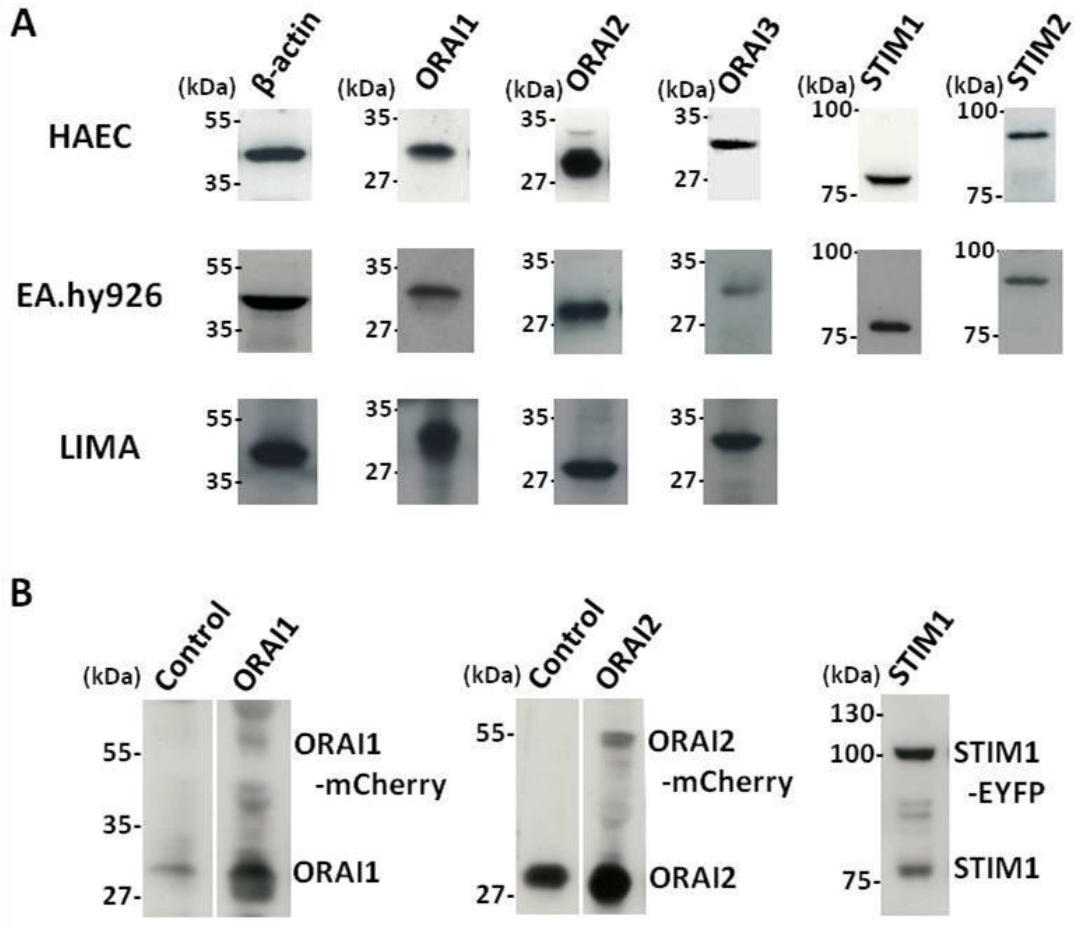

Figure 3-2 ORAI and STIM proteins detected by western blotting. A, Detection of ORAI1-3 and STIM1-2 proteins in human aortic endothelial cells (HAEC), EA.hy926 cells and human left internal mammary artery (LIMA). β-actin was used as positive control. **B,** Detection of ORAI1, ORAI2, and STIM1 in the HEK293 T-REx cells overexpressed with ORAI1-mCherry, ORAI2-mCherry and STIM1-EYFP. The non-transfected cells were used as control. The size of tagged mCherry fluorescent protein is 25.96 kDa and the enhanced yellow fluorescent protein (EYFP) is 26.29 kDa.

The localization of ORAI and STIM channels was examined by immunostaining on the paraffin-embedded human LIMA sections. The staining was positive in the smooth muscle layer and the endothelium (Figure 3-3), suggesting these genes are ubiquitously expressed in vascular endothelial cells and smooth muscle cells. No staining was observed in the negative control group with boiled primary antibodies.

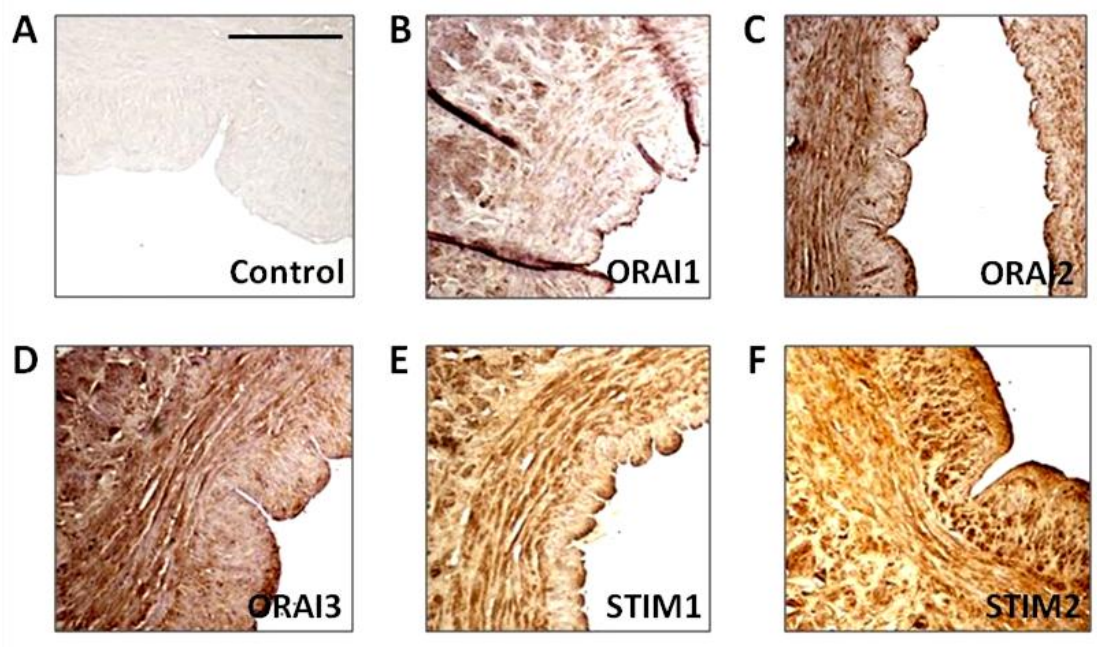

Figure 3-3 Localization of ORAIs and STIMs in human left internal mammary arteries. Immunostaining for ORAI1 (B), ORAI2 (C), ORAI3 (D), STIM1 (E) and STIM2 (F) on paraffin-embedded sections of LIMA using the Vectashield ABC kit with diaminobenzidine substrate. Positive staining shown as brown colour. The boiled primary antibody was set as negative control (Control) (A). The results were reproducible in the human LIMA samples from three patients. Scale bar is 100 µm.

3.3 Regulation of ORAI and STIM expression by high glucose in *in vitro* models

In this section, three sets of experiments were designed to observe the effect of high glucose (25 mM glucose) on the expression of ORAIs and STIMs in endothelial cells, smooth muscle cells and organ cultured blood vessel segments.

3.3.1 Effect of high glucose on the expression of ORAIs and STIMs in endothelial cells

Vascular endothelial EA.hy926 cells were cultured in endothelial medium and treated with 25 mM glucose for 60 hours. The equal molar mannitol was used as control. The mRNA level was quantified by real-time PCR. As demonstrated in Figure 3-4A, the mRNAs of ORAI1, ORAI2, ORAI3, STIM1 and STIM2 were significantly increased after the incubation with 25 mM glucose for 60 hours.

The protein expression of ORAI and STIM isoforms was also examined by western blotting. The band density of ORAIs and STIMs in the high glucose-treated group was significantly higher than the group treated with mannitol (Figure 3-4 B-C). These data suggested that high glucose upregulated the mRNA and protein expression of ORAIs and STIMs in the vascular endothelial cells.

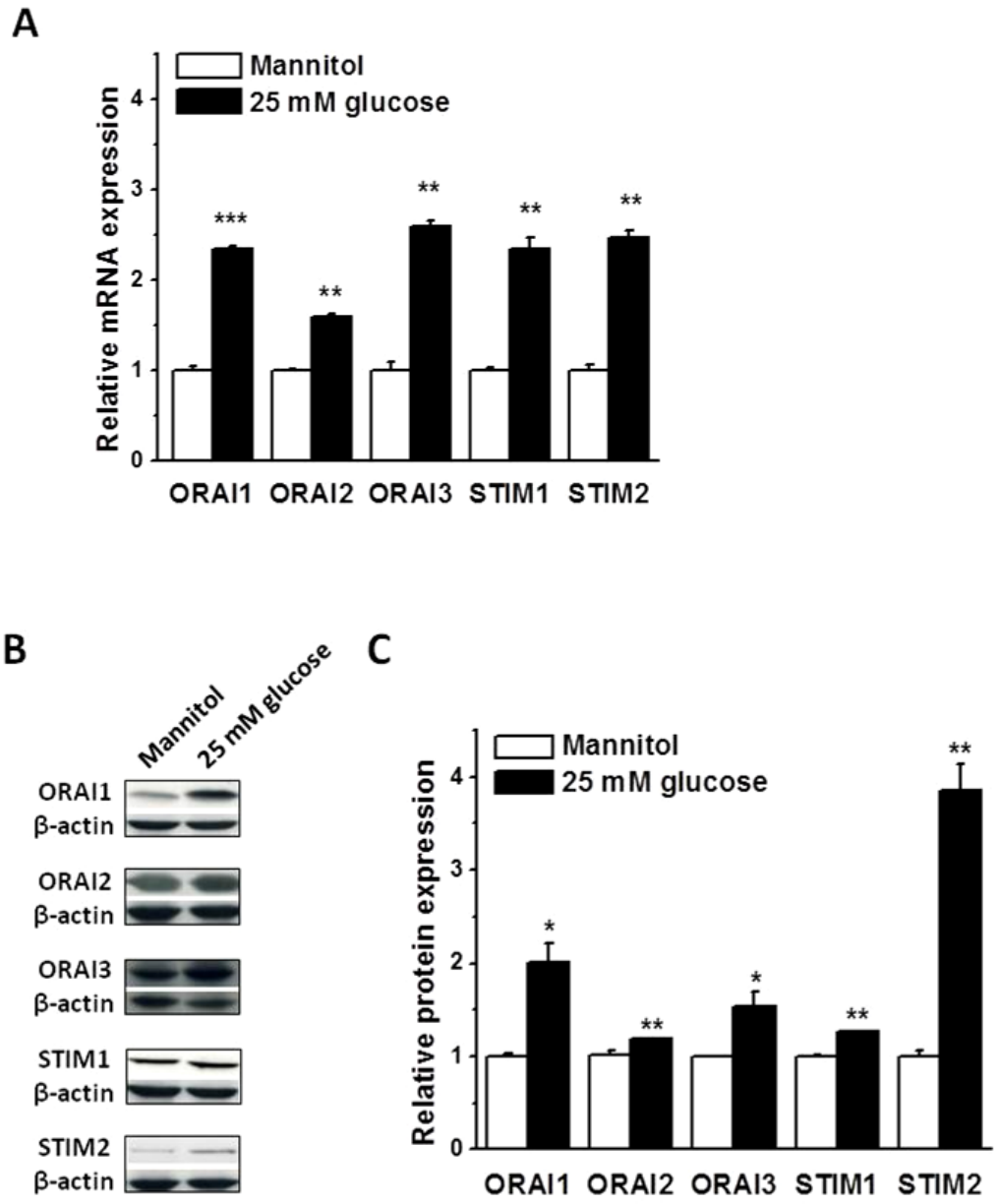

Figure 3-4 Upregulation of ORAI and STIM expression by high glucose. EA.hy926 cells were cultured with high glucose (25 mM) for 60 hours. The mannitol (19.5 mM) plus 5.5 mM glucose was used as equal osmolarity control. The β-actin was used as housekeeping gene for relative quantification. **A,** The mRNA of ORAIs and STIMs was quantified by real-time PCR. The mean data were obtained from three independent experiments and the triplicate PCR reactions were set for each experiment. **B,** Examples of ORAI1-3 and STIM1-2 detected by western blotting. **C,** The density of protein bands was quantified using ImageJ software. Mean data from 3 independent experiments. *$P < 0.05$; **$P < 0.01$; ***$P < 0.001$

3.3.2 Effect of high glucose on the expression of ORAIs and STIMs in smooth muscle cells

The primary cultured human saphenous vein smooth muscle cells within 5 passages were used in the experiment. The cells were incubated with high glucose for 60 hours, and the normal glucose (5.5 mM) was set as control. The mRNA level of ORAI2, STIM1 and STIM2 was significantly upregulated, however, the expression of ORAI1 and ORAI3 was decreased (Figure 3-5A).

Due to the difference in high glucose regulation between endothelial cells and saphenous vein smooth muscle cells, expression was re-examined using rat aortic smooth muscle cells. The rat aortic smooth muscle cells grew much faster than the smooth muscle cells from human saphenous vein, and the cells at passage 2 were used in the experiment. The mRNA expression for ORAI1-3 and STIM1-2 was significantly increased in the cells cultured with high glucose for 60 hours comparing with the group treated with mannitol (Figure 3-5B), suggesting high glucose upregulated the expression of ORAIs and STIMs in the smooth muscle cells.

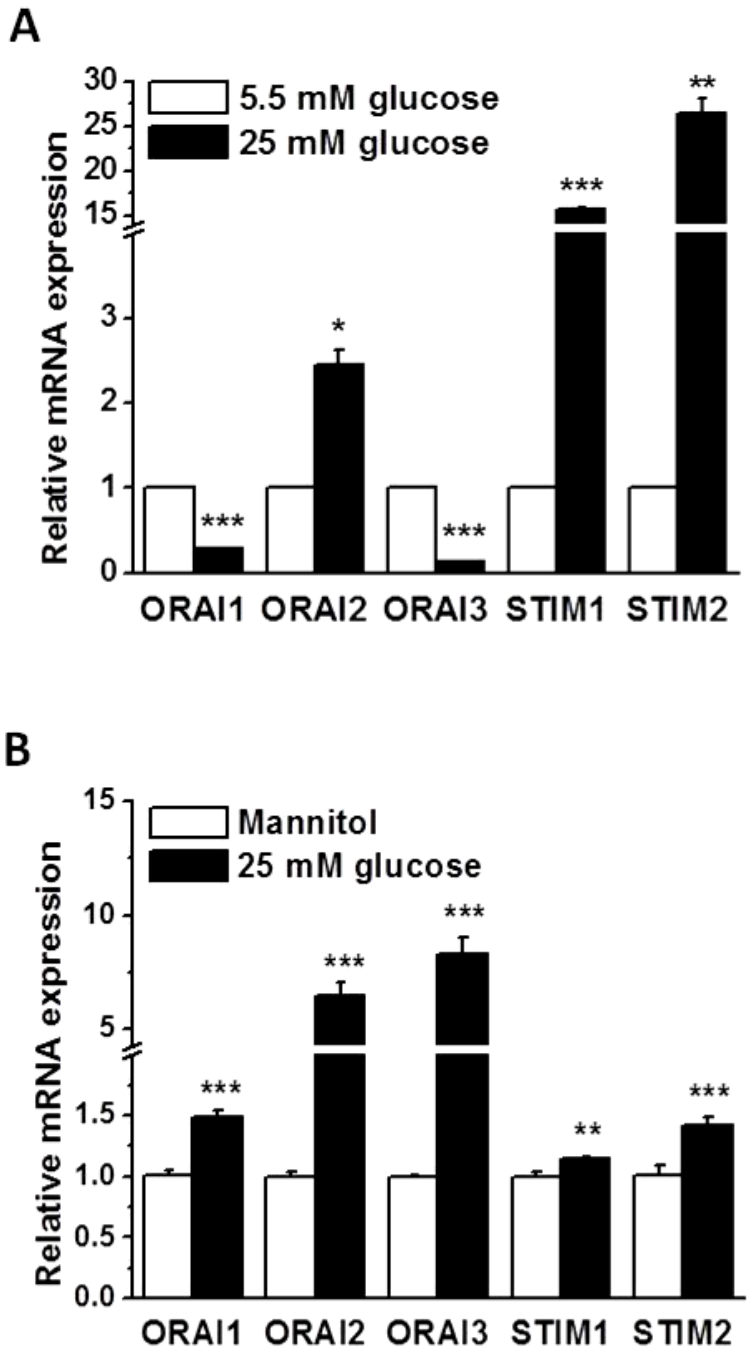

Figure 3-5 ORAI and STIM expression regulated by high glucose in smooth muscle cells. The mRNA level quantified by real-time PCR in (A) human saphenous vein smooth muscle cells and (B) rat aortic smooth muscle cells after treatment with 25 mM glucose for 60 and 48 hours respectively. The mannitol (19.5 mM) plus 5.5 mM glucose was used as equal osmolarity control. The β-actin was used as housekeeping gene for relative quantification. Mean data from 3 independent experiments with triplicate samples. *$P < 0.05$; **$P < 0.01$; ***$P < 0.001$

3.3.3 Effect of high glucose on the expression of ORAIs and STIMs in human blood vessels

LIMA segments from 5 non-diabetic patients (60.4 ± 0.8 years) were cultured under high glucose conditions for 60 hours. The blood vessel segments from same patients were cultured in normal (5.5 mM) glucose in parallel as control. The mRNA expression was detected by real-time PCR. The response of the ORAI and STIM gene expression to high glucose treatment varied among the different patients (Figure 3-6).

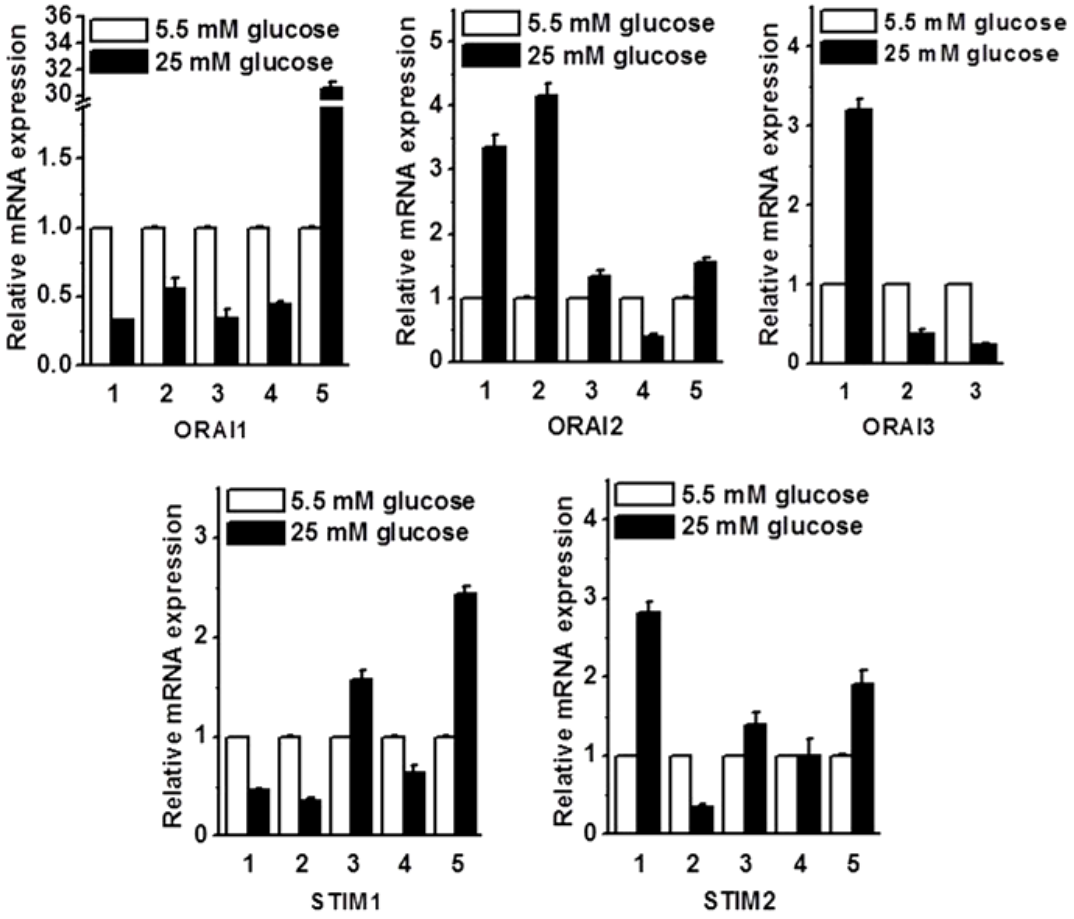

Figure 3-6 Regulation of ORAI and STIM expression by high glucose in organ-cultured human left internal mammary artery. The organ-cultured blood vessels were treated with normal (5.5 mM) and high (25 mM) glucose for 60 hours. The mRNA of ORAIs and STIMs was detected by real-time PCR. The triplicate RT-PCR reactions were performed for each patient. Numbers 1-5 indicate the patient code.

3.4 Regulation of ORAI and STIM expression in diabetes

To further examine the expression of ORAI and STIM in *in vivo* conditions, the aorta samples from Type 2 diabetic patients and kidney samples from Type 1 diabetic mouse models were tested.

3.4.1 Human aorta samples from patients with Type 2 diabetes

Human aorta samples from 4 male Type 2 diabetic (56.7 ± 2.7 years) and 4 male age-matched non-diabetic patient controls (58.5 ± 3.5 years) were used in this study. There was no significant difference in body mass index (BMI, 30 ± 1.6 *vs* 30 ± 2.0 kg/m^2, $P > 0.05$). The mRNA expression of ORAI and STIM isoforms was determined by quantitative real-time PCR using the primers in Table 2-2. Both ORAI and STIM mRNA expression were significantly increased in the diabetic samples (Figure 3-7).

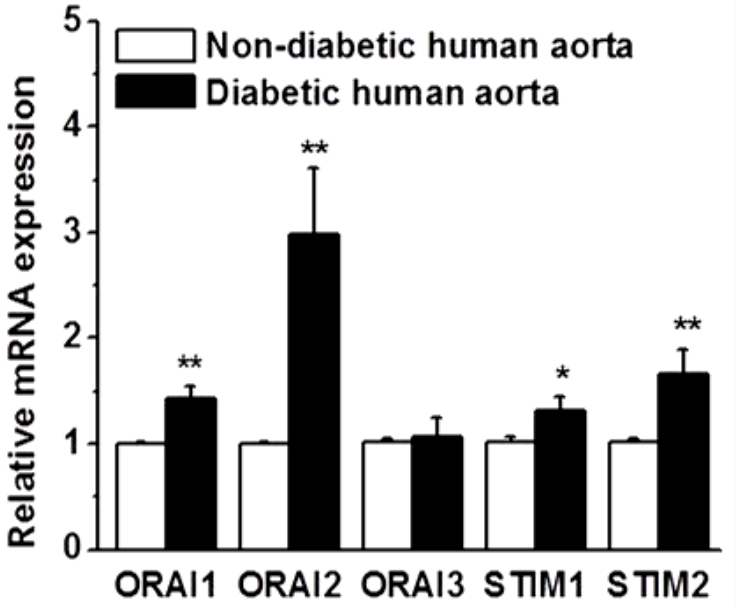

Figure 3-7 ORAI and STIM expression in human aorta. ORAI and STIM expression detected by real-time PCR was increased in aorta samples from diabetic patients (n = 4). Age-matched aorta samples from non-diabetic patients were used as a control (n = 4). The β-actin was used as housekeeping gene for relative quantification. The triplicate RT-PCR reactions were performed for each sample. *P < 0.05; **P < 0.01

3.4.2 Type 1 diabetic mouse models

Since the availability of clinical tissue samples from patients with Type 1 diabetes, the gene regulation was investigated using Type 1 diabetic models. In addition, the vascular tissues in the mouse is very limited, so the kidney samples from STZ-induced diabetic mice and Akita Type 1 diabetic mice were used in the following experiments.

STZ-induced diabetic mice: The STZ-induced Type 1 diabetic mice were used (Table 3-1). The high blood glucose level was developed in the STZ-treated mice after 8 weeks injection of STZ. The body weight of the STZ-treated mice was significantly reduced. The expression of ORAI1-3 and STIM1-2 mRNAs was significantly increased in the kidney samples from STZ-treated mice comparing to control mice (Figure 3-8).

Table 3-1 Blood glucose level and body weight in streptozotocin-induced Type 1 diabetic model

Treatment	n	Start	Final	n	Start	Final
		Vehicle			Streptozotocin	
Blood glucose (mM)	6	9.11±0.33	7.99±0.28	6	9.21±0.39	21.48±1.2***
Weight (kg)	6	23.91±1.6	31.30±1.00	6	22.20±1.3	26.49±0.62***

*** $P < 0.001$, Comparison between the control (vehicle) and streptozotocin-treated mice group.

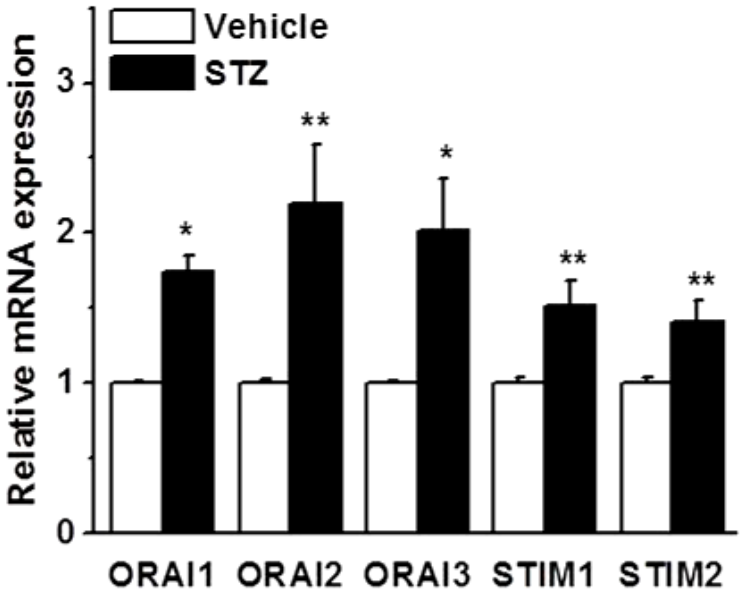

Figure 3-8 ORAI and STIM expression in the kidney from streptozotocin-induced Type 1 diabetic mice. The mRNA of ORAIs and STIMs detected by real-time PCR was increased in kidney samples from streptozotocin (STZ)-treated diabetic mice (n = 6) compared to the kidney samples from the control mice treated with vehicle (n = 6). The β-actin was used as housekeeping gene for relative quantification. The triplicate RT-PCR reactions were performed for each sample. *P < 0.05; **P < 0.01

Akita Type 1 diabetic mice: The Akita mice model is a genetic Type 1 diabetic animal model without significant body weight loss (Yoshioka *et al.*, 1997). Therefore this model was used to further examine the store-operated channel gene expression in Type 1 diabetes. Six Akita mice were used and 6 wild-type mice at the same age were used as control. Blood glucose level and body weight were measured at the start and the end of the experiment (Table 3-2). Akita mice developed significant hyperglycemia, however, the weight of the mice measured at the start and the end of the experiment was similar to that of the wild-type control mice. The mRNA expression of ORAI and STIM isoforms was determined by quantitative real-time PCR using the primers in Table 2-2. ORAI and STIM mRNA expression was significantly higher in the kidney samples from Akita mice than that in the wild-type mice (Figure 3-9).

Table 3-2 Blood glucose level and body weight in Akita Type 1 diabetic model

	n	**Start**	**Final**	**n**	**Start**	**Final**
		Wild-type			Akita	
Blood glucose (mM)	6	7.99±0.99	8.01±1.27	6	21.90±1.91	21.38±1.92***
Weight (kg)	6	18.29±0.42	18.86±0.73	6	18.00±0.75	18.71±0.80

*** $P < 0.001$, Comparison between the control (wild-type) and Akita mice group.

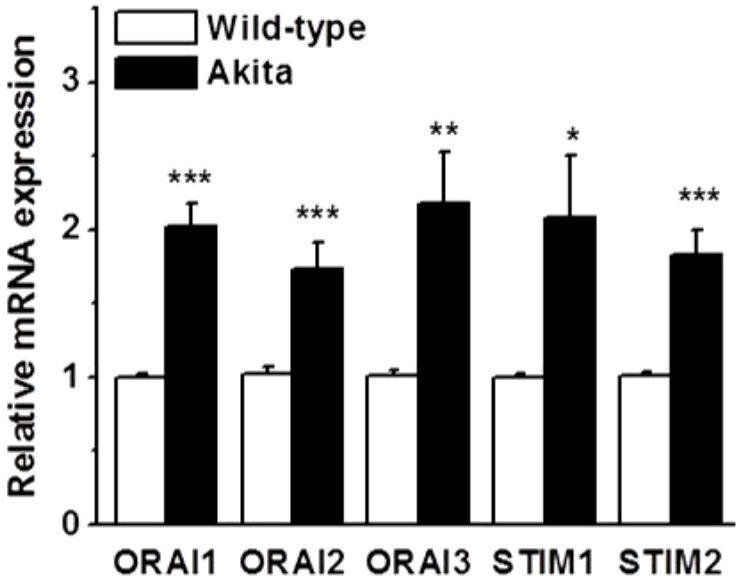

Figure 3-9 ORAI and STIM mRNA expression in the kidney tissues from Akita Type 1 diabetic mice. The mRNA of ORAIs and STIMs detected by real-time PCR was increased in kidney samples from Akita diabetic mice (n = 6) compared to the wild-type mice (n = 6). The β-actin was used as housekeeping gene for relative quantification. The triplicate RT-PCR reactions were performed for each sample. *P < 0.05; **P < 0.01; ***P < 0.001

3.5 Upregulation of ORAI and STIM by high glucose is mediated by calcineurin/ NFAT signalling pathway

To understand the underlying mechanism of ORAI and STIM upregulation by high glucose, the potential role of Ca^{2+}/calcineurin/NFAT signalling pathway was examined, because gene transcription may be affected by the increased intracellular Ca^{2+} through this pathway (Hogan *et al.*, 2003). Using primary cultured rat aortic smooth muscle cells, the expression of ORAI1-3 and STIM1-2 was increased in the cells treated with high glucose. Cyclosporin A (CsA) is a potent calcineurin inhibitor (Crabtree, 2001). The high glucose-induced upregulation of ORAIs and STIMs was prevented by incubation with CsA at 200 nM for 48 hours. On the other hand, the expression of ORAI1-3 was inhibited by application of CsA alone, but no significant effect on STIM1 and STIM2 was observed (Figure 3-10).

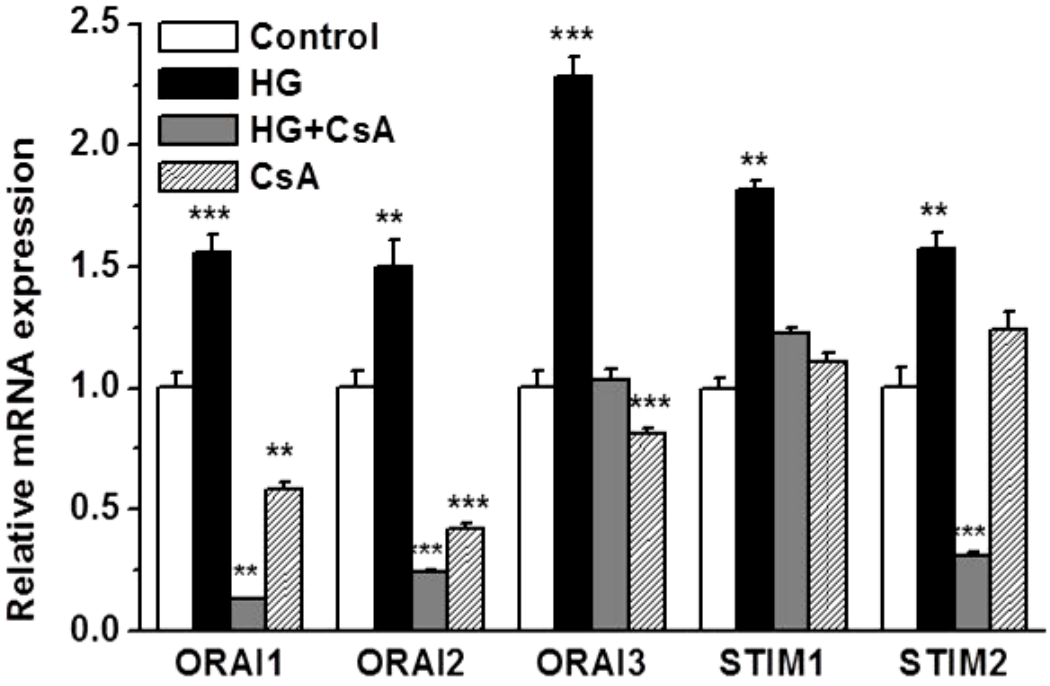

Figure 3-10 Inhibition of high glucose-induced upregulation of ORAI and STIM expression by cyclosporin A. Rat aortic smooth muscle cells were cultured with high glucose (HG, 25 mM), cyclosporin A (CsA, 200 nM), and high glucose plus CsA for 48 hours. The mRNA of ORAIs and STIMs was detected by real-time PCR. The β-actin was used as housekeeping gene for relative quantification. Mean data from 3 independent experiments with triplicate samples. * $P < 0.05$; ** $P < 0.01$; *** $P < 0.001$

The effect of store-operated channel blocker on gene expression was also examined. DES has been shown to block the store-operated Ca^{2+} influx and thus reduce the intracellular Ca^{2+} level (Zakharov *et al.*, 2004). Incubation with DES 10μM for 48 hours significantly reduced the expression of ORAI1-3. However, the expression of STIM1-2 was not changed (Figure 3-11).

These data suggested that the upregulation of ORAIs and STIMs by high glucose is mediated by Ca^{2+}/calcineurin/NFAT signalling pathway.

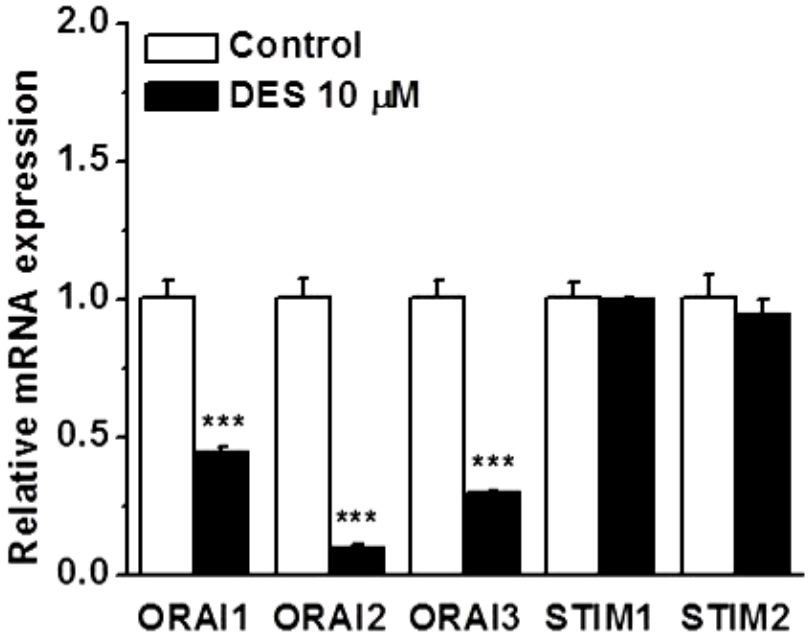

Figure 3-11 Regulation of ORAI and STIM expression by diethylstilbestrol. Rat aortic smooth muscle cells were cultured with diethylstilbestrol (DES) 10 μM for 48 hours. Untreated cells were used as control. The mRNA of ORAIs and STIMs was detected by real-time PCR. The β-actin was used as housekeeping gene for relative quantification. Mean data from 3 independent experiments with triplicate samples. ***$P < 0.001$

3.6 ORAI and STIM expression regulated by homocysteine

The regulation of ORAI and STIM expression by Hcy was observed in the primary cultured human aortic endothelial cells. The mRNA and protein levels of ORAI and STIM isoforms were determined by real-time PCR and western blotting.

The mRNA level of ORAI1, ORAI2 and ORAI3 was significantly downregulated by incubation with 1-100 μM Hcy for 24 hours, but the STIM1 and STIM2 mRNA levels were significantly increased after Hcy treatment (Figure 3-12), suggesting that the effect of Hcy is different from the oxidative stress condition induced by high glucose treatment.

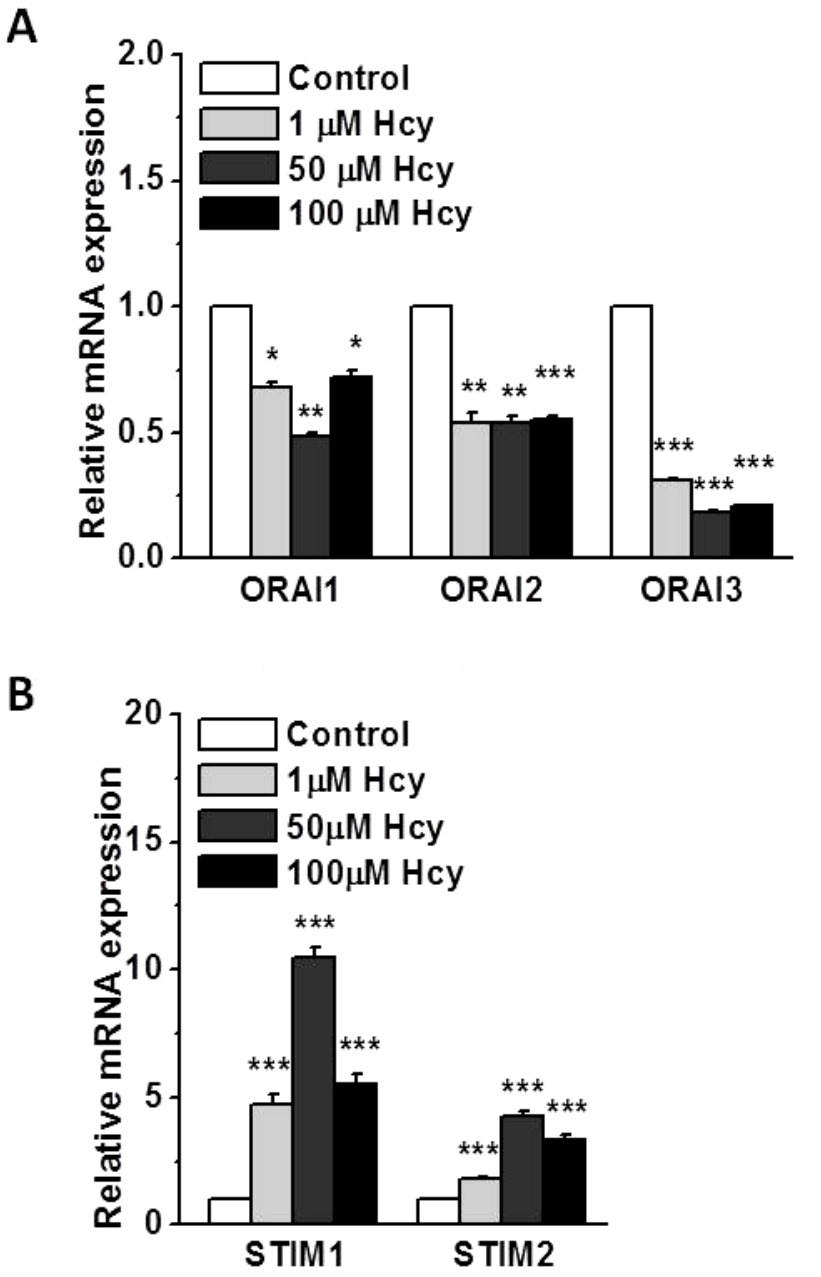

Figure 3-12 Regulation of ORAI and STIM mRNA expression by homocysteine. Human aortic endothelial cells were cultured with homocysteine (Hcy) for 24 hours. The mRNA of ORAIs (A) and STIMs (B) was quantified by real-time PCR. Untreated cells were set as control. The β-actin was used as housekeeping gene for relative quantification. The mean data were obtained from 3 independent experiments and the triplicate PCR reactions were set for each experiment. **P* < 0.05; ***P* < 0.01; ****P* < 0.001

The protein levels of ORAIs and STIMs in human aortic endothelial cells lysate were also examined by western blotting. The protein band density for ORAI1 and ORAI2 proteins was decreased after treatment with 10 μM and 50 μM Hcy, whereas the STIM1 and STIM2 protein levels were increased (Figure 3-13).

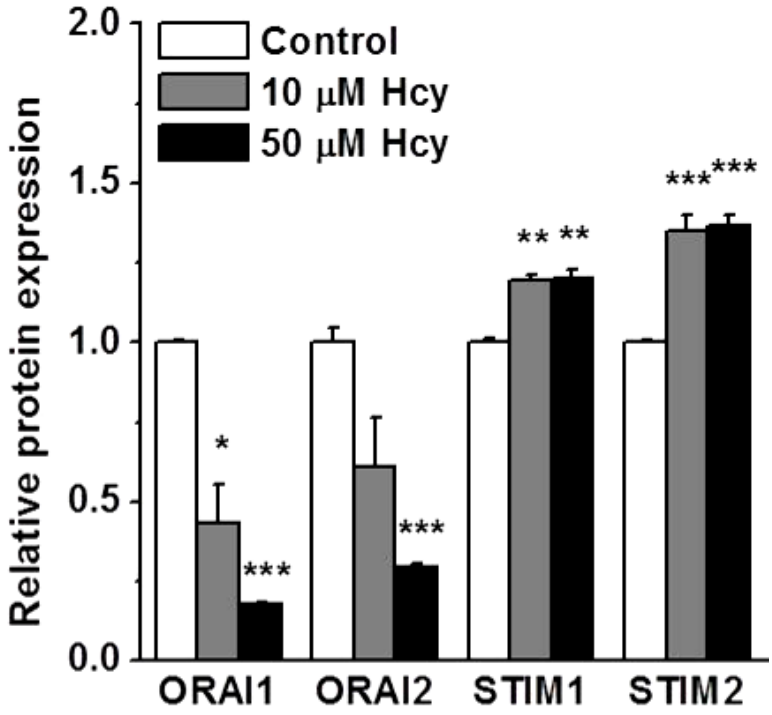

Figure 3-13 Regulation of ORAI and STIM protein expression by homocysteine. Human aortic endothelial cells were cultured with 10 μM or 50 μM homocysteine (Hcy) for 24 hours. Untreated cells were used as control. The density of protein bands detected by western blotting was quantified using ImageJ software. The β-actin was used as control for quantification. Mean data from 3 independent experiments are presented and triplicate protein lanes on the gel were set for each experiment. *$P < 0.05$; **$P < 0.01$; ***$P < 0.001$

3.7 ORAI and STIM regulated by H_2O_2

Due to the different effect of high glucose and Hcy on ORAI and STIM expression, the effect of H_2O_2 was also examined. The mRNA expression of ORAI1-3 and STIM1-2 was upregulated by incubation with 100 μM or 500 μM H_2O_2 for 48 hours in the vascular endothelial cells EA.hy926 (Figure 3-14) suggesting the effect of H_2O_2 was similar to the high glucose treatment.

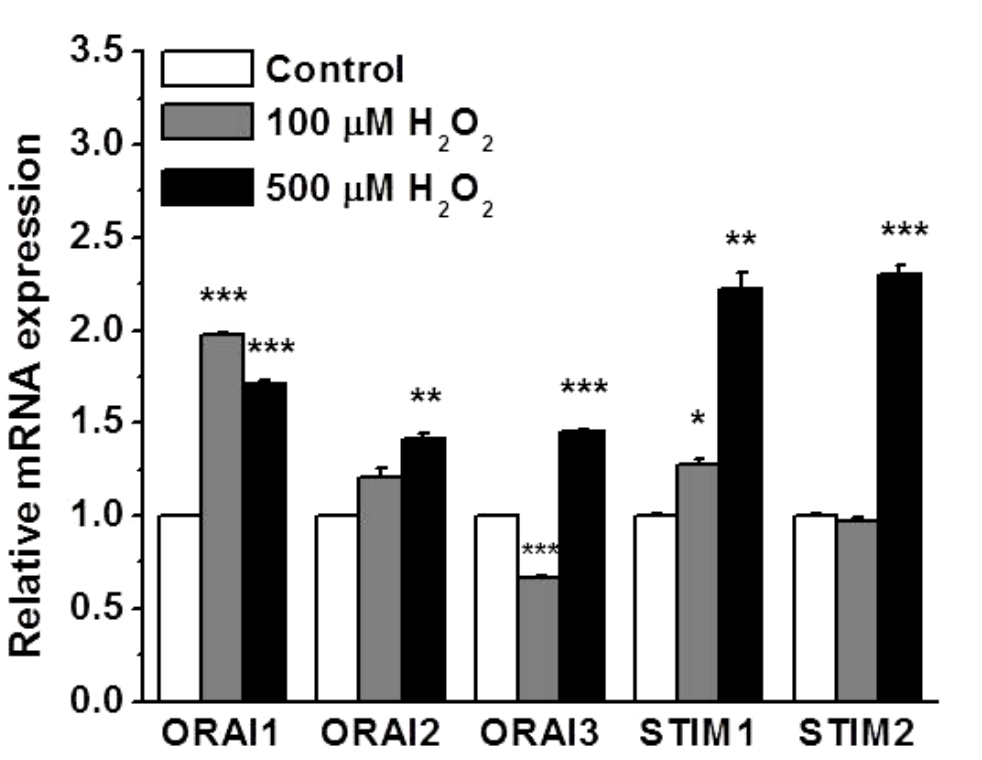

Figure 3-14 Regulation of ORAI and STIM mRNA expression by H_2O_2. The mRNA level quantified by real-time PCR in EA.hy926 cells cultured with H_2O_2 for 48 hours. Untreated cells were used as control. The β-actin was used as housekeeping gene for relative quantification. Mean data from 3 independent experiments with triplicate samples. *$P < 0.05$; **$P < 0.01$; ***$P < 0.001$

3.8 Discussion

The data in this chapter demonstrate that the expression of store-operated Ca^{2+} channel molecules ORAI and STIM is regulated by oxidative stress conditions in human blood vessels and vascular cells, and the upregulation is mediated by the Ca^{2+}/calcineurin/NFAT pathway.

Among the numerous Ca^{2+} influx pathways, one important Ca^{2+} influx path in mammalian cell plasma membrane is store-operated Ca^{2+} entry, the process in which depletion of Ca^{2+} stores in the ER induces Ca^{2+} influx from the extracellular space through the activation of plasma membrane SOC channels (Parekh & Penner, 1997; Parekh & Putney, 2005). STIM and ORAI proteins were found to be the molecular basis of store-operated Ca^{2+} function (Soboloff *et al.*, 2006c). In this thesis, it is shown that ORAI1-3 and STIM1-2 mRNAs and proteins are expressed in human LIMA, saphenous vein, aorta, and human aortic endothelial and smooth muscle cells. This finding is in agreement with the report on the smooth muscle cells of human umbilical artery detected by RT-PCR (Roldan Palomo *et al.*, 2012), and the report on ORAI1 and STIM1 in human pulmonary arterial smooth muscle cells detected by western blotting (Ogawa *et al.*, 2012), which suggests the ubiquitous expression of ORAIs and STIMs in different human vessels. In animals, the expression of STIM1 and ORAI1 has been detected in rat aortic smooth muscle cells using RT-PCR and western blotting (Giachini *et al.*, 2009a; Giachini *et al.*, 2009b; Bisaillon *et al.*, 2010). Additionally, ORAI splice variants in mice have been reported, such as ORAI2L and ORAI2S in a number of tissues including brain, lung, spleen and mouse aortic endothelial cells (Gross *et al.*, 2007), however, there are no such spliced variants in human blood vessels. An actin-binding spliced variant of STIM1 (STIM1L) has been demonstrated in mouse tissues and human T lymphocytes and skeletal muscle (Darbellay *et al.*, 2011), but this has not been investigated in this study. The localization of ORAI and STIM channels in LIMA was also detected by immunohistochemistry staining on the paraffin-embedded tissue sections. ORAI and STIM proteins were positively stained across the artery sections showing that these proteins are expressed in both endothelial and smooth muscle cells. These results suggest that store-operated channel molecules ORAI and STIM are ubiquitously expressed in human blood vessels.

The endothelial cell line EA.hy926 was used in several parts of this study. This cell line was obtained by the fusion of primary human umbilical vein cells with the human lung cancer cell line A549 resulting in having 4n-complement of chromosomes. Nevertheless, Ea.hy926 cells are established as a model for investigating endothelial functions after being demonstrated that they express pure endothelial cell characteristics, such as endothelin-1, prostacyclin, factor VIII-related antigen, and endothelial adhesion molecules (Edgell *et al.*, 1983; Bauer *et al.*, 1992; Rieber *et al.*, 1993; Targosz-Korecka *et al.*, 2013). Primary aortic endothelial and smooth muscle cells were also used as being closest to native cells since aorta is a blood vessel that suffers from atherosclerosis (Kronzon & Tunick, 2006; Hansson & Hermansson, 2011; Bastos Goncalves *et al.*, 2012; van Gils *et al.*, 2012; Robbins *et al.*, 2013)**.**

Three oxidative stress conditions were used in *in vitro* cell models including the incubation with high glucose, Hcy and H_2O_2. ORAI and STIM mRNA expression was significantly upregulated by high glucose in vascular endothelial cells. This upregulation was confirmed at the protein level by western blotting. However, the mRNA expression of these channels in human saphenous vein smooth muscle cells showed a different response to high glucose treatment, as mRNA expression of ORAI1 and ORAI3 was downregulated when ORAI2, STIM1 and STIM2 was upregulated. The reason is unclear, but this could be due to the different location of vascular smooth muscle cells in the body. In addition, the primary cultured smooth muscle cells may have phenotype changes although the cells we used in the study are at early passage numbers, but the cell growth speed for the human saphenous vein smooth muscle cells is much slower than the cells isolated from mouse aorta. Thirdly, the primary cultured smooth muscle cells from human saphenous vein is derived from one patient, therefore it is unclear for potential individual variation. In order to give more evidence of ORAI and STIM mRNA expression in smooth muscle cells, the rat aortic smooth muscle cells were used and the data showed less variation, suggesting that there is a similar effect to the one on vascular endothelial cells. The effect of high glucose on ORAI and STIM expression in blood vessels segments was examined in organ-cultured LIMA segments from non-diabetic patients, but the results are not conclusive due to the big variation between the samples from different patients. Therefore, the further *in vivo* experiments have been

performed using the aorta samples from diabetic patients with age-matched non-diabetic samples as control, which showed less variation and confirmed the conclusions from *in vitro* experiments.

Further *ex vivo* experiments were carried out to examine the ORAI and STIM expression in Type 1 diabetes. Since there were no clinical samples available from Type 1 diabetes, Type 1 diabetic mouse models were used. It is known that diabetes is a clinical condition that affects a broad spectrum of tissues throughout the body including muscle, skin, heart, brain, and kidneys. To extend the findings of high glucose upregulation to other tissues, the expression of ORAI and STIM in kidney samples from two Type 1 diabetic mouse models was examined and the upregulation was evident in the Type 1 diabetic mouse models.

STZ-induced Type 1 diabetic model is a classic Type 1 diabetic mouse model. STZ is a broad-spectrum antibiotic extracted from *Streptomycesacromogenes* (Herr *et al.*, 1959; Rakieten *et al.*, 1963; Brosky & Logothetopoulos, 1969; Junod *et al.*, 1969; Rerup, 1970). It causes rapid and irreversible necrosis of β-cells in the pancreas (Junod *et al.*, 1967). Early studies have revealed that intravenous injection of 25–100 mg/kg STZ to rats was able to produce a dose-dependent hyperglycemia (Junod *et al.*, 1969). The employed dose of STZ and the animal species define the characteristics of diabetes that are developed (Rakieten *et al.*, 1963; Brosky & Logothetopoulos, 1969; Junod *et al.*, 1969; Rerup, 1970). Endogenous chronic oxidative stress can be studied using the STZ-induced diabetic model (Low *et al.*, 1997). In the present study, upregulation of ORAIs and STIMs in the kidney samples from STZ-induced diabetic mice was significant, which is in agreement with the results from endothelial cells cultured in high glucose and the results from diabetic human aorta samples.

Because the STZ mice model showed a significant weight loss, the second Type 1 diabetic mouse model was used. Akita mouse model is a genetic modified Type 1 diabetic model. The Akita mouse model is characterized by progressive hyperglycemia with reduced β-cell mass production but without the characteristics of insulitis or obesity (Yoshioka *et al.*, 1997; Kayo & Koizumi, 1998). Akita mouse has a mutation (C96Y) in the insulin 2 gene (Ins2) (Wang *et al.*, 1999). This mutation changes cysteine to tyrosine in the proinsulin, which disrupts the disulfide bond

formation that causes drastic conformational change. There are two insulin genes, Ins1 and Ins2, that are non-allelic in the mouse but the majority of the total insulin produced in the wild-type mice is transcribed by Ins2 gene. Akita mice heterozygous for the mutation develop severe diabetes; however single Ins1 or Ins2 knockout mutant mice do not develop diabetes indicating there is a significant impact of the mutant insulin of Akita on the dysfunction of β-cells (Leroux *et al.*, 2001). In agreement with the results from the STZ-treated model, ORAI and STIM expression was significantly upregulated in the kidney samples from Akita mice, suggesting that hyperglycemia is an important factor for gene regulation, and weight loss is not a determinant. Taken together, all the *in vivo* and *in vitro* data give the evidence that ORAI and STIM gene expression is changed in diabetes and the upregulation by high glucose or hyperglycemia happens in most cell types, although there are some variations among the isoforms.

The Ca^{2+}/calcineurin/NFAT signalling pathway was specified about 10 years ago and was one of the first signalling pathways identified to connect the cell membrane with the nucleus (Shaw *et al.*, 1988; Flanagan *et al.*, 1991; Liu *et al.*, 1991; Clipstone & Crabtree, 1992). One of the roles of Ca^{2+} is to regulate calcineurin (Klee *et al.*, 1998), which then dephosphorylates and promotes the nuclear import of the cytoplasmic components (NFATc proteins) of NFAT transcription complexes, resulting in the activation of genes expression (Flanagan *et al.*, 1991; Jain *et al.*, 1993; Loh *et al.*, 1996; Beals *et al.*, 1997). The first evidence for the existence of NFAT was derived from analysis of antigen-responsive enhancer elements in the cytokine IL-2 gene promoter in lymphocytes (Durand *et al.*, 1988). So far, NFAT expression or function has been described in several cell types, including mast (Weiss *et al.*, 1996), endothelial (Cockerill *et al.*, 1995), neuronal cells (Ho *et al.*, 1994) and smooth muscle cells (Boss *et al.*, 1998). Distinct tissue-specific patterns are followed for the expression of NFAT isoforms (Hoey *et al.*, 1995). A screen for somatic cell mutations that prevented NFAT transcriptional activation showed many mutations that nullified the activity of the CRAC channels and thus revealed that this was the source of Ca^{2+} required for NFAT import (Fanger *et al.*, 1995; Serafini *et al.*, 1995; Timmerman *et al.*, 1996). The mechanism for the high glucose-induced gene upregulation is unclear; here it is firstly demonstrated that Ca^{2+}/calcineurin/NFAT pathway is important for ORAI channel regulation through the application of CsA,

an inhibitor of calcineurin (Crabtree, 2001). In addition, inhibition of store-operated Ca^{2+} entry by the channel inhibitor DES also decreased the high glucose-induced ORAI and STIM upregulation. These two evidences suggest that Ca^{2+}/calcineurin/NFAT pathway mediates the high glucose-induced store-operated channel gene expression.

Other potential pathways for oxidative stress-induced ORAI and STIM upregulation may also exist. For example, H_2O_2 not only increased the expression of ORAI and STIM as demonstrated in this study, but also activated TRPM2, TRPC1, TRPC5, TRPC6, the I_{CRAC} current and other Ca^{2+}-permeable channels (Xu *et al.*, 2008b; Grupe *et al.*, 2010; Ding *et al.*, 2011; Chen *et al.*, 2012) and subsequently increased the cytosolic Ca^{2+} concentration and activated the downstream calcineurin/NFAT signalling. In addition, the oxidative mechanism has also been suggested for TRPC3 and TRPC6, since the membrane-permeable radical scavenger, tempol, prevented the effect of high glucose (Wuensch *et al.*, 2010). Therefore, the oxidative stress induced by high glucose could directly alter the Ca^{2+} homeostasis or increase Ca^{2+}-permeable channel activity, such as TRPC5, TRPM2, and ORAI1-3, and thus alter the downstream Ca^{2+}/calcineurin signalling and gene transcription (Graier *et al.*, 1997). Although the evidences for the upregulation of ORAIs and STIMs in vascular endothelia cells and smooth muscle cells are obvious, it is still unclear for the response to other Ca^{2+} channels in different cell types, such as the downregulation of TRPC6 seen in diabetic mesangial cells (Graham *et al.*, 2007). Moreover, H_2O_2 was reported to induce apoptosis in primary cultures of human umbilical vein endothelial cells (Xu *et al.*, 2008b) , but this was not examined in the present study. Thus, it is not clear if the apoptotic effect of H_2O_2 is related to the H_2O_2-induced upregulation of ORAI1-3 and STIM1-2 expression reported in the present study. However, no cell death or shape changes were observed.

Another oxidative stress-related pathological condition is hyperhomocysteinemia, which is also an independent risk factor for the development of CVDs (Mayer *et al.*, 1996; Mangiagalli *et al.*, 2004). Although the effects of high glucose and H_2O_2 on the ORAI and STIM expression were similar, Hcy had a differential effect on ORAI channel expression. ORAI expression was decreased in HAECs after incubation with high levels of Hcy. Different concentrations of Hcy were used and revealed that even

the smallest dose has a significant effect on the expression of the channels. The effect was dose-dependent and it achieved maximum at 50 μM. The downregulation of ORAI expression by Hcy may explain the inhibitory effect of Hcy on SOCE reported in HUVECs (Zhang *et al.*, 2005). However, the mechanism of Hcy is still unclear, although Hcy has been demonstrated to induce cell cycle arrest (Outinen *et al.*, 1999) and cause endothelial cell senescence (Zhu *et al.*, 2006) and apoptosis (Zhang *et al.*, 2001). Hcy may play a regulatory role in the expression of ORAI and STIM in vascular endothelial cells, but the underlying mechanism still needs to be investigated in the future.

3.9 Summary

In this chapter, store-operated Ca^{2+} channel molecules ORAI1-3 and STIM1-2 were identified in human blood vessels, vascular endothelial and smooth muscle cells. The expression of these genes was significantly upregulated by oxidative stress conditions in cell culture models and arterial segment organ culture model. The upregulation was also confirmed in the tissue samples obtained from Type 2 diabetic patients and the Type 1 diabetic mice. The upregulation of ORAI and STIM is mediated by the calmodulin/calcineurin/NFAT signalling pathway, which was evidenced by the application of store-operated blocker DES and the calcineurin inhibitor CsA. The effects of high glucose and H_2O_2 on the ORAI and STIM expression are similar, but Hcy may have differential effect on ORAI channel expression. These results suggested that upregulation of ORAI and STIM under oxidative stress conditions could be an important mechanism for the pathogenesis of diabetic vascular disease or oxidative stress-related diseases.

Chapter 4

Effects of Oxidative Stress on Ca^{2+} Influx, the Activity of ORAI Channels and the Role of Cytosolic STIM1 Movement

4.1 Introduction

Ca^{2+} and ROS are important intracellular signalling molecules that regulate the cellular functions (Berridge *et al.*, 2000; Droge, 2002; Ermak & Davies, 2002). There is a cross-regulation between Ca^{2+} and ROS, as Ca^{2+} regulates ROS production in the mitochondria and the cytosol, and ROS affect Ca^{2+} homeostasis in pathophysiological conditions, such as diabetes and atherosclerosis (Droge, 2002; Brookes *et al.*, 2004; Yan *et al.*, 2006). Oxidizing agents such as Hcy and H_2O_2 were reported to inhibit SOCE in different cell types including vascular endothelial cells, pulmonary artery smooth muscle cells and neutrophils (Zhang *et al.*, 2005; Schach *et al.*, 2007; Tintinger *et al.*, 2007; Florea & Blatter, 2008). Using electrophysiology, Ca^{2+} imaging and site-directed mutagenesis, it was found that H_2O_2 inhibited ORAI1, but did not affect ORAI3 (Bogeski *et al.*, 2010). The extracellular Cys^{195} in ORAI1 has been identified as the action site for the differential sensitivity. Nevertheless, the direct effect of high glucose and Hcy on ORAI channel activity is unknown.

The ER Ca^{2+} store depletion is signalled by the ER Ca^{2+} sensor STIM1 to the SOCs in the PM (Liou *et al.*, 2005; Zhang, 2005). It has been demonstrated that dissociation of Ca^{2+} from the ER-luminal domain of STIM1 results in STIM1 oligomerization (clustering or puncta) and redistribution of STIM1 to the subplasmalemmal area (translocation) (Smyth *et al.*, 2008; Hogan *et al.*, 2010). The opening of ORAI channels in the PM is then triggered by STIM1 via the binding of STIM1 to the N-terminus of ORAI, which results in store-operated Ca^{2+} entry (Hogan *et al.*, 2010). The deficiency of I_{CRAC} caused by STIM1 dysfunction has been implicated in SCID syndrome (Picard *et al.*, 2009). The enhanced expression of STIM1 or enhanced store-operated channel activity have been reported in the stroke-prone spontaneously hypertensive rats (Giachini *et al.*, 2009a) and to be involved in the development of cardiomyocyte hypertrophy (Ohba *et al.*, 2009). Recent study demonstrated that STIM1 may be related to oxidative stress, as S-gluthationylation of STIM1 at Cys^{56} induced STIM1 clustering and ORAI1 channel activation, which has been suggested as an ER Ca^{2+} store independent process (Hawkins *et al.*, 2010). Therefore, examining whether high glucose, Hcy and H_2O_2 have any direct effects on STIM1 movement -an essential step for ORAI channel activation- would be interesting.

In this chapter, I aimed to investigate: 1) the acute and chronic effects of high glucose on store-operated and non-store-operated Ca^{2+} influx in vascular endothelial cells using Ca^{2+} imaging; 2) the direct effect of high glucose and Hcy on ORAI1, ORAI2 and ORAI3 channel activity using whole-cell patch clamp recordings in the inducible HEK293 T-REx cells co-expressed with STIM1-EYFP and ORAI1 or ORAI2 or ORAI3; 3) the effects of high glucose, Hcy and H_2O_2 on STIM1 translocation and clustering using live-cell fluorescence imaging on the HEK293 cells stably transfected with STIM1–EYFP; 4) the effect of high glucose or Hcy on endothelial cell functions-proliferation, secretion, migration and tube formation.

4.2 Ca^{2+} influx enhanced by high glucose in endothelial cells

4.2.1 Effect of acute application of high glucose on Ca^{2+} influx

Ca^{2+} influx in the vascular endothelial cells EA.hy926 was monitored using Fura-PE3/AM. In the store-depleted cells by preincubation with TG (1 μM), Ca^{2+} influx evoked after switching from Ca^{2+}-free to Ca^{2+} solution was not affected by acute application of 25 mM glucose (Figure 4-1A). In the non-store-depleted cells, Ca^{2+} influx was also not affected by acute application of 25 mM glucose (Figure 4-1B).

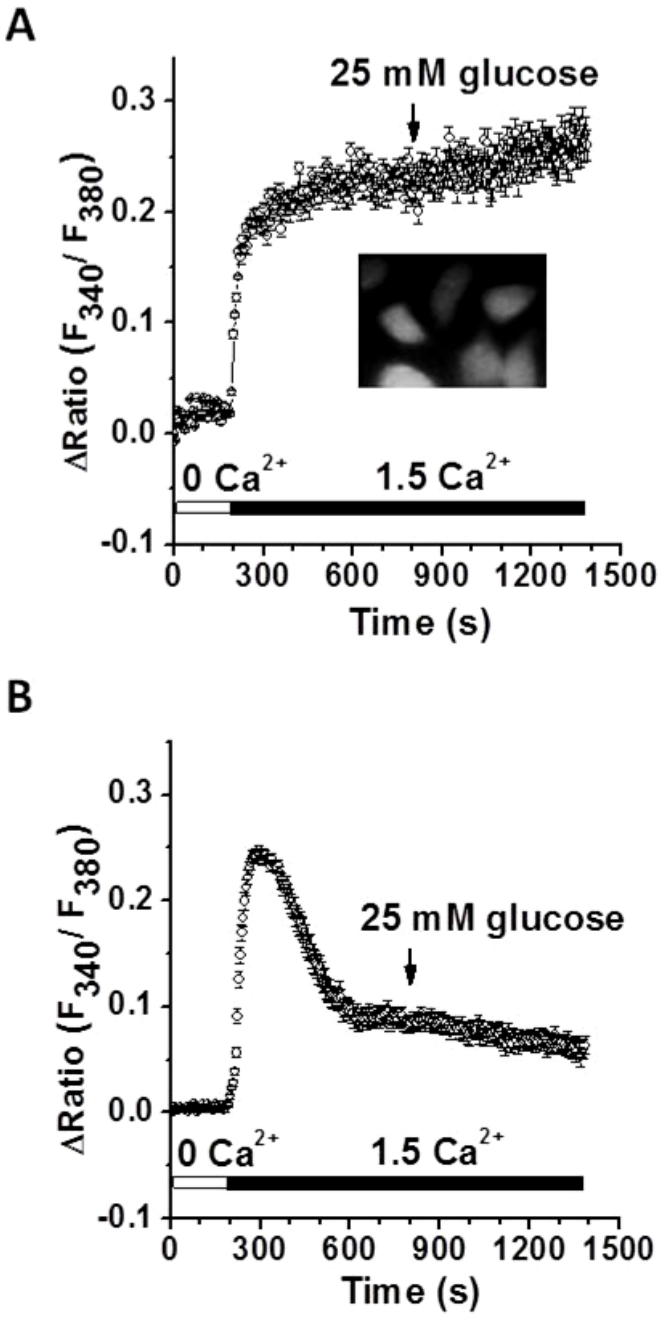

Figure 4-1 Effect of acute high glucose application on Ca^{2+} influx in vascular endothelial cells. The vascular endothelial cells EA.hy926 were loaded with Fura-PE3/AM. **A,** Cells pretreated with 1 μM thapsigargin (TG) for 30 min and the fluorescence at a ratio of F_{340}/F_{380} was monitored before and after perfusion with high glucose (25 mM glucose) (*n* = 17 cells). **B,** Acute application of high glucose on Ca^{2+} influx in the cells without store depletion by TG (*n* = 15 cells).

4.2.2 Effect of chronic treatment with high glucose on Ca^{2+} influx

Ca^{2+} entry was markedly enhanced in the store-depleted cells treated with 25 mM glucose for 72 hours, but the basal Ca^{2+} level was not altered comparing to the cells treated with normal (5.5 mM) glucose for the same time period (Figure 4-2 A-B). The similar experiment was carried out in the cells without store-depletion by TG. Chronic treatment with high glucose also enhanced non-store depletion related component of Ca^{2+} influxes after readmission of Ca^{2+} in the solution (Figure 4-2 C-D). The effects on non-store-depleted Ca^{2+} influx, Ca^{2+} release and the Ca^{2+} influx were further observed in the experiment using the GPCR activator trypsin to actively deplete the ER Ca^{2+} store. The non-store-depleted Ca^{2+} influx was also greater in the cells incubated with high glucose for 72 hours. The Ca^{2+} release signal induced by trysin (0.1 nM) and the subsequent Ca^{2+} influx were significantly higher in the high glucose treated group than that in the control group (Figure 4-3). These data suggest that the store-operated Ca^{2+} influx, non-store-operated Ca^{2+} influx and Ca^{2+} release are enhanced in the cells chronically treated with high glucose.

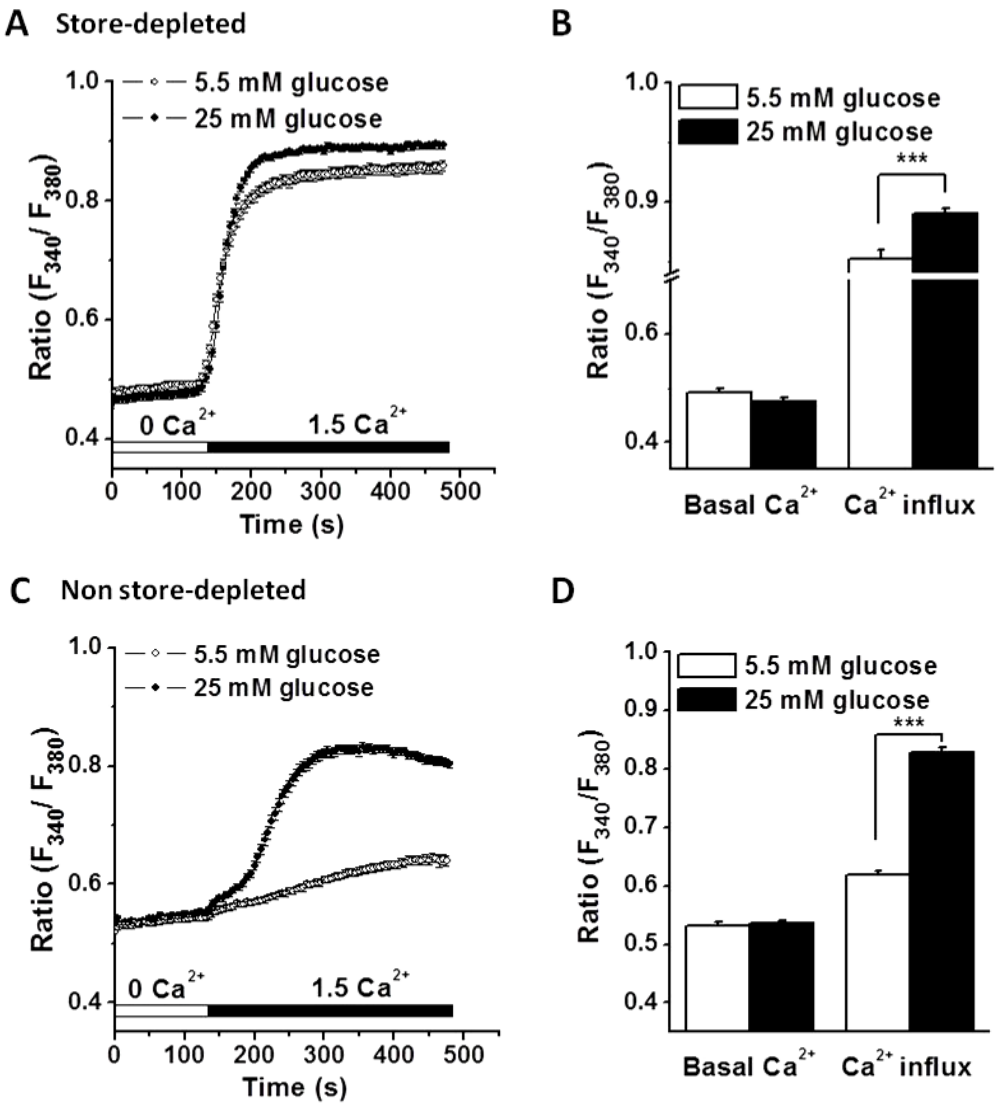

Figure 4-2 Ca^{2+} influx enhanced by chronic treatment with high glucose in store-depleted and non-store-depleted vascular endothelial cells. Human vascular endothelial cells EA.hy926 were loaded with Fura-PE3/AM, and Ca^{2+} was measured as the ratio (F_{340}/F_{380}) of Fura-PE3/AM fluorescence excited at 340 and 380 nm **A,** Store-operated Ca^{2+} influx in the endothelial cells after incubation with or without high glucose for 72 hours. The ER Ca^{2+} store was depleted by preincubation with 1 μM TG for 30 minutes. **B,** Mean ± SEM data showing the ratio measured in the Ca^{2+}-free and 1.5 mM Ca^{2+} solutions in the groups with (n = 52) or without (n = 49) chronic (72 h) incubation with high glucose. **C,** Non-store-operated Ca^{2+} influx in the endothelial cells after incubation with or without high glucose for 72 hours. **D,** Mean ± SEM data showing the ratio measured in Ca^{2+}-free and 1.5 mM Ca^{2+} solutions in the groups with (n = 52) or without (n = 49) chronic (72 h) incubation with high glucose. ***$P < 0.001$

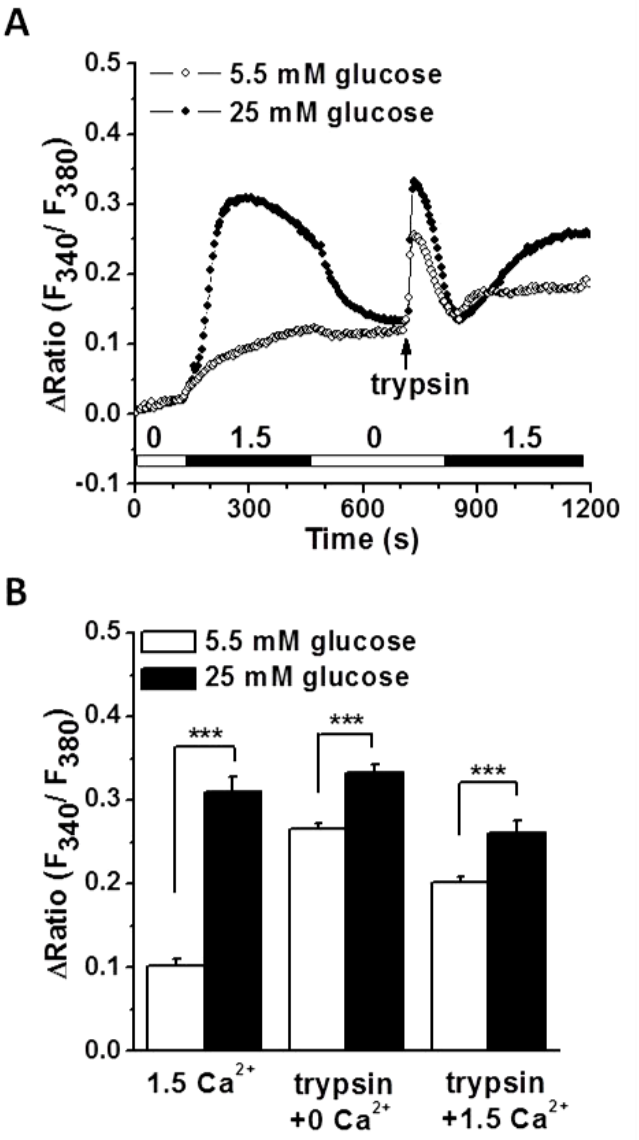

Figure 4-3 Ca^{2+} release and Ca^{2+} influx enhanced by chronic treatment with high glucose in vascular endothelial cells. Human vascular endothelial cells EA.hy926 were loaded with Fura-PE3/AM, and Ca^{2+} was measured as the ratio (F_{340}/F_{380}) of Fura-PE3/AM fluorescence excited at 340 and 380 nm. **A,** After 72 h incubation with or without high glucose, the Ca^{2+} influx was measured after admission of Ca^{2+}, 0.1 nM trypsin, and readmission of Ca^{2+}. **B,** Mean ± SEM data for the Ca^{2+} influx, Ca^{2+} release and Ca^{2+} re-entry in the high glucose-treated (n = 57) and untreated (n = 53) cells. ***P < 0.001

4.3 Functional expression of ORAI and STIM in HEK293 cells

To further examine the effect of oxidative stress conditions on the activity of ORAI1-3 and STIM1, the full-length of ORAI mRNAs were amplified and subcloned into a pcDNA4 vector with tetracycline regulatory system (Tet-On expression system). In this section, the molecular cloning and functional expression of ORAI1-3 channels in the HEK293 T-REx cells were characterized.

4.3.1 Molecular cloning of full length ORAI1-3

Human full-length ORAI1, ORAI2 and ORAI3 coding regions were amplified from the cDNA of HAEC using the primer sets with specific restriction enzyme sites (see Table 2-3). As presented in Figure 4-4, the expected product sizes for ORAI1, ORAI2 and ORAI3 were observed. Successful amplification of full length of ORAI cDNAs was confirmed using restricted enzymes and direct sequencing, for example, ORAI2 cDNA was cut into two bands by SacII (Figure 4-4D). The PCR products for ORAI1 and ORAI2 were cloned into mCherry-tagged pcDNA4/TO vector, and ORAI3 was cloned into mCFP-tagged pcDNA4/TO vector. The ligated products were transformed into DH5α *E. coli* competent cells and the positive colonies were screened by the nest PCR with the specific primers for ORAI1, ORAI2 and ORAI3, which gave the amplicons with the size of 238 bp, 210 bp and 176 bp, respectively (Figure 4-5). Plasmid cDNAs were extracted from the positive clones and the successful cloning of the three ORAI genes were confirmed by sequencing. The examples for ORAI2 sequencing and the alignment of ORAI1 gene sequence against the mCherry-ORAI1 plasmid cDNA are given in Appendix II and III, which had 100% identity to ORAI gene sequences in the GenBank (accession number NM_032790 for ORAI1, NM_001126340 for ORAI2, and NM_152288 for ORAI3).

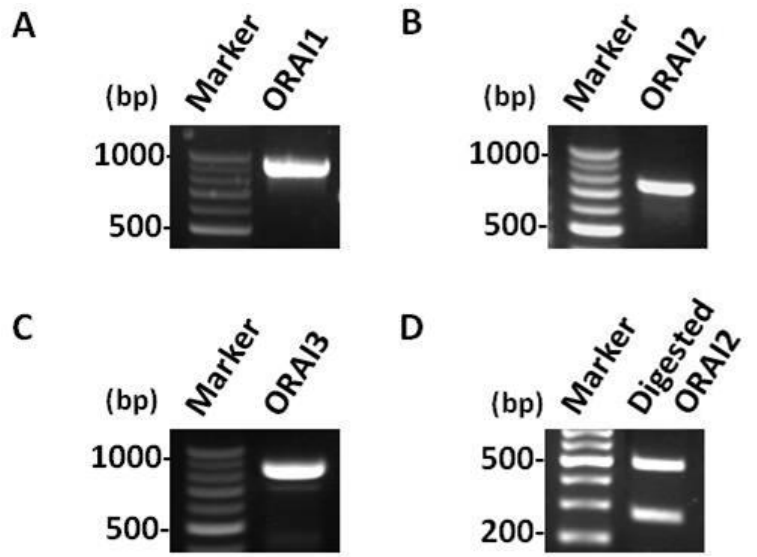

Figure 4-4 Detection of full length ORAI1-3. PCR products were shown in the 1.5% agarose gel stained with 0.5 µg/ml ethidium bromide. The observed product size of PCR amplicons is 939 bp for ORAI1 (A), 790 bp for ORAI2 (B), and 902 bp for ORAI3 (C), which is the same as the predicted size. The expected product sizes after digestion of full length ORAI2 with the restriction enzyme SacII are 271 bp and 519 bp (D).

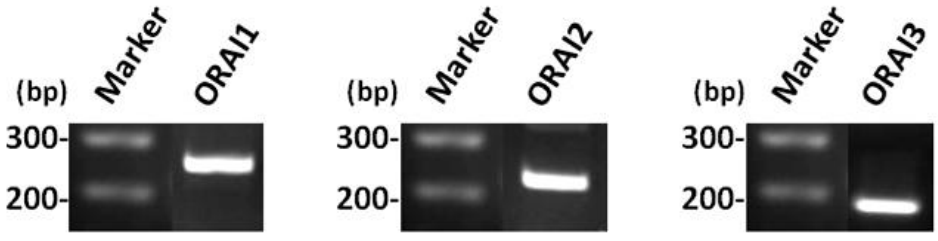

Figure 4-5 Example for the PCR screening of ORAI colonies. PCR products were shown in the 1.5% agarose gel stained with 0.5 µg/ml ethidium bromide. Expression of ORAI1, ORAI2 or ORAI3 was confirmed by PCR in the positive colonies.

4.3.2 Expression of ORAI and STIM in HEK293 cells

Expression of STIM1, ORAI1-3 tagged with EYFP or mCherry or CFP was induced by 1 μM tetracycline and examined by a fluorescent microscope. STIM1-EYFP was mainly localized in the cells, while ORAI1, 2, 3 channels were localized in the PM (Figure 4-6).

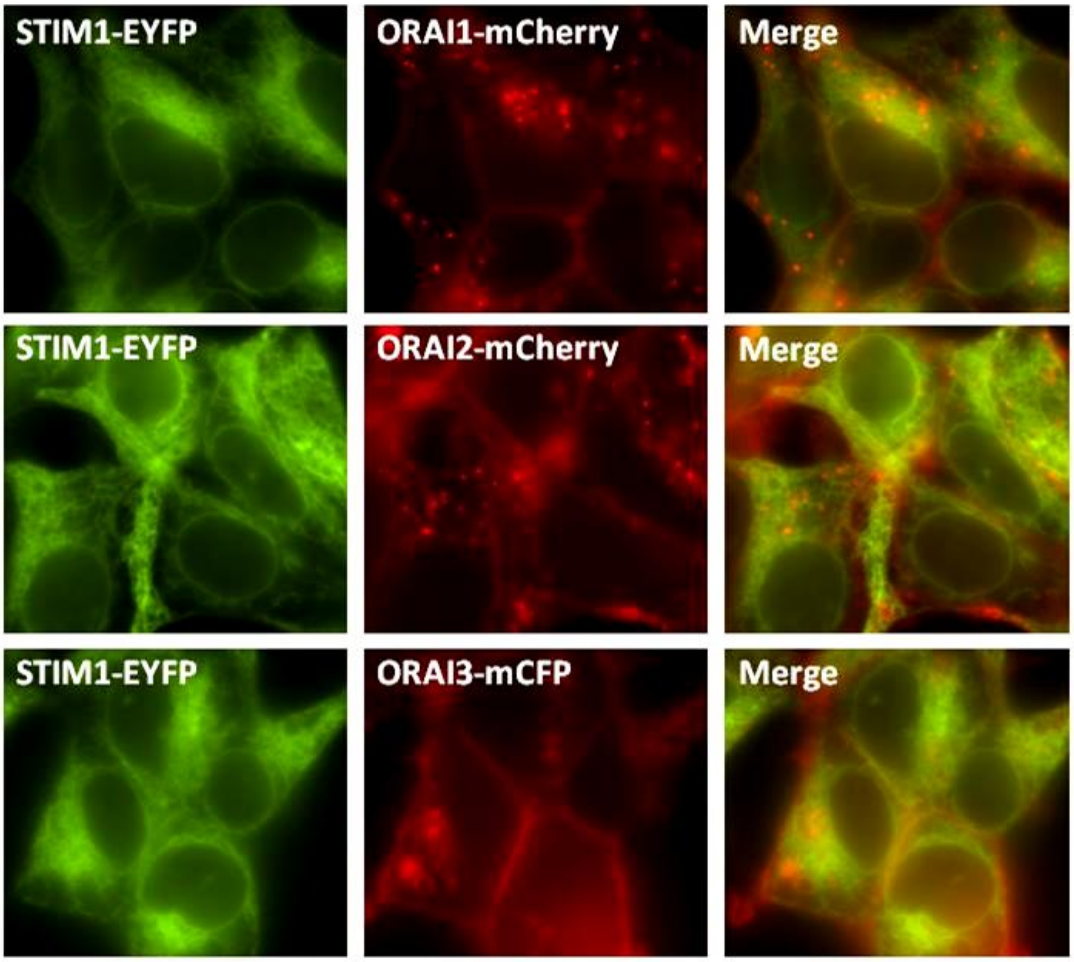

Figure 4-6 Expression pattern for STIM1-EYFP, STIM1-EYFP/TO-mCherry-ORAI1, STIM1-EYFP/TO-mCherry-ORAI2 and STIM1-EYFP/TO-mCFP-ORAI3 in HEK293 cells. ORAI1 and ORAI2 are tagged with the monomeric red fluorescent protein (mCherry), ORAI3 with the monomeric cyan fluorescent protein (mCFP) and STIM1 with the enhanced yellow fluorescent protein (EYFP). Images for EYFP/mCherry/mCFP fluorescence were captured using Nikon fluorescence microscope equipped with a Nikon Plan Fluor 100×/1.30 oil objective.

4.3.3 Characterization of ORAI channels overexpressed in HEK293 cells

The ORAI channel expression in HEK293 cells was induced by tetracycline and the whole-cell current was recorded by patch clamp. As demonstrated in Figure 4-7 A-C, the *IV* curves obtained from the cells expressing STIM1/ORAI1, STIM1/ORAI2 or STIM1/ORAI3 were similar to the reports (Yeromin *et al.*, 2006; Goto *et al.*, 2010). ORAI1 and ORAI2 were activated by 1 μM TG and ORAI3 was activated by 100 μM 2-APB in the cells co-expressed with STIM1. The whole-cell current in the cells expressing STIM1 alone showed similar store-operated current activated by TG, suggesting that the overexpressed STIM1 interacts with the native ORAI channel proteins, which can produce a similar current to that recorded in the STIM1/ORAI co-expressed cells (Figure 4-7D). The non-transfected HEK293 cells had no evident store-operated current (Figure 4-7E). These data suggest the success of functional expression of ORAI/STIM in the cells.

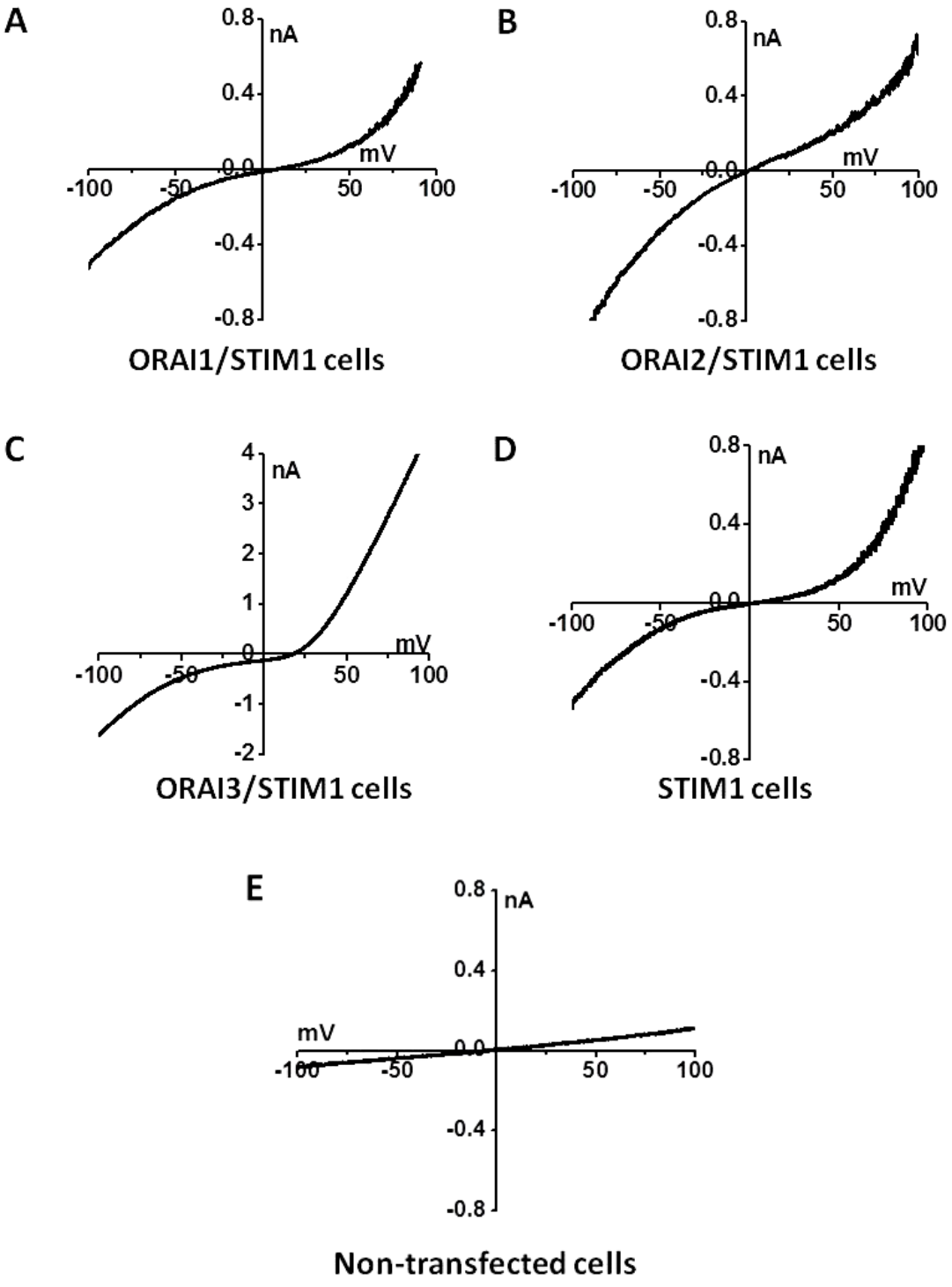

Figure 4-7 Representative *IV* relationships of ORAI1-3 overexpressed in HEK293 T-REx cells. **A,** ORAI1/STIM1 HEK293 T-REx cells. **B,** ORAI2/STIM1 HEK293 T-REx cells. **C,** ORAI3/STIM1 HEK293 T-REx cells. **D,** Non-induced STIM1 HEK293 T-REx cells. **E,** Non-transfected HEK293 T-REx cells. The ORAI1 and ORAI2 channels were activated in bath solution containing 1 μM TG and ORAI3 channels were activated in bath solution containing 100 μM 2-APB.

4.4 ORAI channel activity regulated by oxidative stress

In this section, the direct effects of high glucose and Hcy on ORAI currents were investigated in the overexpression system using patch clamping.

4.4.1 Direct effect of high glucose on ORAI channel activity

Although the expression of ORAI isoforms can be upregulated by high glucose in vascular endothelial cells, the direct effect of high glucose on these channels is still unknown. Therefore, in this section, it is examined whether high glucose affects the ORAI channels directly. The whole-cell patch clamp experiments were performed in the inducible HEK293 T-REx cells co-expressed with STIM1-EYFP and mCherry-tagged ORAI1 or ORAI2, or mCFP-tagged ORAI3. Acute perfusion with high glucose did not change the TG-induced ORAI1 current in the cells co-expressed with ORAI1/STIM1, however, DES, a native store-operated channel blocker (Zakharov *et al.*, 2004), significantly inhibited ORAI1 channel activity (Figure 4-8). The effect of acute perfusion with high glucose on ORAI2/STIM1 was also observed. ORAI2 current was induced by TG, but perfusion with high glucose did not change the current. The ORAI2 current was also sensitive to DES (Figure 4-9). ORAI3 current was activated by 2-APB, but inhibited by DES. High glucose had no direct effect on ORAI3 current (Figure 4-10). In the non-transfected HEK293 T-REx cells, there was no significant current induced by TG or 2-APB (Figure 4-11). These data suggest that high glucose had no direct effect on the ORAI channel activity. The enhanced store-operated Ca^{2+} influx observed in the endothelial cells could be explained by the gene upregulation, rather than the action on the channels per second.

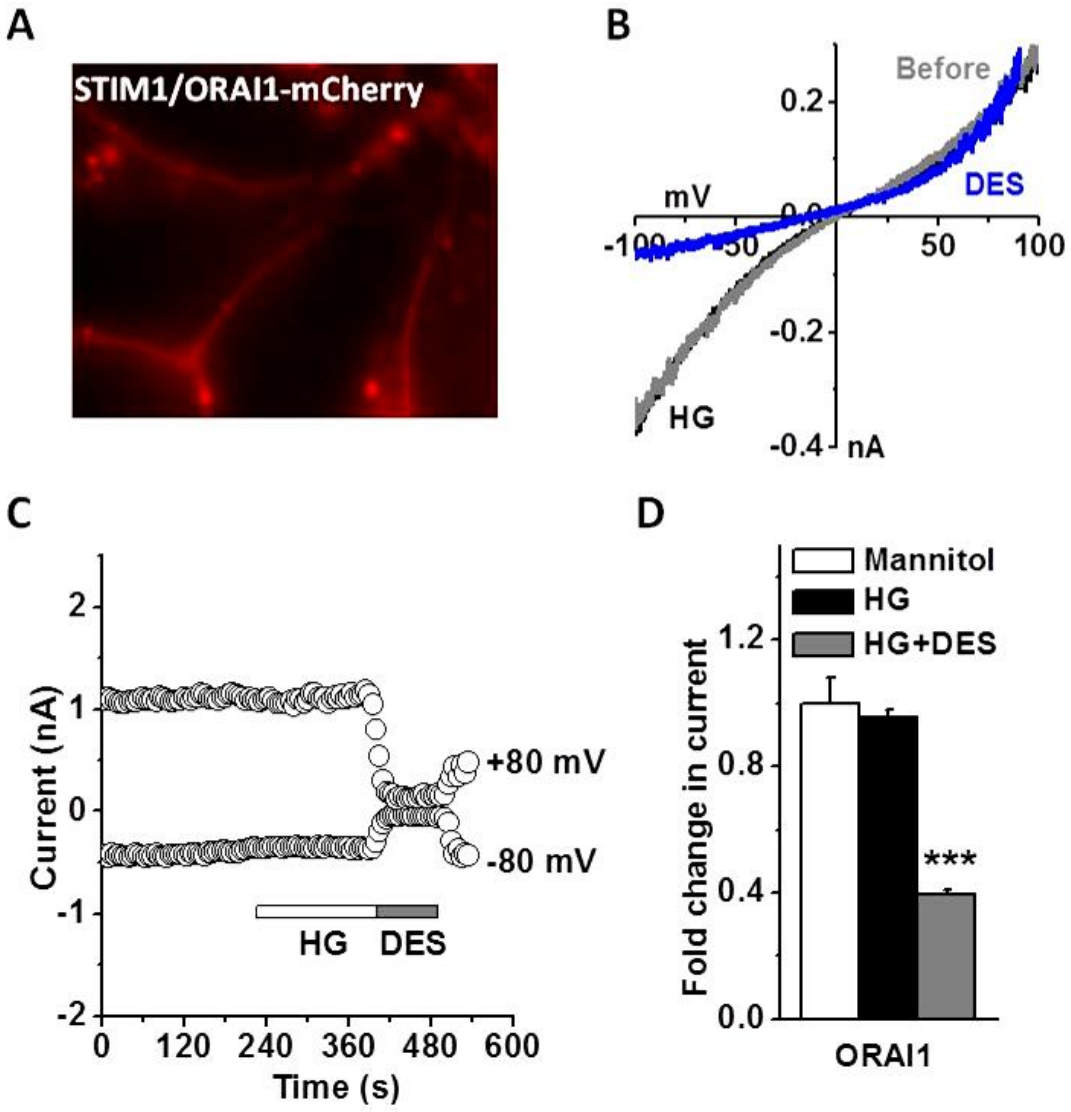

Figure 4-8 ORAI1 channel current not affected by high glucose. **A,** ORAI1-mCherry overexpressing HEK293 T-REx cells co-expressing STIM1. Red fluorescence indicates the expression of ORAI1-mCherry on the plasma membrane. **B,** Representative current-voltage (*IV*) relationship from the recording presented in C. **C,** Representative time-course whole-cell patch clamp recording in ORAI1 overexpressing HEK293 T-REx cell co-expressing STIM1. The bar indicates application of high glucose (25 mM, HG), followed by application of diethylstilbestrol (DES) 10 μM that was used as a channel blocker. **D,** Mean ± SEM data for the inward current (n = 12). ORAI1 channels were activated in bath solution containing 1μM TG. ***$P < 0.001$

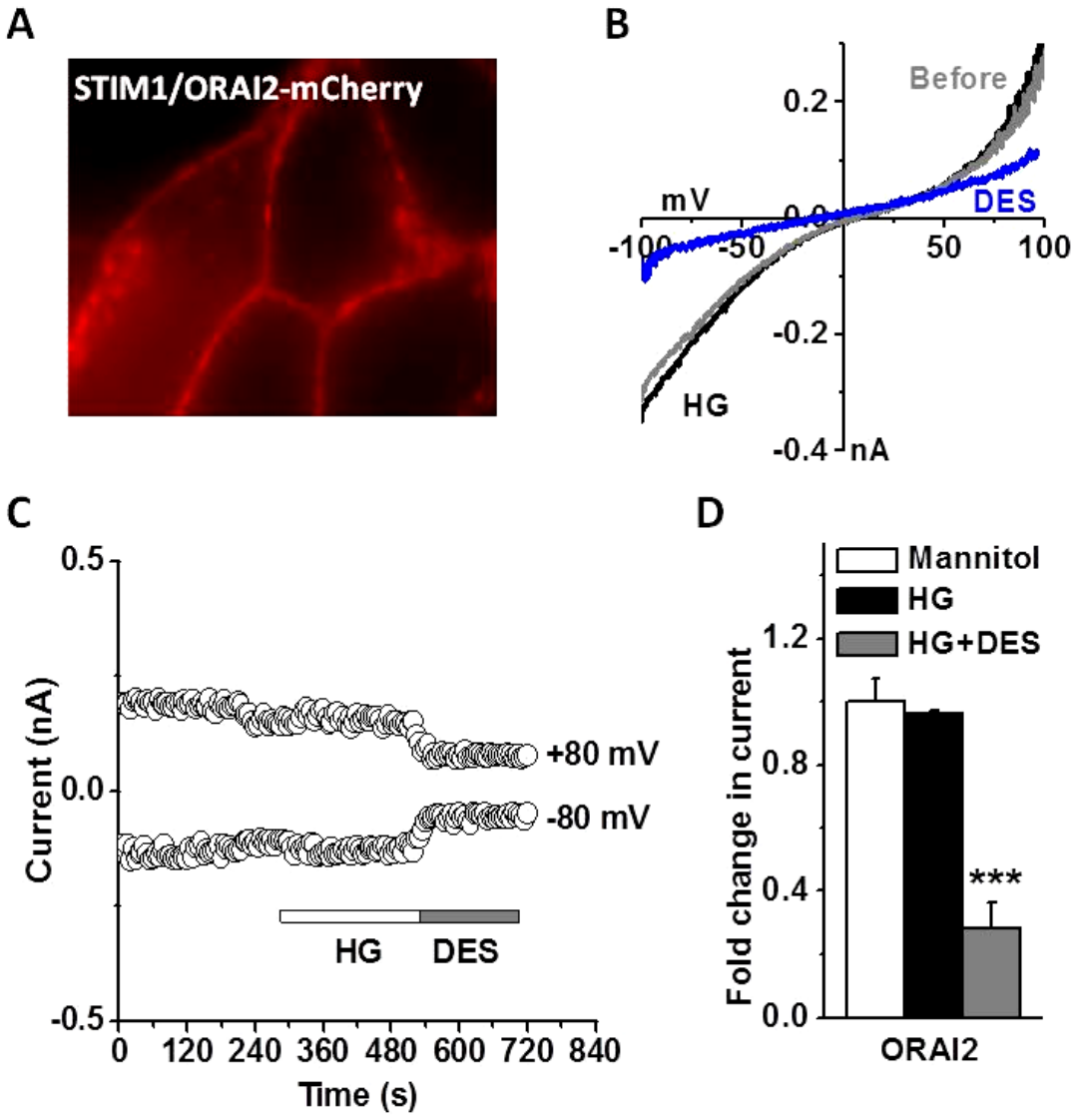

Figure 4-9 ORAI2 channel current not affected by high glucose. A, ORAI2-mCherry overexpressing HEK293 T-REx cells co-expressing STIM1. Red fluorescence indicates the expression of ORAI2-mCherry on the plasma membrane. **B,** Representative *IV* relationship from the recording presented in C. **C,** Representative time-course whole-cell patch clamp recording in ORAI2 overexpressing HEK293 T-REx cell co-expressing STIM1. The bar indicates application of high glucose (25 mM, HG), followed by application of diethylstilbestrol (DES) 10 μM that was used as a channel blocker. **D,** Mean ± SEM data for the inward current (n = 12). ORAI2 channels were activated in bath solution containing 1μM TG. ***P < 0.001

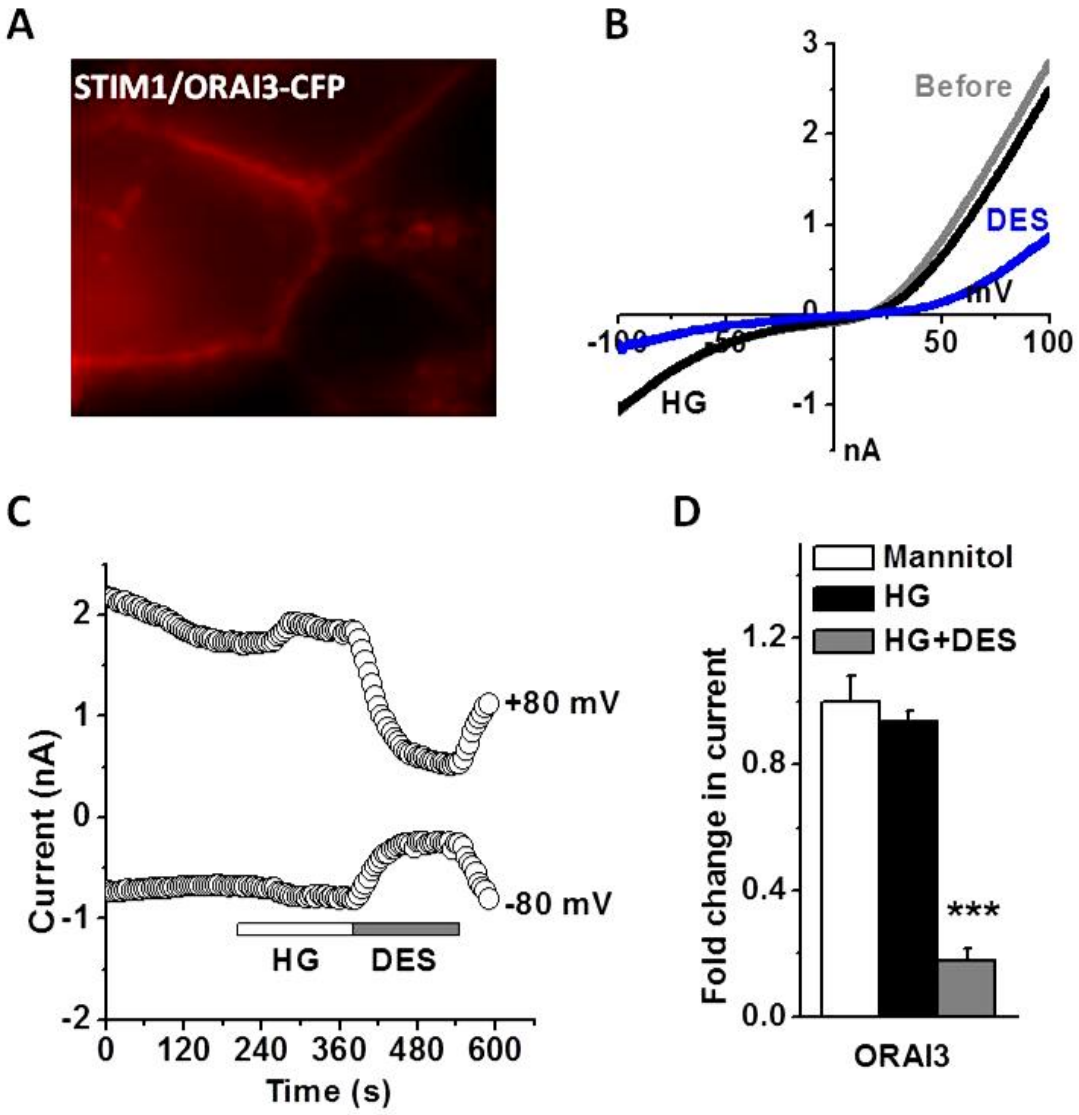

Figure 4-10 ORAI3 channel current not affected by high glucose. A, ORAI3-mCFP overexpressing HEK293 T-REx cells co-expressing STIM1. Red fluorescence indicates the expression of ORAI3-CFP on the plasma membrane. **B,** Representative current-voltage (*IV*) relationship from the recording presented in C. **C,** Representative time-course whole-cell patch clamp recording in ORAI3 overexpressing HEK293 T-REx cell co-expressing STIM1. The bar indicates application of high glucose (25 mM, HG), followed by application of diethylstilbestrol (DES) 10 μM that was used as a channel blocker. **D,** Mean ± SEM data for the inward current (n = 12). ORAI3 channels were activated in bath solution containing 100μM 2-APB. ***$P < 0.001$

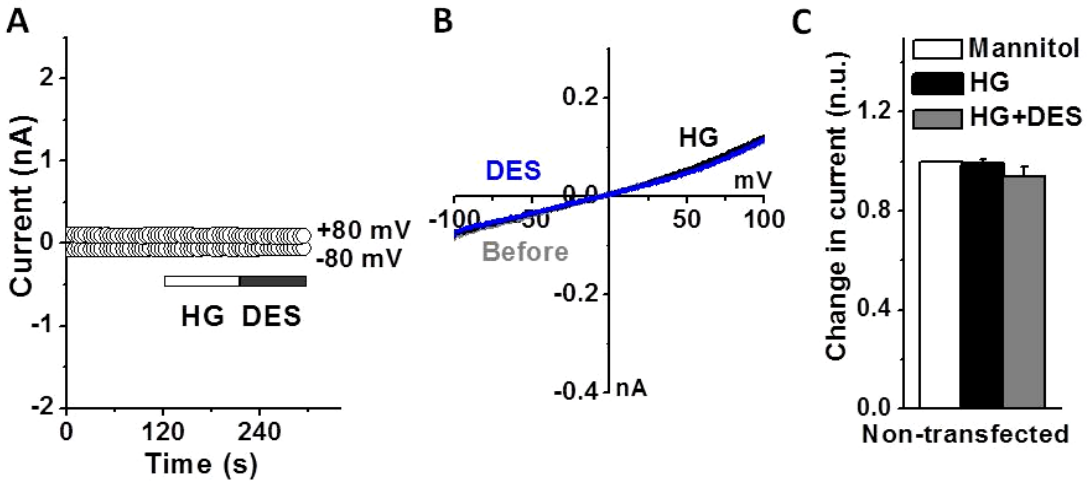

Figure 4-11 No significant current induced by TG in the non-transfected HEK293 T-REx cells and the effect of high glucose. A, Representative time-course whole-cell patch clamp recording in non-transfected HEK293 T-REx cells in the presence of 1 μM TG. The bar indicates application of high glucose (25 mM, HG) and diethylstilbestrol (DES, 10 μM). **B,** Representative *IV* relationship for the recording in A. **C,** Mean ± SEM data for the inward current (n = 6).

4.4.2 Direct effect of homocysteine on ORAI channel activity

Since the expression of ORAI isoforms can be downregulated by Hcy in vascular endothelial cells, but the direct effect of Hcy on these channels is unknown, the effect of Hcy on ORAI channel activity was examined. Whole-cell patch clamp experiments were performed in the inducible HEK293 T-REx cells overexpressing ORAI1, ORAI2 and ORAI3 co-expressed with STIM1. Acute perfusion with Hcy inhibited the TG-induced ORAI1 and ORAI2 currents and the 2-APB-induced ORAI3 current (Figure 4-12 A-C). Similar to the results in 4.4.1, DES significantly inhibited the channel activity of all three ORAI isoforms. Hcy had no significant effect on the endogenous current recorded in the non-transfected HEK293 T-REx cells (Figure 4-12D).

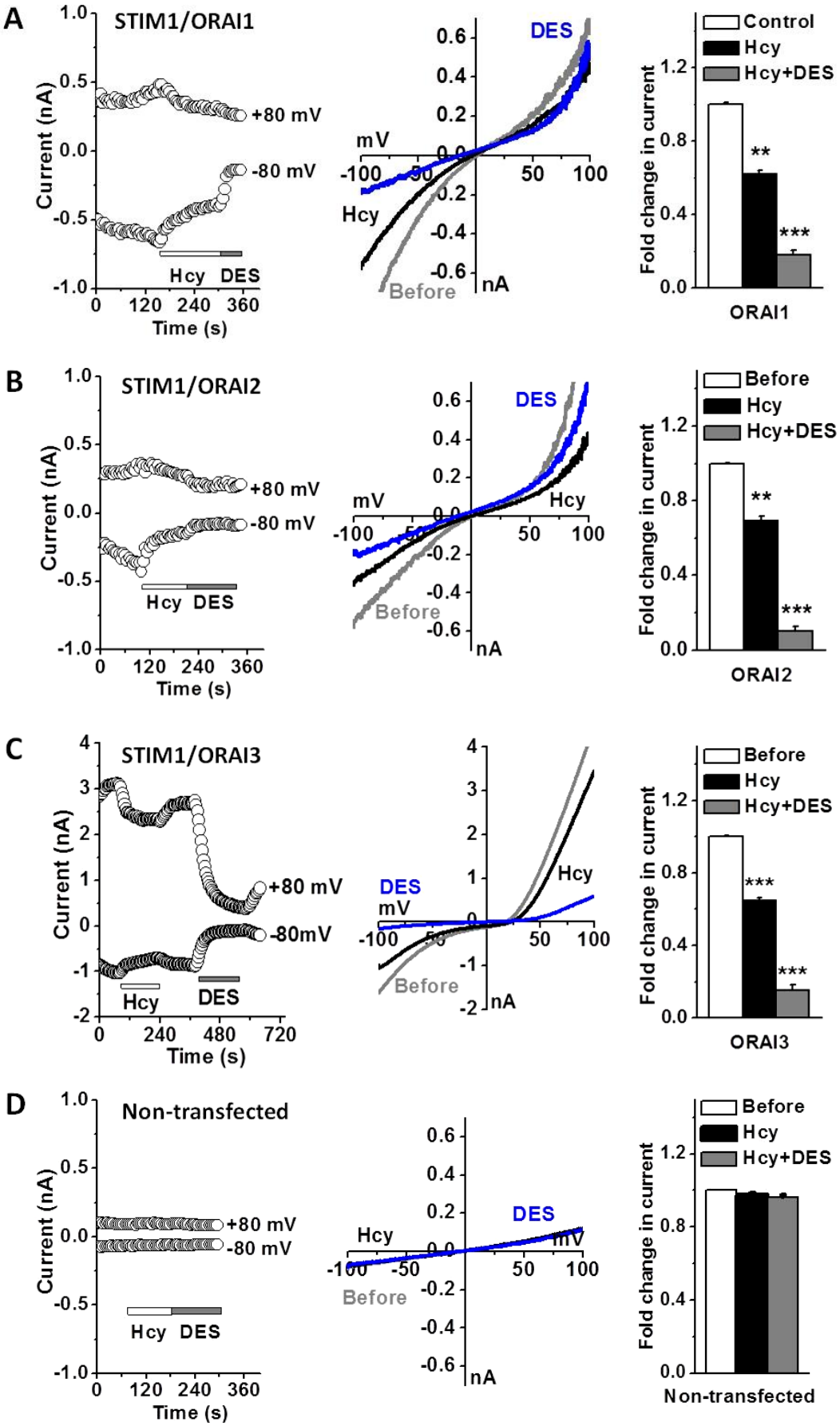
A
STIM1/ORAI1
Current (nA)
+80 mV
-80 mV
Hcy DES
Time (s)
DES
Hcy
Before
mV
nA
Control
Hcy
Hcy+DES
Fold change in current
**
***
ORAI1
B
STIM1/ORAI2
Current (nA)
+80 mV
-80 mV
Hcy DES
Time (s)
DES
Hcy
Before
mV
nA
Before
Hcy
Hcy+DES
Fold change in current
**
***
ORAI2
C
STIM1/ORAI3
Current (nA)
+80 mV
-80mV
Hcy
DES
Time (s)
DES
Hcy
Before
mV
nA
Before
Hcy
Hcy+DES
Fold change in current
***
***
ORAI3
D
Non-transfected
Current (nA)
+80 mV
-80 mV
Hcy DES
Time (s)
DES
Hcy
Before
mV
nA
Before
Hcy
Hcy+DES
Fold change in current
Non-transfected

Figure 4-12 ORAI1-3 channel currents inhibited by homocysteine. Whole-cell current was recorded in the inducible HEK293 T-REx cells co-expressed with STIM1-EYFP and ORAI1-3. **A,** ORAI1. **B,** ORAI2. **C,** ORAI3. **D,** Non-transfected. Representative time-course whole-cell patch clamp recordings and *IV* curves are presented. The bar indicates application of homocysteine (Hcy) 100 μM, followed by application of diethylstilbestrol (DES, 10 μM). Bar charts present the averaged data for the inward current measured at -80 mV (n = 5 for each group). The ORAI1 and ORAI2 channels were activated in bath solution containing 1 μM TG and ORAI3 channel was activated in bath solution containing 100 μM 2-APB. $^{**}P < 0.01$; $^{***}P < 0.001$

4.5 STIM1 translocation and clustering regulated by oxidative stress

In this section, the effects of high glucose, Hcy and H_2O_2 on cytosolic STIM1 movement were investigated in the overexpression system using live cell fluorescent imaging to examine if this mechanism plays a role in the oxidative stress-induced increase of SOCE (section 4.2) or upregulation of SOCs (Chapter 3).

4.5.1 STIM1 translocation regulated by high glucose

In the HEK293 T-REx cells overexpressing STIM1-EYFP, the STIM1-EYFP subplasmalemmal translocation and puncta formation was evoked by 1 μM TG. Acute perfusion with 25 mM glucose did not cause STIM1 clustering or change the TG-induced STIM1 movement (Figure 4-13). The effect of chronic application of high glucose was also observed in the cells without store depletion. Incubation of STIM1 cells with high glucose for 72 hours did not evoke cytosolic STIM1 clustering and translocation. The TG-induced cytosolic STIM1 movement was not altered by the incubation with high glucose (Figure 4-14).

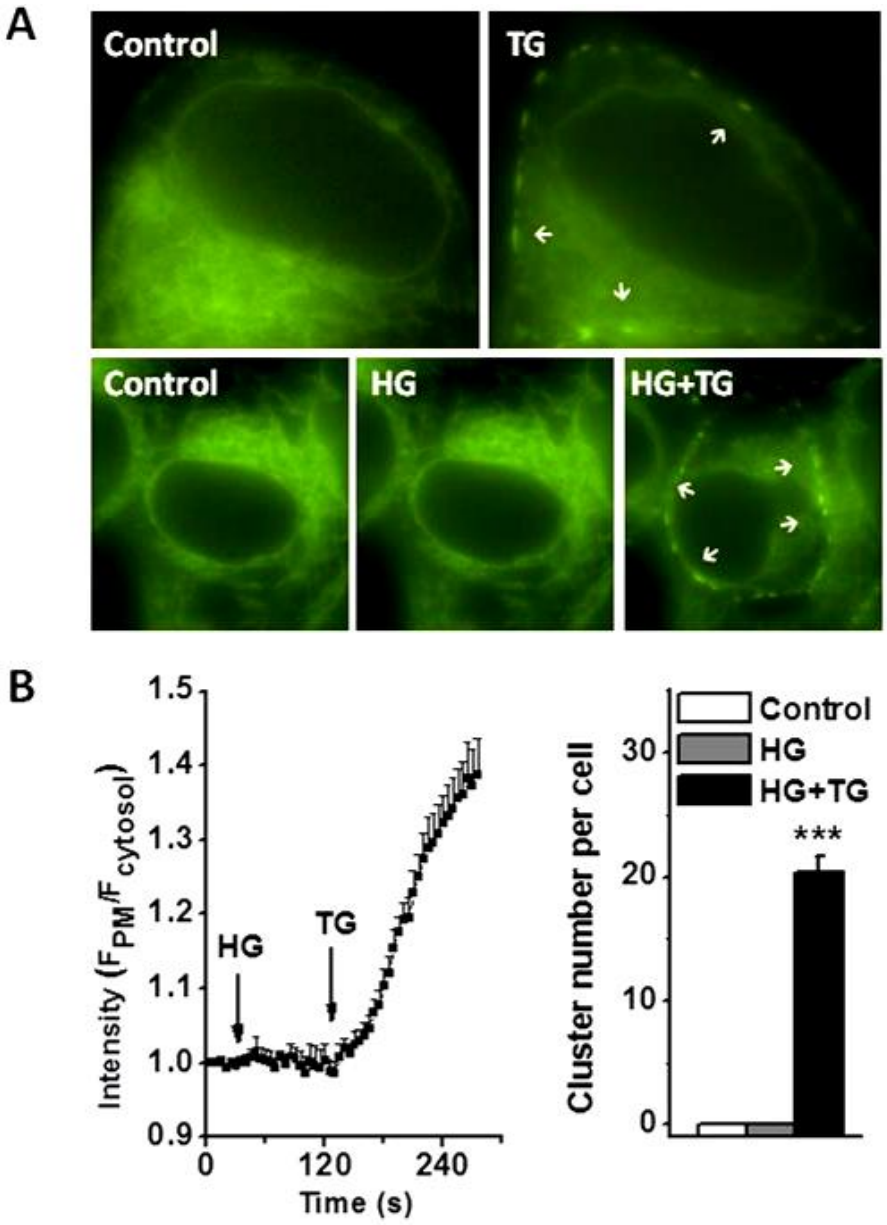

Figure 4-13 STIM1 translocation and clustering not affected by acute application of high glucose in the stable transfected STIM1–EYFP cells. A, STIM1 puncta formation at the PM of cells in Ca^{2+} bath solution induced by TG and the effect of high glucose (25 mM glucose, HG) after acute application. The arrows indicate the subplasmalemmal STIM1 clusters (puncta). Also see the supplementary Videos 1-3 in the CD attached to the thesis. **B,** The dynamic changes of ratio of fluorescent intensity in the PM (F_{PM}) and the cytosol ($F_{cytosol}$) of cells in response to HG acute application followed by TG (1 μM) application in Ca^{2+} bath solution and the number of STIM1 clusters on the PM before and after application of HG or HG plus TG (n = 15 cells in each group). The regions of interest (ROIs) of the PM and the nearby cytosol were manually selected. ***$P < 0.001$

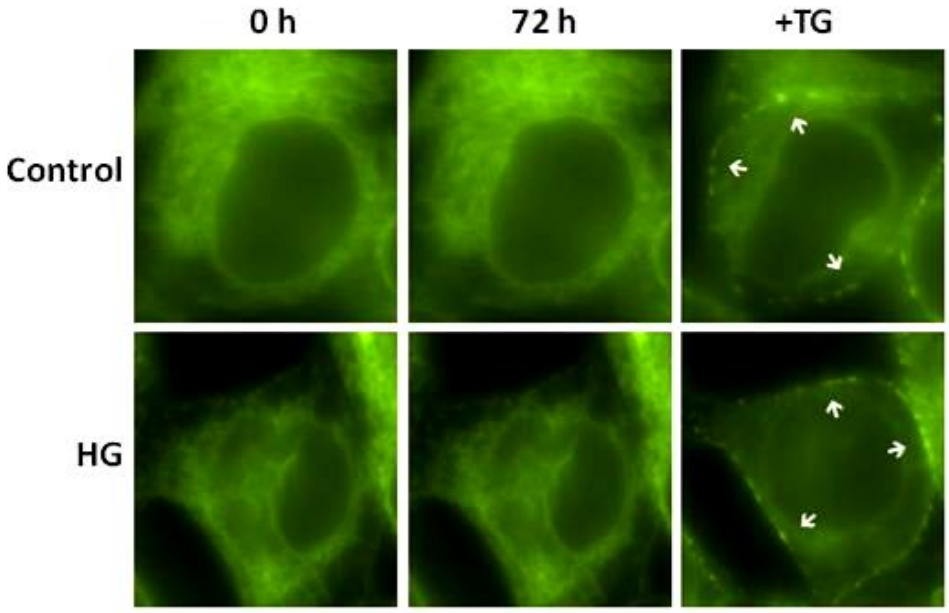

Figure 4-14 STIM1 translocation and clustering not affected by chronic treatment with high glucose in the stable transfected STIM1–EYFP cells. The stable transfected STIM1–EYFP cells were incubated with high glucose (25 mM glucose, HG) for 72 hours. STIM1 clustering was induced by application of TG (1 μM). The arrows indicate the subplasmalemmal STIM1 puncta.

4.5.2 STIM1 translocation regulated by homocysteine

No STIM1 puncta formation was observed following acute perfusion with 10 or 50 μM Hcy in the stable transfected STIM1–EYFP cells (Figure 4-15). However, STIM1 puncta appeared after addition of 1 μM TG in the bath solution, suggesting that Hcy does not interfere with STIM1 movement during store-operated channel activation. Similar to the effect of high glucose treatment, Hcy did not show any effect on the STIM1 movement by chronic incubation with 50 μM of Hcy for 24 hours (Figure 4-16).

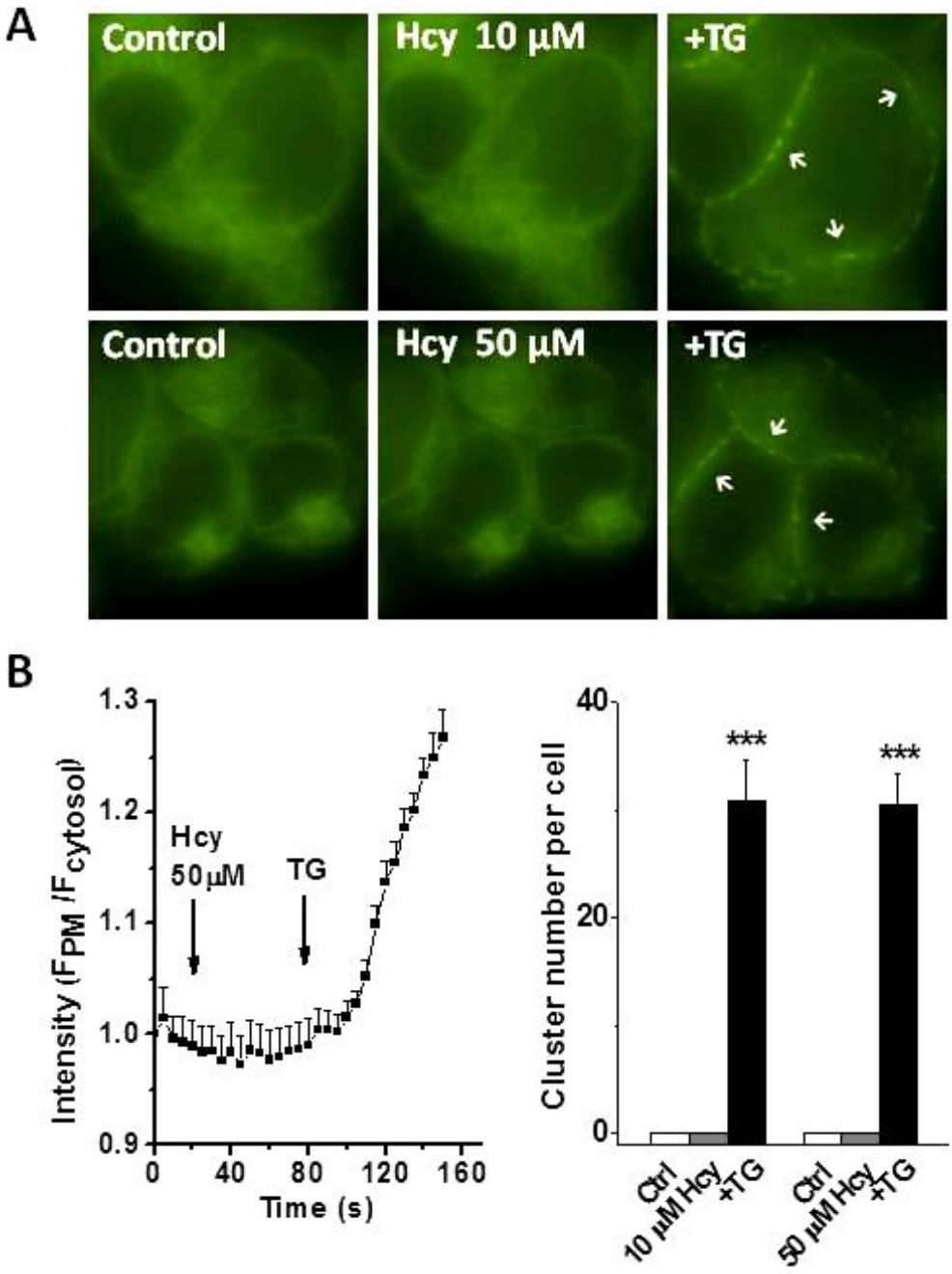

Figure 4-15 No effect of acute application of homocysteine on STIM1 movement in the stable transfected STIM1–EYFP cells. A, The effect of Hcy 10 or 50 µM acute application on STIM1 clustering and translocation. The arrows indicate the subplasmalemmal STIM1 puncta. **B,** The dynamic changes of ratio of fluorescent intensity in the PM (F_{PM}) and the cytosol ($F_{cytosol}$) of cells in response to Hcy acute application followed by TG (1 µM) application in Ca^{2+} bath solution and the number of STIM1 clusters on the PM before and after application of Hcy or Hcy plus TG (*n* = 12 cells in each group). The ROIs of the PM and the nearby cytosol were manually selected. ****P* < 0.001

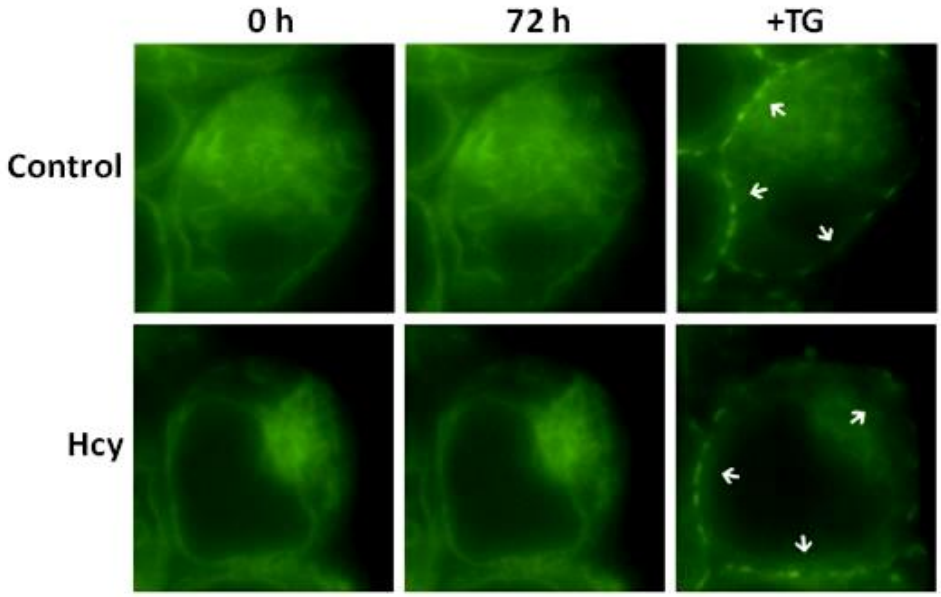

Figure 4-16 No effect of chronic treatment with homocysteine on STIM1 translocation and clustering in the stable transfected STIM1–EYFP cells. The stable transfected STIM1–EYFP cells were incubated with 50 μM Hcy for 24 hours. STIM1 clustering was induced by application of TG (1 μM). The arrows indicate the subplasmalemmal STIM1 puncta.

4.5.3 STIM1 translocation regulated by H_2O_2

In the HEK293 T-REx cells overexpressing STIM1-EYFP, acute application of 100 μM, 500 μM or 1 mM H_2O_2 did not cause STIM1 clustering or change the TG-induced STIM1 movement (Figure 4-17). These data suggest that H_2O_2 does not interfere with STIM1 movement during store-operated channel activation. No significant effects were also observed after incubation with 100 μM H_2O_2 for 48 hours (Figure 4-18).

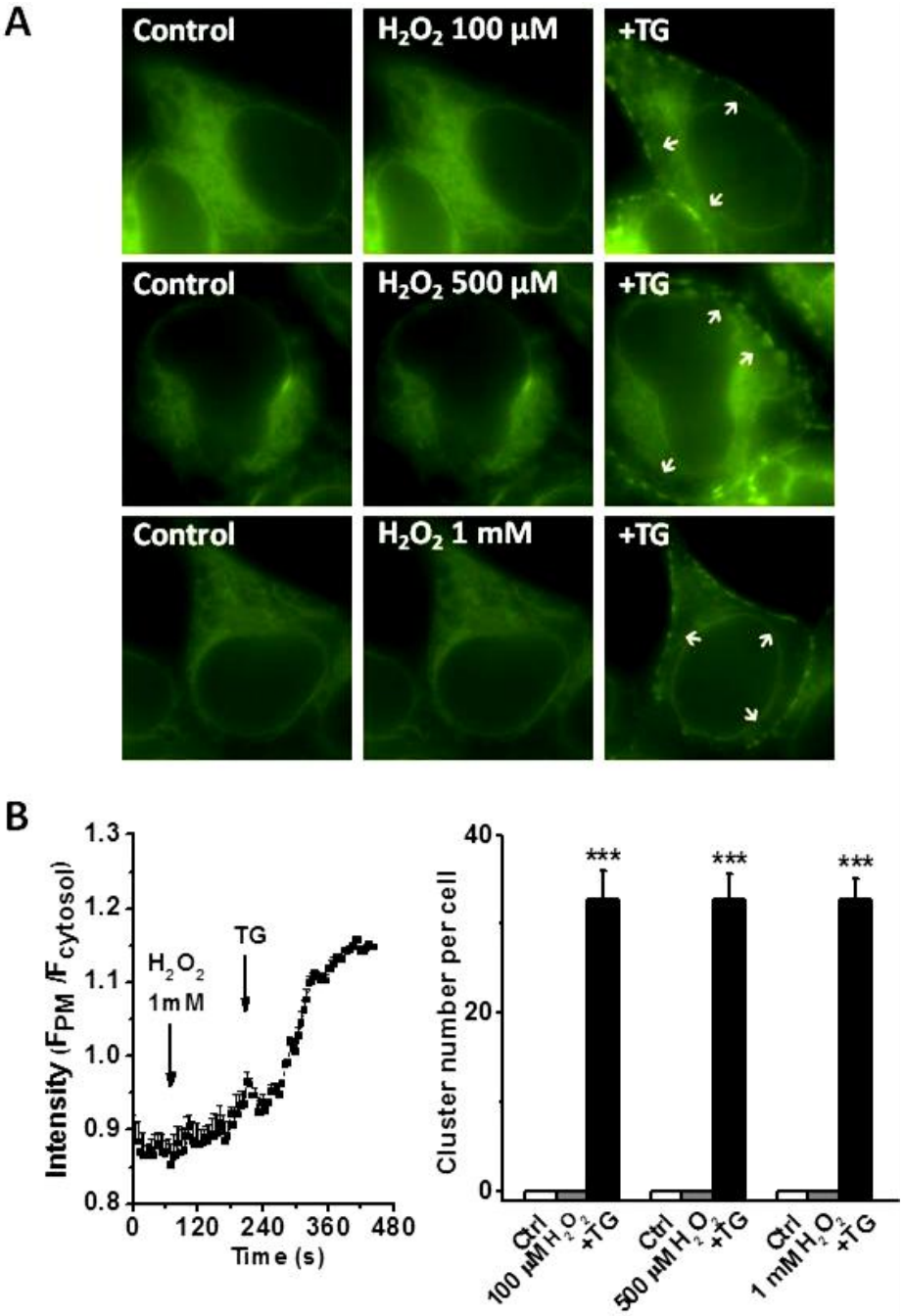

Figure 4-17 STIM1 translocation and clustering not affected by acute application of H_2O_2 in the stable transfected STIM1–EYFP cells. A, The acute effect of H_2O_2 100 μM, 500 μM or 1 mM on STIM1 clustering and translocation. The arrows indicate the subplasmalemmal STIM1 puncta. **B,** The dynamic changes of ratio of fluorescent intensity in the PM (F_{PM}) and the cytosol ($F_{cytosol}$) of cells in response to H_2O_2 acute application followed by TG (1 μM) application in Ca^{2+} bath solution and the number of STIM1 clusters on the PM before and after application of H_2O_2 or H_2O_2 plus TG (n = 11 cells in each group). The ROIs of the PM and the nearby cytosol were manually selected. ***$P < 0.001$

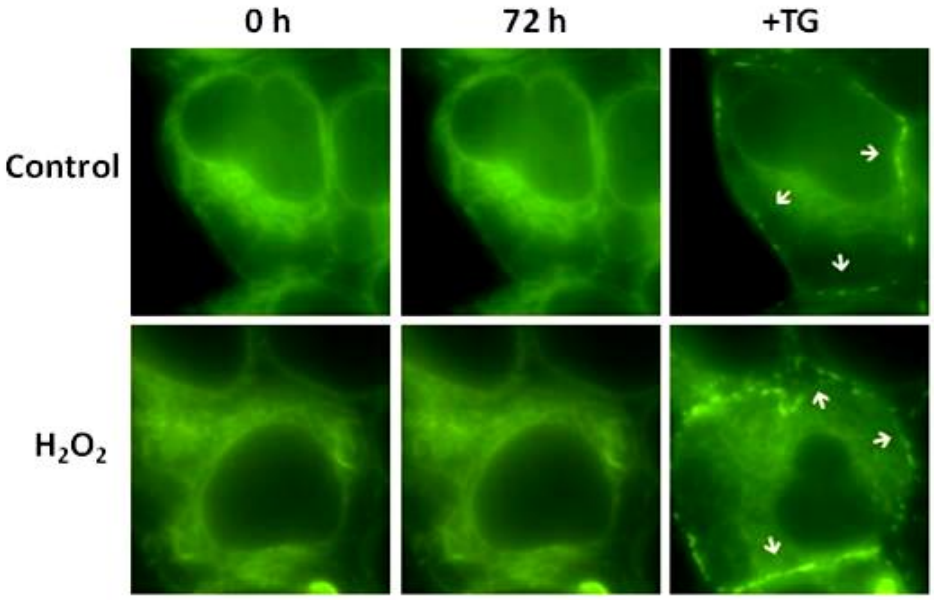

Figure 4-18 STIM1 translocation and clustering not affected by chronic treatment with H_2O_2 in the stable transfected STIM1–EYFP cells. The stable transfected STIM1–EYFP cells were incubated with 100 μM H_2O_2 for 48 hours. STIM1 clustering was induced by application of TG (1 μM). The arrows indicate the subplasmalemmal STIM1 puncta.

4.6 Endothelial function regulated by oxidative stress and the involvement of ORAI channels

4.6.1 Effect of high glucose on endothelial cell migration and tube formation

The effect of high glucose on endothelial cell migration was investigated using wound healing assay (Liang *et al.*, 2007). The EA.hy926 cells were cultured in the endothelial cell medium and treated with 25 mM glucose for 24 hours. The cell number migrated into the wound area was decreased in the high glucose-treated group compared to the group cultured in normal glucose (Figure 4-19 A-B). The experiment on tube formation revealed that EA.hy926 cells cultured under high glucose conditions lost their ability to form network connections between endothelial cells by 18% (Figure 4-19 C-D). These results suggest that endothelial cell migration and tube formation are inhibited by high glucose.

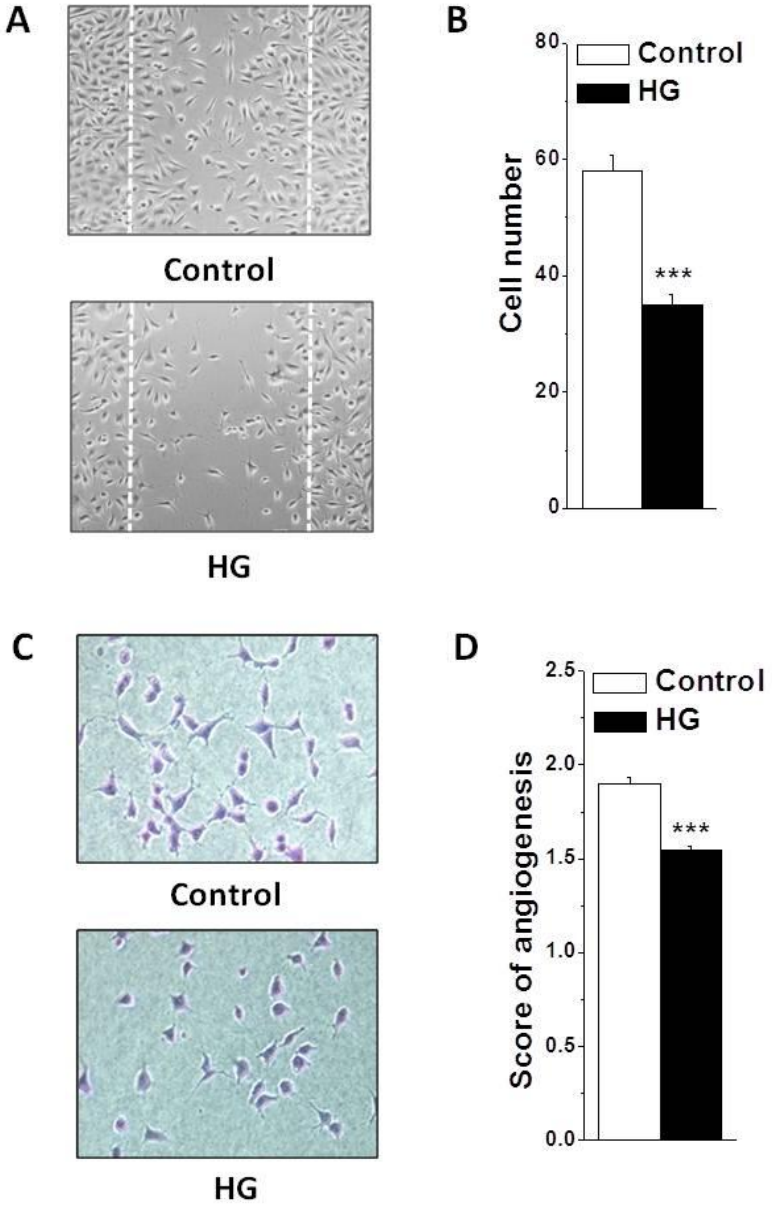

Figure 4-19 Migration and tube formation of endothelial cells inhibited by high glucose. A, Example of endothelial cells migration in the control and the high glucose (HG, 25 mM)-treated group. The migrated cells across the edge of the wound (dot line) were counted after 24 hours treatment with or without HG. **B,** Mean ± SEM data for the numbers of migrated cells (n = 5 experiments, 8 microscopic fields were recorded for each experiment). **C,** Example of endothelial cell tube formation in the control and the HG-treated group after 24 hours culture. **D,** Mean ± SEM data for the score of angiogenesis in the control and the HG treated group (n = 8 experiments, 4 microscopic fields were recorded for each experiment). ***P < 0.001

4.6.2 Involvement of ORAI channels in IL-6 secretion in endothelial cells

ORAI1-3 genes were silenced by siRNA transfection in HAECs. The gene silencing was confirmed by real-time PCR (Figure 4-20A). After transfection with ORAI siRNAs for 24 hours by incubation with the transfectants, the cell culture medium was collected and the amount of IL-6 secreted from the cells was measured using ELISA. IL-6 released from HAEC was significant increased after transfection with ORAI1 siRNAs comparing with the group transfected with scramble siRNA. The groups transfected with ORAI2 or ORAI3 siRNAs showed a tendency to increase the secretion of IL-6 (Figure 4-20B), suggesting that ORAI channels are involved in the IL-6 secretion in the endothelial cells.

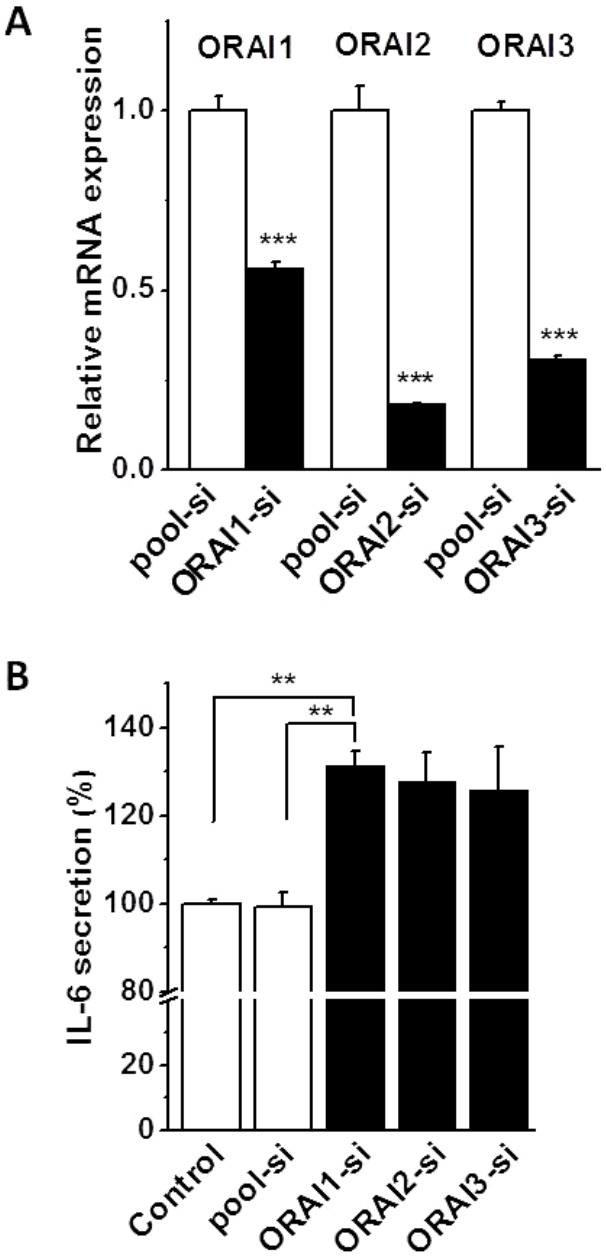

Figure 4-20 IL-6 secretion increased after ORAI silencing in HAEC. A, Silencing of ORAI1, ORAI2 and ORAI3 expression by siRNA transfection in HAEC was confirmed by real-time PCR. **B,** The effect on IL-6 secretion of HAEC after transfection with ORAI1, ORAI2 or ORAI3 siRNA (ORAI-si) and pool siRNA (pool-si) and mock transfection without siRNA (control). The amount of IL-6 was measured by ELISA in the medium collected at 12 hours incubation upon removal of the transfectants (n = 4 wells per experiment). ** $P < 0.01$; *** $P < 0.001$

4.6.3 Involvement of homocysteine in endothelial cell proliferation and IL-6 secretion

The data in 4.4.2 have demonstrated that Hcy can directly inhibit ORAI; therefore, the effect of Hcy on endothelial cell proliferation and the secretion of IL-6 were also examined. The HAECs were cultured in endothelial cell medium and the cell proliferation was measured by WST-1 assay. After incubation with Hcy at different concentrations for 12 hours, the cell proliferation was significantly inhibited (Figure 4-21A). The IL-6 released to the cell culture medium was measured and the amount of IL-6 was decreased by Hcy treatment (Figure 4-21B).

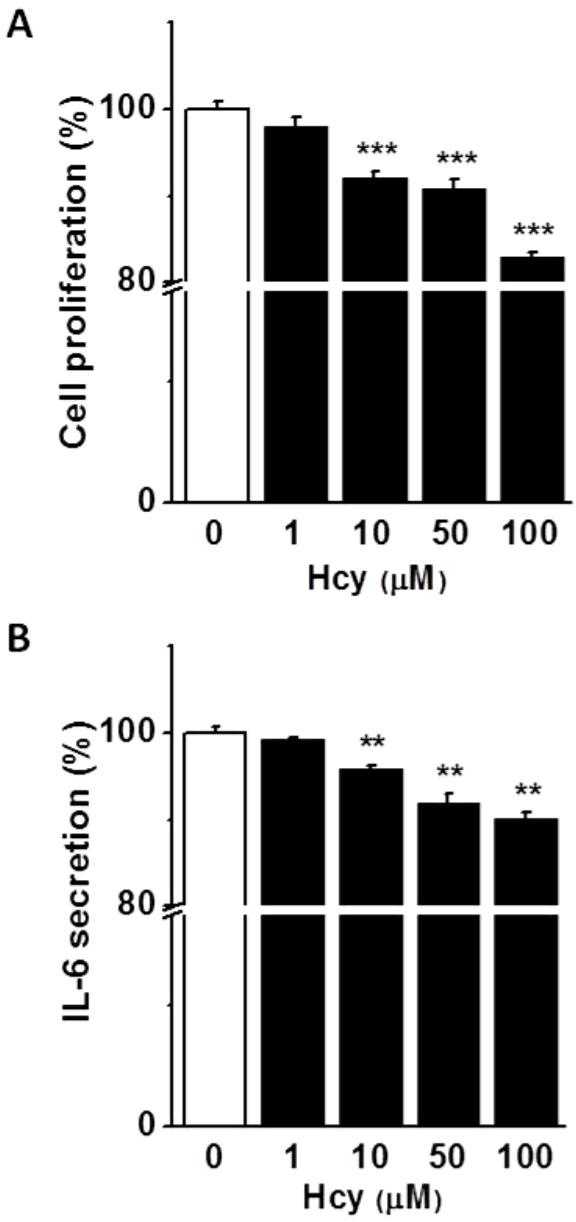

Figure 4-21 HAEC proliferation and IL-6 secretion inhibited by homocysteine. Cells were incubated with 1μM, 10μM, 50μM or 100μM Hcy in endothelial cell medium containing 10% FCS for 48 hours. Untreated cells were used as control. **A,** The cell proliferation was detected by WST-1 assay (n = 6). **B,** The IL-6 secretion was monitored by ELISA after 12 hours incubation with Hcy (n = 6). *** $P < 0.001$

4.7 Discussion

The data in this chapter show that SOCE is enhanced by chronic high glucose treatment in vascular endothelial cells. This enhancement is not mediated by the action on ORAI channel itself, because high glucose does not change the ORAI currents directly in the cells overexpressing ORAI channels. Cytosolic STIM1 movement is also not involved in this effect, because acute application or chronic treatment with high glucose, Hcy or H_2O_2 have no direct effect on the STIM1-EYFP translocation and clustering or the TG-induced STIM1 clustering and translocation. Nevertheless, ORAI1-3 channel activity was directly inhibited by Hcy and it is firstly demonstrated here that DES inhibits ORAI1-3 channels. In addition, the endothelial functions including cell proliferation, migration, tubular formation and IL-6 secretion were also studied by application of high glucose or Hcy or transfected with ORAI siRNAs.

Intracellular Ca^{2+} level or Ca^{2+} homeostasis has been shown to be affected by high glucose in early studies (Kimura *et al.*, 1998a; Kimura *et al.*, 1998b; Pieper & Dondlinger, 1998). The response to high glucose could be different depending on the acute application or chronic treatment. Acute application with high glucose had less effect on Ca^{2+} influx seen in this study and early reports (Graier *et al.*, 1993), but chronic treatment by incubation with high glucose for 2-4 days significantly increased the Ca^{2+} influx in the EA.hy926 cells seen in this study, in HUVECs (Tamareille *et al.*, 2006) and in bovine aorta endothelial cells (Bishara & Ding, 2010). These findings suggest that the upregulation of ORAI and STIM expression may be the main mechanism to explain the high glucose-induced increase in intracellular Ca^{2+} level, because high glucose did not change the ORAI channel activity in the cells overexpressing ORAI1-3. Ca^{2+} release and OAG-induced Ca^{2+} influx was also increased in vascular endothelial cells by chronic treatment with high glucose (Liu *et al.*, 2008), suggesting the involvement of other Ca^{2+} permeable channels in the high glucose-regulated Ca^{2+} homeostasis.

In order to examine the direct effects of oxidative stress on ORAI channels, the STIM1/ORAI1, STIM1/ORAI2 or STIM1/ORAI3 were expressed in the HEK293 cells using Tet-On expression system. The currents in the cells can be activated by

TG for ORAI1-2 and 2-APB for ORAI3, which is in agreement with the previous reports (Yeromin *et al.*, 2006; DeHaven *et al.*, 2008), suggesting the cloning and functional expression system are successful in this study. In addition, the ORAI protein PM localization in the expressed cells, the dependence of STIM1, and characteristics of ORAI current *IV* curves also indicate that the Tet-On system can be used for studying the store-operated ORAI channel properties.

After the characterization of the currents in the inducible STIM1/ORAI HEK293 cells, the effect of the oxidative stress-inducing compounds on ORAI channel activity was examined directly by acute perfusion. No direct effects of high glucose on ORAI1-3 currents were observed in the whole-cell patch clamp experiments. However, the data in this chapter show for the first time that Hcy inhibits ORAI1-3 channel current directly, which could be the molecular mechanism to explain the inhibition of SOCE in the endothelial cells demonstrated in our lab (unpublished data) and others (Zhang *et al.*, 2005). These results taken together with the downregulation of ORAI isoforms mRNA and protein expression by Hcy observed in previous chapter may suggest a differential effect between Hcy and high glucose or H_2O_2 and indicate that the effect of Hcy on store-operated channels is mediated by both direct effect on channel itself and the regulation on gene expression.

The direct effect of DES, a native store-operated channel blocker (Zakharov *et al.*, 2004), on ORAI1, ORAI2 and ORAI3 channel current was firstly examined in the present study. DES at 10 μM inhibited all the three ORAI isoforms channel activity. DES also inhibited the expression of ORAI1-3 mRNA in vascular endothelial cells, suggesting that DES affects ORAIs via the regulation of gene expression and the direct action on channel activity per second. 2-APB is another store-operated channel blocker in many native cells, however, 2-APB showed differential effects on ORAI channels, i.e., inhibition on ORAI1 and ORAI2 currents, but stimulation on ORAI3 channel, which is consistent with the previous reports (Peinelt *et al.*, 2008; Schindl *et al.*, 2008).

The active or passive Ca^{2+} store depletion in the ER is an essential step for subplasmalemmal STIM1 clustering and movement that follows after the application of SERCA blockers TG and cyclopiazonic acid (Liou *et al.*, 2005; Zhang, 2005), or through IP_3R activation by many GPCR agonists such as carbachol (Smyth *et al.*,

2008) and ATP/ UTP, respectively (Ross *et al.*, 2007; Chvanov *et al.*, 2008). Since this mechanism has been regarded as a crucial step for the SOCE process, the effect of oxidative stress on STIM1 clustering and translocation was tested in the stably transfected STIM1-EYFP cells. TG-induced STIM1 clustering and translocation was confirmed in the stably transfected STIM1 cells and oxidative stress conditions were mimicked by acute application or chronic exposure to high glucose, Hcy or H_2O_2. SOCE was increased by chronic treatment with high glucose but high glucose did not evoke STIM1 clustering or affect the TG-induced STIM1 clustering. Although there was a direct inhibition of ORAI1-3 current by Hcy, no effect was observed on STIM1 clustering and movement or the TG-induced STIM1 clustering and movement, suggesting that Hcy may not interference with the channel activation process. Moreover, H_2O_2 had no acute or chronic effect on STIM1 clustering and movement, despite the fact that the I_{CRAC} current was reported to be activated by H_2O_2 (Grupe *et al.*, 2010).This is probably because these compounds do not cause a big Ca^{2+} release, thus no STIM1 clustering and subsequently movement is promoted.

In addition, we recently examined the link of cytosolic STIM1 movement to mitochondrial functions (Zeng *et al.*, 2012). Reagents that affect mitochondrial oxidative stress and damage, such as H_2O_2 and mercury, showed no effect on STIM clustering and translocation, which further supports the findings in this chapter. However, reagents that induce mitochondrial Ca^{2+} release, such as the mitochondrial metabolic inhibitors 4-(trifluoromethoxy)phenylhydrazone (FCCP) and sodium azide, or the non-steroidal anti-inflammatory drug flufenamic acid, were able to induce a pattern of cytosolic STIM1 clustering, but no subplasmalemmal translocation.

Changes in the intracellular free Ca^{2+} concentration are key factors for cellular functions. Oxidative stress-induced alteration of Ca^{2+} concentration triggers various cellular processes. However, different cells may have different outcomes depending on the expression levels of each isoforms and their partner proteins. In the present study, high glucose and Hcy were used to examine their effect on endothelial cell functions. Migration and proliferation of EA.hy926 cells was significantly inhibited by high glucose treatment, while high glucose was reported to induce apoptosis (Tamareille *et al.*, 2006) or the inhibition of cell proliferation in HUVECs (Xu *et al.*,

2009). However, retinal endothelial cells and ECV304 cells may have different properties, because it has been reported that high glucose may stimulate the migration and tubular formation in these cells (Shigematsu *et al.*, 1999; Huang & Sheibani, 2008). The capillary-like structure formation was decreased in the HUVECs (Luo *et al.*, 2008), which could be due to the inhibition of cell proliferation under high glucose conditions (Xu *et al.*, 2009).

For the effects of Hcy on endothelial functions, the IL-6 secretion, endothelial cell proliferation and ORAI channel activity were all changed by Hcy, suggesting the effects and mechanisms of Hcy could be multifaceted and need to be further investigated. The effects of Hcy on ORAI gene expression and channel activity could be difficult to explain the decrease in IL-6 secretion, because the gene silence of ORAIs seems to increase the production of IL-6.

4.8 Summary

In this chapter, store-operated and non-store-operated Ca^{2+} influx were found to be increased after chronic treatment with high glucose in vascular endothelial cells. However, ORAI1-3 channel currents and STIM1 clustering and translocation are not affected by high glucose, which suggests that the high glucose-induced enhancement of intracellular Ca^{2+} level may be explained only by the upregulation of ORAI and STIM expression in diabetic conditions and not by a direct effect on the channel activity. On the other hand, Hcy inhibits ORAI1-3 channel currents, which may be mediated by a mechanism different from the oxidative stress conditions induced by high glucose or H_2O_2. However, the store-operated channel activation mechanism via the interference with intracellular STIM1 clustering and translocation in not involved in this process since no STIM1 clustering and translocation was observed after treatment with Hcy. Moreover, direct evidence of DES as a pan inhibitor of ORAI1-3 channels is provided by the data in this chapter, which is useful for future pharmacological research. The vascular endothelial cell functions- proliferation, secretion, migration and tube formation- were inhibited by high glucose or Hcy. All these findings give a new molecular insight of store-operated Ca^{2+} signalling

pathway under oxidative stress conditions, which may be developed as new potential therapeutic targets for the treatment of diabetic vascular complications.

Chapter 5

Osmolarity Sensitivity of ORAI Channels

5.1 Introduction

Hyperosmolar hyperglycaemic state (HHS) is a complication of diabetes mellitus, which may lead to a life-threatening endocrine emergency. HHS is characterized by marked hyperglycemia (blood glucose more than 33.3 mM) and high serum osmolarity (usually higher than 320 mOsm/kg), but without significant hyperketonaemia (<3 mmol/L) or acidosis (pH>7.3, bicarbonate >15 mmol/L) (Chiasson *et al.*, 2003; Kitabchi *et al.*, 2008). There are several Ca^{2+}-permeable channels regulated by osmolarity, however, the involvement of store-operated channels in the hyperosmolarity is unknown.

Changes in osmolarity induce osmotic pressure that results in alterations in cell volume. A rapid osmotic swelling or shrinkage is induced upon sudden exposure of cells to hypo- or hyperosmotic solutions, respectively, affecting mechanisms involved in the regulation of gene expression and metabolism (Lang *et al.*, 1998). Anabolic metabolism and proliferation is stimulated by cell swelling whereas catabolism, insulin resistance and sensitivity to apoptotic stimuli are induced by cell shrinkage (Haussinger & Lang, 1992; Lang *et al.*, 1998; Schliess *et al.*, 2001).

The alteration of intracellular Ca^{2+} level has been demonstrated under hyperosmotic conditions, which could be one of the potential mechanisms for the hyperosmolar state (Kajimura & Curry, 1999; Paemeleire *et al.*, 1999; Marchenko & Sage, 2000; Sanchez & Wilkins, 2004). Some Ca^{2+} permeable channels are regulated by osmolarity, for instance, the transient receptor potential vanilloid 2 (TRPV2) that can be activated by hypoosmolarity-triggered cell swelling in mouse aortic smooth muscle cells (Muraki *et al.*, 2003). TRPV4 has also been demonstrated as an osmolarity-sensitive channel (Strotmann *et al.*, 2000). In addition, hyperosmolarity-induced cell shrinkage causes rapid production of ROS in human hepatocytes, suggesting a link between hyperosmolarity and oxidative stress (Becker *et al.*, 2007; Schliess *et al.*, 2007). Due to the relevance of Ca^{2+} signalling and ROS production under hyperosmolarity state and the regulation of ORAI and STIM channel molecules by oxidative stress, the involvement of ORAIs and STIMs in the pathophysiology of hyperosmolarity is examined here.

In this chapter, I aimed to investigate the effect of hyperosmolarity on vascular endothelial cell migration, store-operated Ca^{2+} influx and the expression of ORAI and STIM channel molecules in vascular endothelial cells. The direct effect of hyperosmolarity on ORAI1-3 channel current and on STIM1 clustering and translocation was also investigated in the inducible ORAI/STIM1 HEK293 cells.

5.2 Effect of hyperosmolarity on endothelial cell migration

The effect of hyperosmolarity on endothelial cell migration was investigated using wound healing assay (Liang *et al.*, 2007). The EA.hy926 was cultured in endothelial cell medium and treated with 19.5 mM mannitol for 24 hours. The cell number migrated into the wound area was decreased in the mannitol-treated group compared to the control group cultured in normal glucose (Figure 5-1), suggesting the hyperosmolarity decreases the endothelial cell migration.

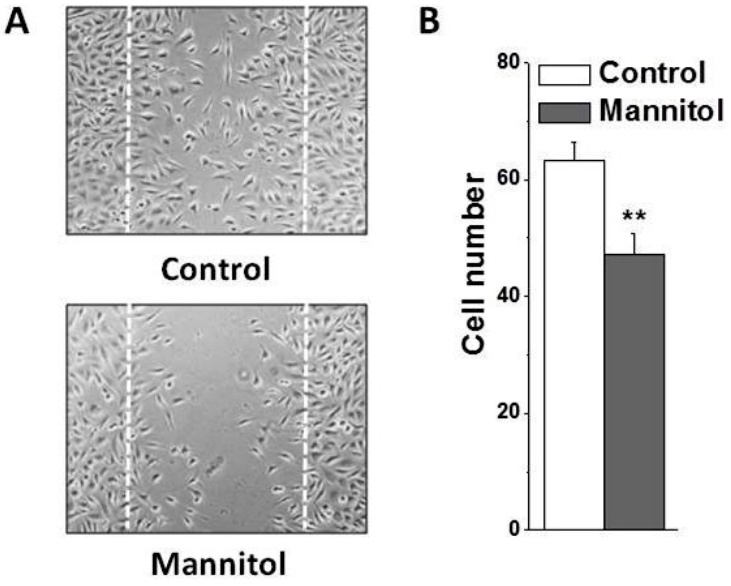

Figure 5-1 Effect of hyperosmolarity on endothelial cell migration. A, Example of endothelial cells migration in the control (without mannitol) and the mannitol (19.5 mM)-treated group. The migrated cells across the edge of the wound (dot line) were counted after 24 hours treatment. **B,** Mean ± SEM data for the numbers of migrated cells (*n* = 5 experiments, 8 pictures per experiment).

5.3 Ca^{2+} entry decreased by hyperosmolarity in vascular endothelial cells

EA.hy926 cells were cultured in endothelial medium with the addition of 19.5 mM mannitol for 72 hours. The intracellular Ca^{2+} concentration was monitored by Ca^{2+} imaging. Mannitol inhibited Ca^{2+} influx evoked after changing from Ca^{2+}-free to Ca^{2+} solution. No difference was observed between control and mannitol-treated cells in Ca^{2+} peak after admission of 1 μM trypsin, suggesting that mannitol has no effect on Ca^{2+} release. However, the Ca^{2+} influx after readmission of Ca^{2+} solution after store-depletion by trypsin was inhibited by mannitol (Figure 5-2).

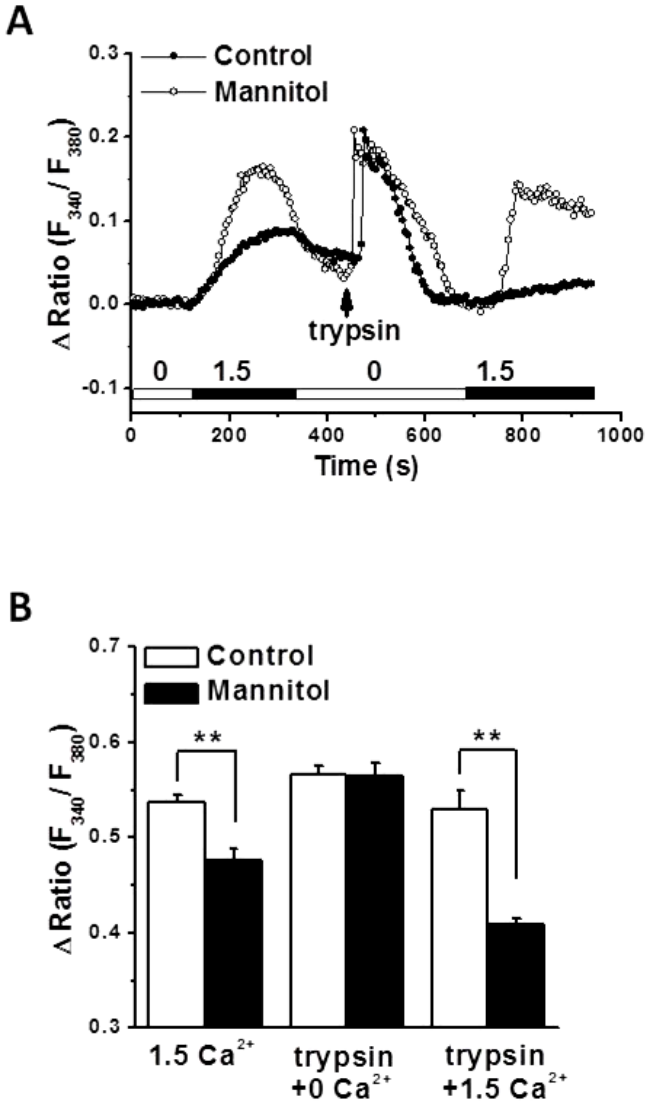

Figure 5-2 Ca^{2+} influx inhibited by mannitol in EA.hy926 cells. The EA.hy926 cells were cultured in the endothelial cell medium. The changes in $[Ca^{2+}]_i$ was measured as ratios of fluorescence excited at 340 and 380 nm in the Fura-PE3/AM loaded cells. **A,** Ca^{2+} imaging in untreated (control) and mannitol (19.5 mM)-treated cells. **B,** Mean ± SEM data for the Ca^{2+} influx, Ca^{2+} release and Ca^{2+} re-entry in the mannitol-treated (n = 12) and untreated (n = 10) cells. $^{**}P < 0.01$

5.4 ORAI and STIM expression downregulated by hyperosmolarity

The mRNA level of ORAI1, ORAI2, ORAI3, STIM1, and STIM2 was significantly decreased in the EA.hy926 cells incubated with 19.5 mM mannitol for 60 hours, comparing with the normal osmolarity group with 5.5 mM glucose (Figure 5-3A). Using western blotting, the protein expression of ORAI and STIM isoforms was also significantly reduced by 19.5mM mannitol treatment (Figure 5-3 B-C).

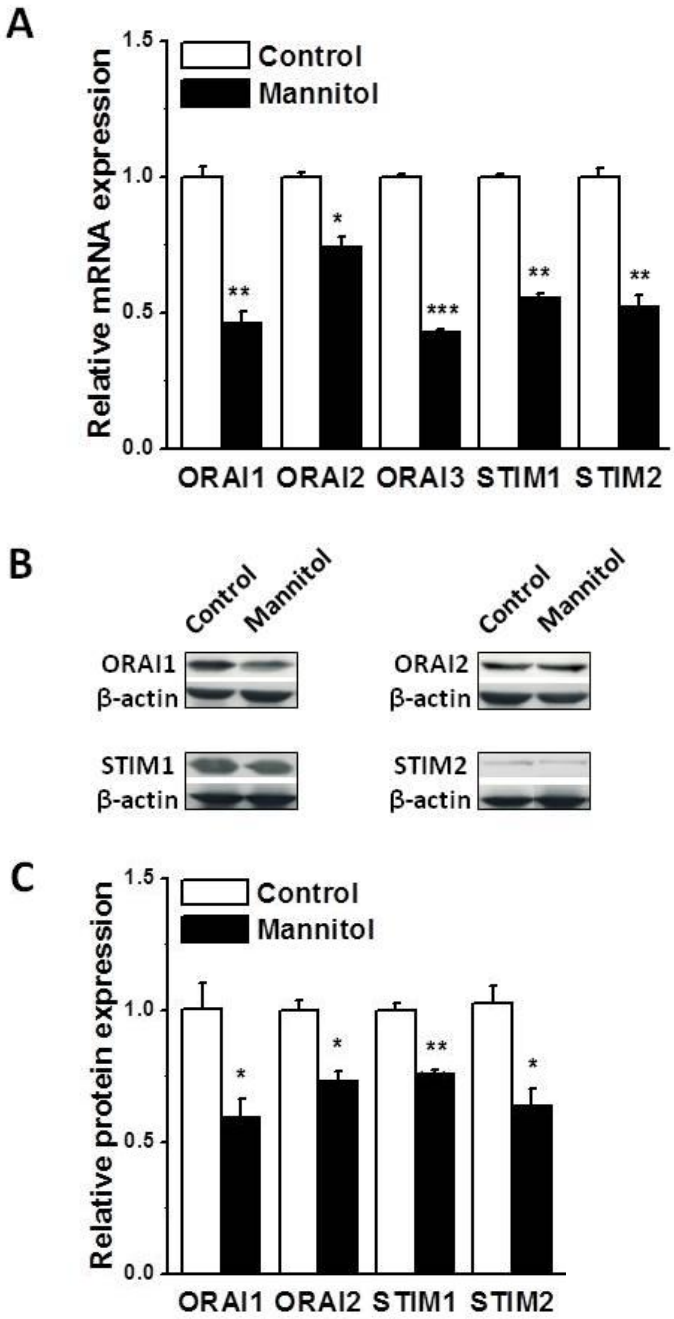

Figure 5-3 Downregulation of ORAI and STIM expression by hyperosmolarity. **A,** EA.hy926 cells were cultured with mannitol (19.5 mM) in normal glucose (5.5 mM) for 60 hours. The cells in the control group were incubated in normal medium containing 5.5 mM glucose. The mRNA expression was detected by real-time PCR and β-actin was used as internal house-keeping gene control for quantification. **B,** Example of the detection of ORAI and STIM proteins by western blotting. The β-actin was used as control for quantification. **C.** Mean data from 3 independent experiments with triplicate samples are presented. $*P < 0.05$, $**P < 0.01$, $***P < 0.001$

5.5 Inhibition of ORAI channels by hyperosmolarity

Since the expression of ORAI isoforms can be downregulated by hyperosmolarity in vascular endothelial cells, but the direct effect of hyperosmolarity on these channels is unknown, therefore, I examined whether mannitol affects the ORAI channels directly. Whole-cell patch clamp experiments were performed in the inducible HEK293 T-REx cells co-expressed with STIM1-EYFP and mCherry-tagged ORAI1 or ORAI2, or mCFP-tagged ORAI3 to obtain the *IV* relationship of the channels. When a stable current was observed, acute perfusion with 19.5 mM mannitol inhibited the TG-induced ORAI1 and ORAI2 currents and the 2-APB-induced ORAI3 current (Figure 5-4). Perfusion with 9.75 mM mannitol had 52% of the inhibitory effect that perfusion with 19.5 mM mannitol had on ORAI1 current (Figure 5-4A).

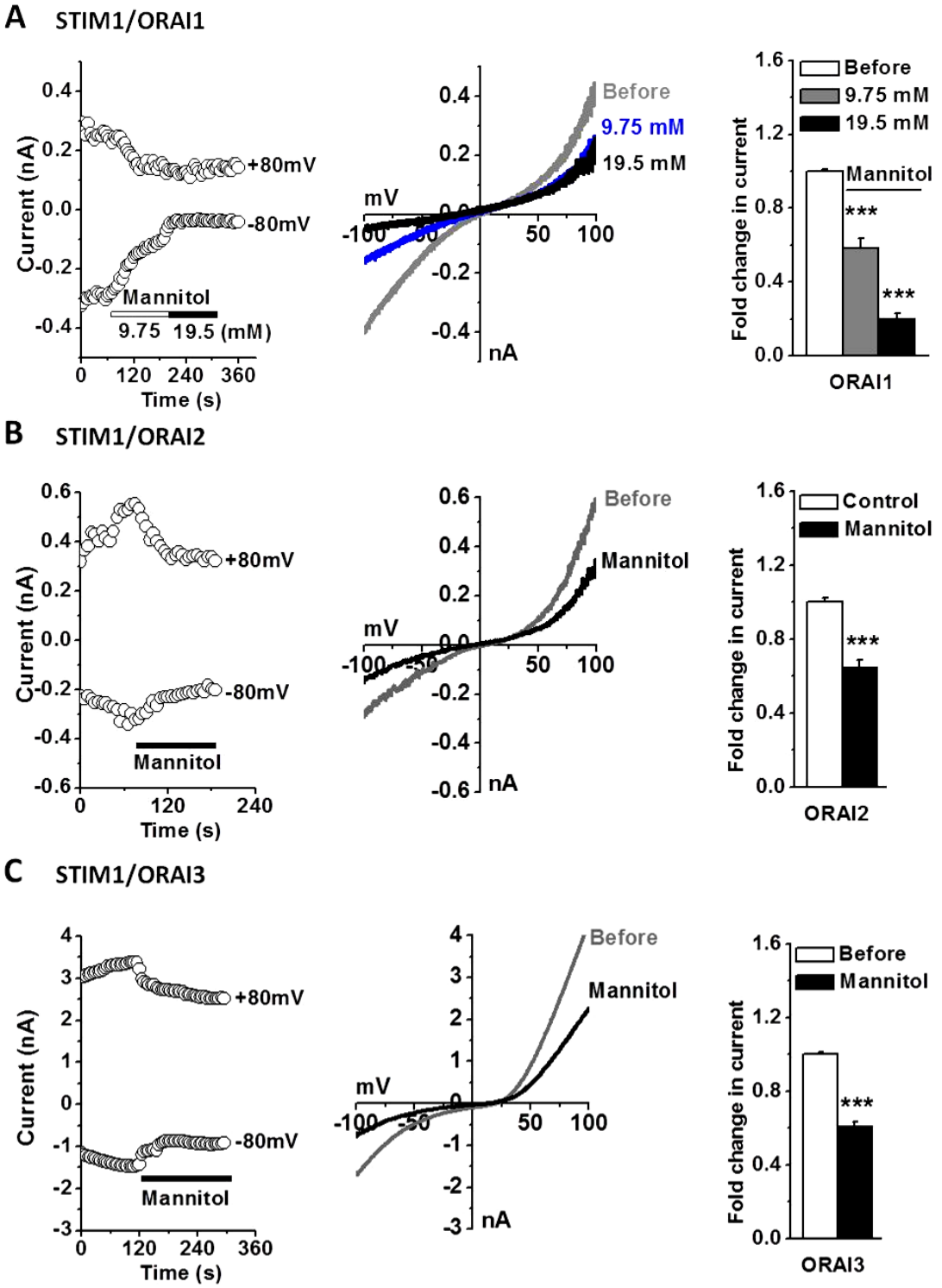

Figure 5-4 Effect of mannitol on ORAI1-3 channel activity. Whole-cell current was recorded in the inducible HEK293 T-REx cells co-expressed with STIM1-EYFP and ORAI1-3. **A,** ORAI1. **B,** ORAI2. **C,** ORAI3. The ORAI1 and ORAI2 currents were activated by 1 μM TG in the bath solution, and ORAI3 current was activated by 100 μM 2-APB in the bath solution. Representative *IV* curves and time-courses are presented. Bar charts present the averaged data showing the effect of 9.75 mM or 19.5 mM mannitol on ORAI1 channel activity or the effect of 19.5 mM mannitol on ORAI2,3 channel activity (n = 9 for each group). ***$P < 0.001$

5.6 Effect of hyperosmolarity on STIM1 clustering and translocation

Activation of ORAI channels is triggered by STIM1 subplasmalemmal translocation and clustering (Zhang, 2005; Zeng *et al.*, 2012), so the effect of STIM1 translocation and clustering was also examined. In the HEK293 T-REx cells overexpressing STIM1-EYFP, no STIM1 translocation and puncta formation was observed after treatment with mannitol (19.5 mM) for 72 hours. STIM1 translocation and puncta formation was evoked by TG (Figure 5-5). These data suggest that mannitol has no direct effect on the STIM1 movement.

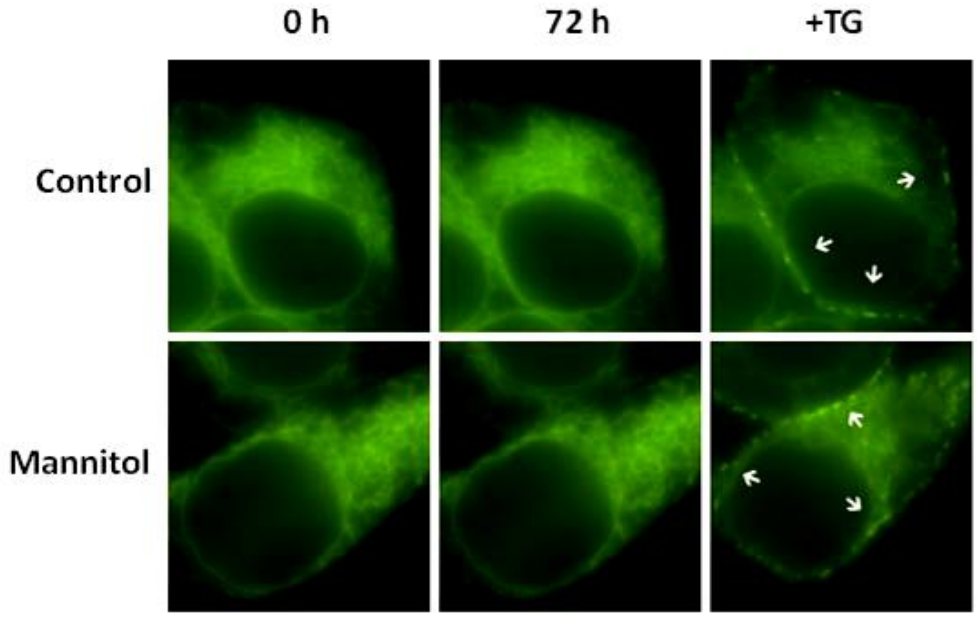

Figure 5-5 Effect of hyperosmolarity on STIM1 translocation and clustering. The stable transfected HEK293 STIM1-EYFP cells were cultured in DMEM/F-12+GlutaMax™-I media and treated with mannitol 19.5 mM for 72 hours, followed by application of TG 1 μM. Untreated cells were used as control. The arrows indicate the subplasmalemmal STIM1 puncta. ***$P < 0.001$

5.7 Discussion

The results in this chapter show that hyperosmolarity decreases endothelial cell migration, store-operated Ca^{2+} influx and the expression of ORAI and STIM in vascular endothelial cells. Hyperosmolarity also inhibits ORAI channel activity directly without effecting cytosolic STIM1 movement during store-operated Ca^{2+} channel activation.

Endothelial cell migration was reported to be regulated by Ca^{2+} influx through TRPC5,6 channels (Chaudhuri *et al.*, 2008) and hyperosmolarity increased Ca^{2+} concentration in endothelial cells and hepatocytes (Paemeleire *et al.*, 1999; Krumschnabel *et al.*, 2003). Some Ca^{2+} channels are directly affected by osmolarity changes. For instance, L-type Ca^{2+} channel activity was enhanced in rat portal vein smooth muscle cells after superfusion with hypotonic solution. The mechanism could be through the activation of protein kinase C (Ding *et al.*, 2004). Another report showed that increased osmolarity reduced the activity of voltage-gated L-type Ca^{2+} channel currents in rat anterior pituitary cells (Ben-Tabou De-Leon *et al.*, 2006). However, there is no report regarding the role of hyperosmolarity in the regulation of SOC channels.

Mannitol was used in the present study to mimic a condition of hyperosmolarity. Whole-cell patch clamp experiments using the inducible ORAI/STIM1 HEK293 cells revealed that mannitol has a direct inhibitory effect on ORAI1-3 channel current. The corresponding concentration of high glucose had no effect on channel activity, thus it is suggested that the observed inhibition of channel current was an effect of osmolarity. Additionally, ORAI1 channel showed a dose-response inhibition under perfusion with mannitol solution. In agreement with this result, the results in this chapter demonstrated that hyperosmolarity inhibited SOCE in vascular endothelial cells. Moreover, the expression of ORAI and STIM was downregulated by hyperosmolarity. However, STIM1 puncta formation and movement was not affected by chronic treatment with mannitol, suggesting that STIM1 translocation does not play any role on mannitol-inhibited store-operated Ca^{2+} influx. This is a novel mechanism that needs to be elucidated in depth. The direct effect of hyperosmolarity on channel current may have a big significance in pathology as it is

presented here that migration of endothelial cells was inhibited by hyperosmolarity and it is already known that hyperosmolarity can be seen in diabetic conditions such as the HHS observed in Type 2 diabetes (Kitabchi *et al.*, 2008).

5.8 Summary

The data in this chapter demonstrate that ORAI is an osmolarity-sensitive channel. Hyperosmolarity decreased SOCE in vascular endothelial cells via direct inhibition of ORAI channel current and downregulation of ORAI and STIM channel expression. Migration of vascular endothelial cells is also inhibited by hyperosmolarity. Since HHS is a severe complication of diabetes, the novel mechanism of the sensitivity of ORAI channels to hyperosmolarity and the relevance to endothelial functions may provide a new understanding of the pathological mechanisms of diabetes and diabetic vascular complications.

Chapter 6

General Discussion

6.1 Main results and significance of the study

In this study, ORAI1-3 and STIM1-2 were detected in vascular endothelial cells and smooth muscle cells and it was found that their mRNA and protein expression is upregulated by chronic treatment with high glucose in cell models. Expression of ORAI1-3 and STIM1-2 is also upregulated in human aorta from Type 2 diabetic patients and kidney tissues from streptozotocin-induced and Akita Type 1 diabetic mouse models. CsA and store-operated channel blocker DES prevent the high glucose-induced gene upregulation. H_2O_2 also upregulates ORAI1-3 and STIM1-2; however, Hcy increases STIM1-2 expression, but downregulates ORAI1-3. Store-operated Ca^{2+} influx is enhanced by chronic treatment with high glucose in endothelial cells but there is no effect if treated acutely. High glucose has no direct effect on ORAI1-3 currents, but Hcy decreases the currents in HEK-293 cells overexpressing STIM1/ORAI1-3. STIM1-EYFP translocation and clustering after Ca^{2+} store-depletion are not affected by oxidative stress. It is also demonstrated here that hyperosmolarity inhibits ORAI1-3 currents and SOCE and downregulates ORAI1-3 and STIM1-2 gene expression, but does not alter cytosolic STIM1-EYFP translocation. These data are novel and important for understanding the pathophysiology of diabetic blood vessels. The upregulation of ORAI and STIM store-operated Ca^{2+} channel molecules is one of the mechanisms contributing to the impaired Ca^{2+} homeostasis in diabetic blood vessels or oxidative stress-related vascular injury.

6.2 Mechanism of high glucose-induced upregulation of SOCE

Based on the findings in Chapters 3-4, the model for the mechanisms of high glucose-induced upregulation of ORAI and STIM is proposed in Figure 6-1. High glucose increases intracellular Ca^{2+} concentration. The Ca^{2+} will bind the Ca^{2+} sensor protein calmodulin, which activates the phosphatase calcineurin. The activation of calcineurin results in dephosphorylation and nuclear import of NFAT proteins, and thus leads to the change of ORAI and STIM gene transcription. The effect of high glucose is prevented by inhibition of calcineurin with CsA or inhibition of SOCE

with DES, which provides the evidence of calcineurin and Ca^{2+} in the signalling pathway. Since there is no direct effect of high glucose on ORAI channel current or STIM1 translocation, the upregulation of store-operated channel genes could be the main mechanism for the high glucose-induced intracellular Ca^{2+} overload. The Ca^{2+}/calcineurin/NFAT pathway regulated by high glucose could be a positive feedback mechanism between the channel expression and SOCE.

Moreover, it is already known that high glucose induce the overproduction of ROS, such as H_2O_2, via both the NADPH oxidase system and the mitochondrial metabolism (Peiro *et al.*, 2001; Mortuza *et al.*, 2013) and this could be another potential pathway for upregulation of ORAI and STIM. This is based on the evidence that ORAI and STIM expression was upregulated by H_2O_2 and also I_{CRAC} current and other Ca^{2+}-permeable channels were activated by H_2O_2 (Xu *et al.*, 2008b; Grupe *et al.*, 2010; Chen *et al.*, 2012). This activation may lead to increased intracellular Ca^{2+} concentration and subsequently activation of the downstream calcineurin/NFAT pathway.

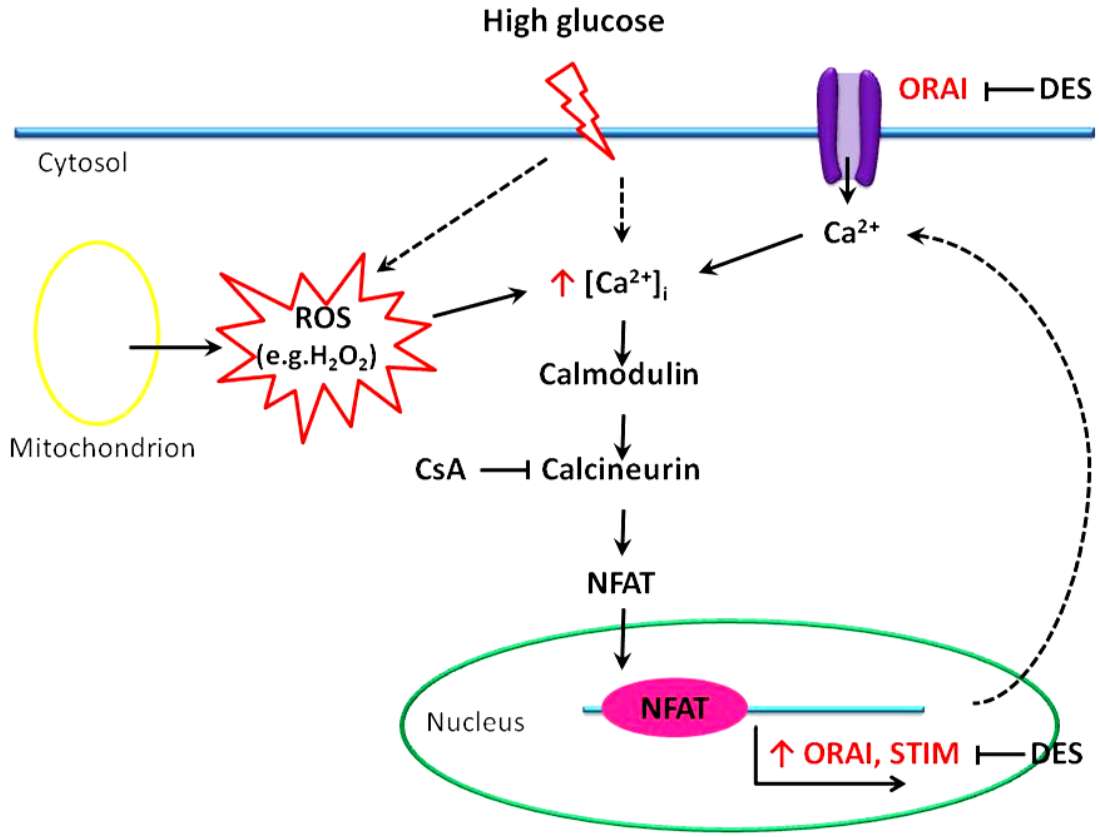

Figure 6-1 Mechanism of store-operated Ca^{2+} entry regulated by high glucose. High glucose increases SOCE by upregulation of ORAI and STIM *in vitro* and *in vivo* via the Ca^{2+}/calcineurin/NFAT pathway. Application of cyclosporin A (CsA) or diethylstilbestrol (DES) prevents the effect. High glucose-induced oxidative stress (ROS production) could be another potential pathway for upregulation.

6.3 Limitations of the study

There are some limitations in this thesis such as the low number of the clinical samples collected. The waiting time for the collection of the clinical samples is long since the cases do not appear very often, thus more samples need to be collected in the future. Moreover, Type 1 diabetic tissue from mouse models was used in this study, because obtaining blood vessels from patients with Type 1 diabetes was not possible as this population does not often undergo cardiac surgery.

In addition, more evidence is needed for the activity of the Ca^{2+}/calcineurin/NFAT pathway with regards to the high glucose-induced upregulation of ORAI and STIM. The conclusion was based on the inhibition of this effect by CsA although this chemical is also an inhibitor of other cellular processes, such as the mitochondrial permeability transition pore and the Ca^{2+} entry through the Ca^{2+} uniporter in mitochondria (Montero *et al.*, 2004; Chalmers & McCarron, 2008). Nevertheless, CsA was used by many studies to prove the involvement of the Ca^{2+}/calcineurin/NFAT pathway in the promotion of gene expression (Demozay *et al.*, 2011; Nijenhuis *et al.*, 2011; Rosenkranz *et al.*, 2011). Other blockers of this pathway or RNA interference for NFAT could be used to further confirm this.

6.4 Future directions

Vascular endothelial cell functions were shown to be regulated by oxidative stress conditions. Besides demonstrating the involvement of ORAI channels in IL-6 secretion, other vascular cell functions such as migration and angiogenesis should be investigated using siRNAs for ORAI/STIM or specific blockers of the ORAI current such as DES. This would provide a bigger insight into the role of these proteins in the disruption of vascular cell functions under oxidative stress conditions and a clinical link to prevention of any vascular dysfunction would be examined as a therapeutic diagnosis.

Changes in Ca^{2+} concentration through ORAI channels potentially have an effect on diabetes and hyperglycaemia. A study on the effect of RNS on ORAI and STIM

channel molecules would also be a promising field for future research. This would provide further information about the effect of oxidative stress on ORAI, STIM and SOCE.

6.5 Conclusion

The data in this thesis demonstrate for the first time that high glucose increases SOCE by upregulation of ORAI and STIM via the Ca^{2+}/calcineurin/NFAT pathway in vascular cells, but there is no direct effect on the channel itself or STIM1 movement. ORAI and STIM expression is also increased when the cells are treated with H_2O_2. Hcy, on the other hand, is firstly shown to inhibit ORAI channel activity directly as well as the expression of ORAI. Additionally, SOCE is inhibited by hyperosmolarity and this may be mediated by the direct inhibitory effect on ORAI channel activity or ORAI and STIM expression. These findings suggest that the regulation of the store-operated channel activity or related gene expression is a potential critical step in the pathophysiology of vascular disease in patients with diabetes or oxidative stress-related diseases.

References

Abdullaev IF, Bisaillon JM, Potier M, Gonzalez JC, Motiani RK & Trebak M. (2008). Stim1 and Orai1 mediate CRAC currents and store-operated calcium entry important for endothelial cell proliferation. *Circulation Research* **103,** 1289-1299.

Alberti KG & Zimmet PZ. (1998). Definition, diagnosis and classification of diabetes mellitus and its complications. Part 1: diagnosis and classification of diabetes mellitus provisional report of a WHO consultation. *Diabetic Medicine* **15,** 539-553.

Ambudkar IS, Ong HL, Liu X, Bandyopadhyay B & Cheng KT. (2007). TRPC1: The link between functionally distinct store-operated calcium channels. *Cell Calcium* **42,** 213-223.

American Diabetes Association. (2005). Diagnosis and classification of diabetes mellitus. *Diabetes Care* **28,** s37-s42.

Ansley DM & Wang B. (2013). Oxidative stress and myocardial injury in the diabetic heart. *The Journal of Pathology* **229,** 232-241.

Aranda E & Owen GI. (2009). A semi-quantitative assay to screen for angiogenic compounds and compounds with angiogenic potential using the EA.hy926 endothelial cell line. *Biological Research* **42,** 377-389.

Avogaro A, Albiero M, Menegazzo L, de Kreutzenberg S & Fadini GP. (2011). Endothelial dysfunction in diabetes. *Diabetes Care* **34,** S285-S290.

Bae YS, Kang SW, Seo MS, Baines IC, Tekle E, Chock PB & Rhee SG. (1997). Epidermal growth factor (EGF)-induced generation of hydrogen peroxide. *The Journal of Biological Chemistry* **272,** 217-221.

Bastos Goncalves F, Voute MT, Hoeks SE, Chonchol MB, Boersma EE, Stolker RJ & Verhagen HJ. (2012). Calcification of the abdominal aorta as an independent predictor of cardiovascular events: a meta-analysis. *Heart (British Cardiac Society)* **98,** 988-994.

Bauer J, Margolis M, Schreiner C, Edgell CJ, Azizkhan J, Lazarowski E & Juliano RL. (1992). In vitro model of angiogenesis using a human endothelium-derived permanent cell line: contributions of induced gene expression, G-proteins, and integrins. *Journal of Cellular Physiology* **153,** 437-449.

Baynes JW. (1991). Role of oxidative stress in development of complications in diabetes. *Diabetes* **40,** 405-412.

Baynes JW & Thorpe SR. (1999). Role of oxidative stress in diabetic complications: a new perspective on an old paradigm. *Diabetes* **48,** 1-9.

Beals CR, Clipstone NA, Ho SN & Crabtree GR. (1997). Nuclear localization of NF-ATc by a calcineurin-dependent, cyclosporin-sensitive intramolecular interaction. *Genes & Development* **11,** 824-834.

Becker S, Reinehr R, Graf D, vom Dahl S & Haussinger D. (2007). Hydrophobic bile salts induce hepatocyte shrinkage via NADPH oxidase activation. *Cellular Physiology and Biochemistry* **19,** 89-98.

Beech DJ, Bahnasi YM, Dedman AM & Al-Shawaf E. (2009). TRPC channel lipid specificity and mechanisms of lipid regulation. *Cell Calcium* **45,** 583-588.

Ben-Tabou De-Leon S, Ben-Zeev G & Nussinovitch I. (2006). Effects of osmotic shrinkage on voltage-gated Ca^{2+} channel currents in rat anterior pituitary cells. *American Journal of Physiology - Cell Physiology* **290,** C222-C232.

Bergmeier W, Oh-hora M, McCarl C-A, Roden RC, Bray PF & Feske S. (2009). R93W mutation in Orai1 causes impaired calcium influx in platelets. *Blood* **113,** 675-678.

Berridge MJ. (2012). Calcium signalling remodelling and disease. *Biochemical Society Transactions* **40,** 297-309.

Berridge MJ, Bootman MD & Lipp P. (1998). Calcium - a life and death signal. *Nature* **395,** 645-648.

Berridge MJ, Bootman MD & Roderick HL. (2003). Calcium signalling: dynamics, homeostasis and remodelling. *Nature Reviews Molecular Cell Biology* **4,** 517-529.

Berridge MJ, Lipp P & Bootman MD. (2000). The versatility and universality of calcium signalling. *Nature Reviews Molecular Cell Biology* **1,** 11-21.

Bhandari S, Watson N, Long E, Sharpe S, Zhong W, Xu SZ & Atkin SL. (2008). Expression of somatostatin and somatostatin receptor subtypes 1-5 in human normal and diseased kidney. *Journal of Histochemistry & Cytochemistry* **56,** 733-743.

Bird GS, DeHaven WI, Smyth JT & Putney Jr JW. (2008). Methods for studying store-operated calcium entry. *Methods* **46,** 204-212.

Bird GS, Hwang SY, Smyth JT, Fukushima M, Boyles RR & Putney JW. (2009). STIM1 is a calcium sensor specialized for digital signaling. *Current Biology* **19,** 1724-1729.

Bisaillon JM, Motiani RK, Gonzalez-Cobos JC, Potier M, Halligan KE, Alzawahra WF, Barroso M, Singer HA, Jourd'heuil D & Trebak M. (2010). Essential role for STIM1/Orai1-mediated calcium influx in PDGF-induced smooth muscle migration. *American Journal of Physiology - Cell Physiology* **298,** C993-1005.

Bishara NB & Ding H. (2010). Glucose enhances expression of TRPC1 and calcium entry in endothelial cells. *American Journal of Physiology - Heart and Circulatory Physiology* **298,** H171-178.

Bogeski I, Kappl R, Kummerow C, Gulaboski R, Hoth M & Niemeyer BA. (2011). Redox regulation of calcium ion channels: Chemical and physiological aspects. *Cell Calcium* **50,** 407-423.

Bogeski I, Kummerow C, Al-Ansary D, Schwarz EC, Koehler R, Kozai D, Takahashi N, Peinelt C, Griesemer D, Bozem M, Mori Y, Hoth M & Niemeyer BA. (2010). Differential redox regulation of ORAI ion channels: A mechanism to tune cellular calcium signaling. *Science Signaling* **3,** ra24.

Boss V, Abbott KL, Wang X-F, Pavlath GK & Murphy TJ. (1998). The cyclosporin A-sensitive nuclear factor of activated T cells (NFAT) proteins are expressed in vascular smooth muscle cells. *The Journal of Biological Chemistry* **273,** 19664-19671.

Boushey C, Beresford S, Omenn G & Motulsky A. (1995). A quantitative assessment of plasma homocysteine as a risk factor for vascular disease:

probable benefits of increasing folic acid intakes. *JAMA: The Journal of the American Medical Association* **274,** 1049-1057.

Brandman O, Liou J, Park WS & Meyer T. (2007). STIM2 is a feedback regulator that stabilizes basal cytosolic and endoplasmic reticulum Ca^{2+} levels. *Cell* **131,** 1327-1339.

Braun A, Varga-Szabo D, Kleinschnitz C, Pleines I, Bender M, Austinat M, Bosl M, Stoll G & Nieswandt B. (2009). Orai1 (CRACM1) is the platelet SOC channel and essential for pathological thrombus formation. *Blood* **113,** 2056-2063.

Broad LM, Cannon TR & Taylor CW. (1999). A non-capacitative pathway activated by arachidonic acid is the major Ca^{2+} entry mechanism in rat A7r5 smooth muscle cells stimulated with low concentrations of vasopressin. *The Journal of Physiology* **517,** 121-134.

Brookes PS, Yoon Y, Robotham JL, Anders MW & Sheu S-S. (2004). Calcium, ATP, and ROS: a mitochondrial love-hate triangle. *American Journal of Physiology - Cell Physiology* **287,** C817-C833.

Brosky G & Logothetopoulos J. (1969). Streptozotocin diabetes in the mouse and guinea pig. *Diabetes* **18,** 606-611.

Brownlee M. (2001). Biochemistry and molecular cell biology of diabetic complications. *Nature* **414,** 813-820.

Brownlee M. (2005). The pathobiology of diabetic complications: A unifying mechanism. *Diabetes* **54,** 1615-1625.

Brownlee M & Cerami A. (1981). The biochemistry of the complications of diabetes mellitus. *Annual Review of Biochemistry* **50,** 385-432.

Butterfield DA, Castegna A, Lauderback CM & Drake J. (2002). Evidence that amyloid beta-peptide-induced lipid peroxidation and its sequelae in Alzheimer's disease brain contribute to neuronal death. *Neurobiology of Aging* **23,** 655-664.

Carafoli E. (1991). Calcium pump of the plasma membrane. *Physiological Reviews* **71,** 129-153.

Carafoli E. (2002). Calcium signaling: A tale for all seasons. *Proceedings of the National Academy of Sciences USA* **99,** 1115-1122.

Ceriello A. (2003). New insights on oxidative stress and diabetic complications may lead to a "causal" antioxidant therapy. *Diabetes Care* **26,** 1589-1596.

Chalmers S & McCarron JG. (2008). The mitochondrial membrane potential and Ca^{2+} oscillations in smooth muscle. *Journal of Cell Science* **121,** 75-85.

Chaudhuri P, Colles SM, Bhat M, Van Wagoner DR, Birnbaumer L & Graham LM. (2008). Elucidation of a TRPC6-TRPC5 channel cascade that restricts endothelial cell movement. *Molecular Biology of the Cell* **19,** 3203-3211.

Chen GL, Zeng B, Eastmond S, Elsenussi SE, Boa AN & Xu SZ. (2012). Pharmacological comparison of novel synthetic fenamate analogues with econazole and 2-APB on the inhibition of TRPM2 channels. *British Journal of Pharmacology* **167,** 1232-1243.

Chen Y, Smith ML, Chiou GX, Ballaron S, Sheets MP, Gubbins E, Warrior U, Wilkins J, Surowy C, Nakane M, Carter GW, Trevillyan JM, Mollison K & Djuric SW. (2002). TH1 and TH2 cytokine inhibition by 3,5-bis(trifluoromethyl)pyrazoles, a novel class of immunomodulators. *Cellular Immunology* **220,** 134-142.

Cheng H, Lederer WJ & Cannell MB. (1993). Calcium sparks: elementary events underlying excitation-contraction coupling in heart muscle. *Science* **262,** 740-744.

Cheng KT, Liu X, Ong HL & Ambudkar IS. (2008). Functional requirement for Orai1 in store-operated TRPC1-STIM1 channels. *The Journal of Biological Chemistry* **283,** 12935-12940.

Cheng KT, Liu X, Ong HL, Swaim W & Ambudkar IS. (2011). Local Ca^{2+} entry via Orai1 regulates plasma membrane recruitment of TRPC1 and controls cytosolic Ca^{2+} signals required for specific cell functions. *PLoS Biology* **9,** e1001025.

Chiarugi P & Cirri P. (2003). Redox regulation of protein tyrosine phosphatases during receptor tyrosine kinase signal transduction. *Trends in Biochemical Sciences* **28,** 509-514.

Chiasson JL, Aris-Jilwan N, Belanger R, Bertrand S, Beauregard H, Ekoe JM, Fournier H & Havrankova J. (2003). Diagnosis and treatment of diabetic ketoacidosis and the hyperglycemic hyperosmolar state. *Canadian Medical Association Journal* **168,** 859-866.

Chung AW, Au Yeung K, Chum E, Okon EB & van Breemen C. (2009). Diabetes modulates capacitative calcium entry and expression of transient receptor

potential canonical channels in human saphenous vein. *European Journal of Pharmacology* **613,** 114-118.

Chvanov M, Walsh C, Haynes L, Voronina S, Lur G, Gerasimenko O, Barraclough R, Rudland P, Petersen O, Burgoyne R & Tepikin A. (2008). ATP depletion induces translocation of STIM1 to puncta and formation of STIM1–ORAI1 clusters: translocation and re-translocation of STIM1 does not require ATP. *Pflügers Archiv - European Journal of Physiology* **457,** 505-517.

Clapham DE. (2003). TRP channels as cellular sensors. *Nature* **426,** 517-524.

Clapham DE. (2007). Calcium Signaling. *Cell* **131,** 1047-1058.

Clipstone NA & Crabtree GR. (1992). Identification of calcineurin as a key signalling enzyme in T-lymphocyte activation. *Nature* **357,** 695-697.

Cockerill GW, Bert AG, Ryan GR, Gamble JR, Vadas MA & Cockerill PN. (1995). Regulation of granulocyte-macrophage colony-stimulating factor and E-selectin expression in endothelial cells by cyclosporin A and the T- cell transcription factor NFAT. *Blood* **86,** 2689-2698.

Cosentino F, Sill J & Katusic Z. (1994). Role of superoxide anions in the mediation of endothelium-dependent contractions. *Hypertension* **23,** 229-235.

Crabtree GR. (2001). Calcium, calcineurin, and the control of transcription. *The Journal of Biological Chemistry* **276,** 2313-2316.

Cypser JR & Johnson TE. (2002). Multiple stressors in Caenorhabditis elegans induce stress hormesis and extended longevity. *The Journals of Gerontology Series A: Biological Sciences and Medical Sciences* **57,** B109-B114.

Darbellay B, Arnaudeau S, Bader CR, Konig S & Bernheim L. (2011). STIM1L is a new actin-binding splice variant involved in fast repetitive Ca^{2+} release. *The Journal of Cell Biology* **194,** 335-346.

de Diego-Otero Y, Romero-Zerbo Y, Bekay Re, Decara J, Sanchez L, Fonseca FR-d & Arco-Herrera Id. (2008). [alpha]-Tocopherol protects against oxidative stress in the Fragile X knockout mouse: an experimental therapeutic approach for the Fmr1 deficiency. *Neuropsychopharmacology* **34,** 1011-1026.

DeHaven WI, Jones BF, Petranka JG, Smyth JT, Tomita T, Bird GS & Putney JW. (2009). TRPC channels function independently of STIM1 and Orai1. *The Journal of Physiology* **587,** 2275-2298.

DeHaven WI, Smyth JT, Boyles RR, Bird GS & Putney JW. (2008). Complex actions of 2-aminoethyldiphenyl borate on store-operated calcium entry. *The Journal of Biological Chemistry* **283,** 19265-19273.

DeHaven WI, Smyth JT, Boyles RR & Putney JW. (2007). Calcium inhibition and calcium potentiation of Orai1, Orai2, and Orai3 calcium release-activated calcium channels. *The Journal of Biological Chemistry* **282,** 17548-17556.

Demozay D, Tsunekawa S, Briaud I, Shah R & Rhodes CJ. (2011). Specific glucose-induced control of insulin receptor substrate-2 expression is mediated via Ca^{2+}-dependent calcineurin/NFAT signaling in primary pancreatic islet beta-cells. *Diabetes* **60,** 2892-2902.

Deng X, Wang Y, Zhou Y, Soboloff J & Gill DL. (2009). STIM and Orai: dynamic intermembrane coupling to control cellular calcium signals. *The Journal of Biological Chemistry* **284,** 22501-22505.

Dermitzakis ET & Clark AG. (2009). Genetics. Life after GWA studies. *Science* **326,** 239-240.

Ding Y, Schwartz D, Posner P & Zhong J. (2004). Hypotonic swelling stimulates L-type Ca^{2+} channel activity in vascular smooth muscle cells through PKC. *American Journal of Physiology - Cell Physiology* **287,** C413-421.

Ding Y, Winters A, Ding M, Graham S, Akopova I, Muallem S, Wang Y, Hong JH, Gryczynski Z, Yang S-H, Birnbaumer L & Ma R. (2011). Reactive oxygen species-mediated TRPC6 protein activation in vascular myocytes, a mechanism for vasoconstrictor-regulated vascular tone. *The Journal of Biological Chemistry* **286,** 31799-31809.

Droge W. (2002). Free radicals in the physiological control of cell function. *Physiological Reviews* **82,** 47-95.

Durand DB, Shaw JP, Bush MR, Replogle RE, Belagaje R & Crabtree GR. (1988). Characterization of antigen receptor response elements within the interleukin-2 enhancer. *Molecular and Cellular Biology* **8,** 1715-1724.

Dziadek MA & Johnstone LS. (2007). Biochemical properties and cellular localisation of STIM proteins. *Cell Calcium* **42,** 123-132.

Edgell CJ, McDonald CC & Graham JB. (1983). Permanent cell line expressing human factor VIII-related antigen established by hybridization. *Proceedings of the National Academy of Sciences* **80,** 3734-3737.

Ermak G & Davies KJA. (2002). Calcium and oxidative stress: from cell signaling to cell death. *Molecular Immunology* **38,** 713-721.

Evans JL, Goldfine ID, Maddux BA & Grodsky GM. (2002). Oxidative stress and stress-activated signaling pathways: a unifying hypothesis of type 2 diabetes. *Endocrine Reviews* **23,** 599-622.

Fanger CM, Hoth M, Crabtree GR & Lewis RS. (1995). Characterization of T cell mutants with defects in capacitative calcium entry: genetic evidence for the physiological roles of CRAC channels. *The Journal of Cell Biology* **131,** 655-667.

Faouzi M, Hague F, Potier M, Ahidouch A, Sevestre H & Ouadid-Ahidouch H. (2010). Down-regulation of Orai3 arrests cell-cycle progression and induces apoptosis in breast cancer cells but not in normal breast epithelial cells. *Journal of Cellular Physiology* **226,** 542-551.

Feske S. (1996). Severe combined immunodeficiency due to defective binding of the nuclear factor of activated T cells in T lymphocytes of two male siblings. *European Journal of Immunology* **26,** 2119-2126.

Feske S. (2009). ORAI1 and STIM1 deficiency in human and mice: roles of store-operated Ca^{2+} entry in the immune system and beyond. *Immunological Reviews* **231,** 189-209.

Feske S. (2010). CRAC channelopathies. *Pflügers Archiv - European Journal of Physiology* **460,** 417-435.

Feske S. (2011). Immunodeficiency due to defects in store-operated calcium entry. *Annals of the New York Academy of Sciences* **1238,** 74-90.

Feske S, Gwack Y, Prakriya M, Srikanth S, Puppel S-H, Tanasa B, Hogan PG, Lewis RS, Daly M & Rao A. (2006). A mutation in Orai1 causes immune deficiency by abrogating CRAC channel function. *Nature* **441,** 179-185.

Fill M & Copello JA. (2002). Ryanodine receptor calcium release channels. *Physiological Reviews* **82,** 893-922.

Flanagan WM, Corthesy B, Bram RJ & Crabtree GR. (1991). Nuclear association of a T-cell transcription factor blocked by FK-506 and cyclosporin A. *Nature* **352,** 803-807.

Florea SM & Blatter LA. (2008). The effect of oxidative stress on Ca^{2+} release and capacitative Ca^{2+} entry in vascular endothelial cells. *Cell Calcium* **43,** 405-415.

Fox CS, Coady S, Sorlie PD, Levy D, Meigs JB, D'Agostino RB, Sr., Wilson PW & Savage PJ. (2004). Trends in cardiovascular complications of diabetes. *JAMA* **292,** 2495-2499.

Franzius D, Hoth M & Penner R. (1994). Non-specific effects of calcium entry antagonists in mast cells. *Pflügers Archiv - European Journal of Physiology* **428,** 433-438.

Freichel M, Suh SH, Pfeifer A, Schweig U, Trost C, Weiszgerber P, Biel M, Philipp S, Freise D, Droogmans G, Hofmann F, Flockerzi V & Nilius B. (2001). Lack of an endothelial store-operated Ca^{2+} current impairs agonist-dependent vasorelaxation in TRP4-/- mice. *Nature Cell Biology* **3,** 121-127.

Frischauf I, Muik M, Derler I, Bergsmann J, Fahrner M, Schindl R, Groschner K & Romanin C. (2009). Molecular determinants of the coupling between STIM1 and Orai channels. *The Journal of Biological Chemistry* **284,** 21696-21706.

Gems D & Partridge L. (2008). Stress-response hormesis and aging: "that which does not kill us makes us stronger". *Cell Metabolism* **7,** 200-203.

Ghosh J & Myers CE. (1998). Inhibition of arachidonate 5-lipoxygenase triggers massive apoptosis in human prostate cancer cells. *Proceedings of the National Academy of Sciences USA* **95,** 13182-13187.

Giachini FR, Chiao CW, Carneiro FS, Lima VV, Carneiro ZN, Dorrance AM, Tostes RC & Webb RC. (2009a). Increased activation of stromal interaction molecule-1/Orai-1 in aorta from hypertensive rats: a novel insight into vascular dysfunction. *Hypertension* **53,** 409-416.

Giachini FR, Webb RC & Tostes RC. (2009b). STIM and Orai proteins: players in sexual differences in hypertension-associated vascular dysfunction? *Clinical Science (London)* **118,** 391-396.

Givertz MM & Colucci WS. (1998). New targets for heart-failure therapy: endothelin, inflammatory cytokines, and oxidative stress. *Lancet* **352 Suppl 1,** SI34-38.

Golbidi S, Ebadi SA & Laher I. (2011). Antioxidants in the treatment of diabetes. *Current Diabetes Reviews* **7,** 106-125.

Goldin A, Beckman JA, Schmidt AM & Creager MA. (2006). Advanced glycation end products: sparking the development of diabetic vascular injury. *Circulation* **114,** 597-605.

Golovina VA, Platoshyn O, Bailey CL, Wang J, Limsuwan A, Sweeney M, Rubin LJ & Yuan JXJ. (2001). Upregulated TRP and enhanced capacitative Ca^{2+} entry in human pulmonary artery myocytes during proliferation. *American Journal of Physiology - Heart and Circulatory Physiology* **280,** H746-755.

Goto J-I, Suzuki AZ, Ozaki S, Matsumoto N, Nakamura T, Ebisui E, Fleig A, Penner R & Mikoshiba K. (2010). Two novel 2-aminoethyl diphenylborinate (2-APB) analogues differentially activate and inhibit store-operated Ca^{2+} entry via STIM proteins. *Cell Calcium* **47,** 1-10.

Graham S, Ding M, Sours-Brothers S, Yorio T, Ma J-X & Ma R. (2007). Downregulation of TRPC6 protein expression by high glucose, a possible mechanism for the impaired Ca^{2+} signaling in glomerular mesangial cells in diabetes. *American Journal of Physiology - Renal Physiology* **293,** F1381-F1390.

Graier WF, Simecek S, Hoebel BG, Wascher TC, Dittrich P & Kostner GM. (1997). Antioxidants prevent high-D-glucose-enhanced endothelial Ca^{2+}/cGMP response by scavenging superoxide anions. *European Journal of Pharmacology* **322,** 113-122.

Graier WF, Wascher TC, Lackner L, Toplak H, Krejs GJ & Kukovetz WR. (1993). Exposure to elevated D-glucose concentrations modulates vascular endothelial cell vasodilatory response. *Diabetes* **42,** 1497-1505.

Griendling KK, Sorescu D, Lassegue B & Ushio-Fukai M. (2000). Modulation of protein kinase activity and gene expression by reactive oxygen species and their role in vascular physiology and pathophysiology. *Arteriosclerosis, Thrombosis, and Vascular Biology* **20,** 2175-2183.

Gross SA, Wissenbach U, Philipp SE, Freichel M, Cavalie A & Flockerzi V. (2007). Murine ORAI2 splice variants form functional Ca^{2+} release-activated Ca^{2+} (CRAC) channels. *The Journal of Biological Chemistry* **282,** 19375-19384.

Grupe M, Myers G, Penner R & Fleig A. (2010). Activation of store-operated I(CRAC) by hydrogen peroxide. *Cell Calcium* **48,** 1-9.

Guo R-w & Huang L. (2008). New insights into the activation mechanism of store-operated calcium channels: roles of STIM and Orai. *Journal of Zhejiang University - Science B* **9,** 591-601.

Gwack Y, Srikanth S, Feske S, Cruz-Guilloty F, Oh-hora M, Neems DS, Hogan PG & Rao A. (2007). Biochemical and functional characterization of Orai proteins. *The Journal of Biological Chemistry* **282,** 16232-16243.

Halliwell B, Gutteridge JMC & Lester Packer ANG. (1990). Role of free radicals and catalytic metal ions in human disease: an overview. In *Methods in Enzymology*, pp. 1-85. Academic Press.

Hansson GK & Hermansson A. (2011). The immune system in atherosclerosis. *Nature Immunology* **12,** 204-212.

Harrison DG. (1997). Cellular and molecular mechanisms of endothelial cell dysfunction. *The Journal of Clinical Investigation* **100,** 2153-2157.

Harteneck C, Plant TD & Schultz G. (2000). From worm to man: three subfamilies of TRP channels. *Trends in Neurosciences* **23,** 159-166.

Haussinger D & Lang F. (1992). Cell volume and hormone action. *Trends in Pharmacological Sciences* **13,** 371-373.

Hawkins BJ, Irrinki KM, Mallilankaraman K, Lien Y-C, Wang Y, Bhanumathy CD, Subbiah R, Ritchie MF, Soboloff J, Baba Y, Kurosaki T, Joseph SK, Gill DL & Madesh M. (2010). S-glutathionylation activates STIM1 and alters mitochondrial homeostasis. *The Journal of Cell Biology* **190,** 391-405.

He L-P, Hewavitharana T, Soboloff J, Spassova MA & Gill DL. (2005). A functional link between store-operated and TRPC channels revealed by the 3,5-bis(trifluoromethyl)pyrazole derivative, BTP2. *The Journal of Biological Chemistry* **280,** 10997-11006.

Herr RR, Eble TE, Bergy ME & Jahnke HK. (1959). Isolation and characterization of streptozotocin. *Antibiotics Annual* **7,** 236-240.

Hewavitharana T, Deng X, Soboloff J & Gill DL. (2007). Role of STIM and Orai proteins in the store-operated calcium signaling pathway. *Cell Calcium* **42,** 173-182.

Hex N, Bartlett C, Wright D, Taylor M & Varley D. (2012). Estimating the current and future costs of Type 1 and Type 2 diabetes in the UK, including direct health costs and indirect societal and productivity costs. *Diabetic Medicine* **29,** 855-862.

Hidalgo C & Donoso P. (2008). Crosstalk between calcium and redox signaling: from molecular mechanisms to health implications. *Antioxidants & Redox Signaling* **10,** 1275-1312.

Ho AM, Jain J, Rao A & Hogan PG. (1994). Expression of the transcription factor NFATp in a neuronal cell line and in the murine nervous system. *The Journal of Biological Chemistry* **269,** 28181-28186.

Hoeben A, Landuyt B, Highley MS, Wildiers H, Van Oosterom AT & De Bruijn EA. (2004). Vascular endothelial growth factor and angiogenesis. *Pharmacological Reviews* **56,** 549-580.

Hoey T, Sun YL, Williamson K & Xu X. (1995). Isolation of two new members of the NF-AT gene family and functional characterization of the NF-AT proteins. *Immunity* **2,** 461-472.

Hofer AM, Fasolato C & Pozzan T. (1998). Capacitative Ca^{2+} entry Is closely linked to the filling state of internal Ca^{2+} stores: a study using simultaneous measurements of I_{CRAC} and intraluminal [Ca^{2+}]. *The Journal of Cell Biology* **140,** 325-334.

Hofmann T, Obukhov AG, Schaefer M, Harteneck C, Gudermann T & Schultz G. (1999). Direct activation of human TRPC6 and TRPC3 channels by diacylglycerol. *Nature* **397,** 259-263.

Hofmann T, Schaefer M, Schultz G & Gudermann T. (2000). Transient receptor potential channels as molecular substrates of receptor-mediated cation entry. *Journal of Molecular Medicine* **78,** 14-25.

Hofmann T, Schaefer M, Schultz G & Gudermann T. (2002). Subunit composition of mammalian transient receptor potential channels in living cells. *Proceedings of the National Academy of Sciences of the United States of America* **99,** 7461-7466.

Hogan PG, Chen L, Nardone J & Rao A. (2003). Transcriptional regulation by calcium, calcineurin, and NFAT. *Genes & Development* **17,** 2205-2232.

Hogan PG, Lewis RS & Rao A. (2010). Molecular basis of calcium signaling in lymphocytes: STIM and ORAI. *Annual Review of Immunology* **28,** 491-533.

Hopson KP, Truelove J, Chun J, Wang Y & Waeber C. (2011). S1P activates store-operated calcium entry via receptor- and non-receptor-mediated pathways in vascular smooth muscle cells. *American Journal of Physiology - Cell Physiology* **300,** C919-C926.

Hoth M & Penner R. (1992). Depletion of intracellular calcium stores activates a calcium current in mast cells. *Nature* **355,** 353-356.

Hoth M & Penner R. (1993). Calcium release-activated calcium current in rat mast cells. *The Journal of Physiology* **465,** 359-386.

Huang GN, Zeng W, Kim JY, Yuan JP, Han L, Muallem S & Worley PF. (2006). STIM1 carboxyl-terminus activates native SOC, I_{CRAC} and TRPC1 channels. *Nature Cell Biology* **8,** 1003-1010.

Huang Q & Sheibani N. (2008). High glucose promotes retinal endothelial cell migration through activation of Src, PI3K/Akt1/eNOS, and ERKs. *American Journal of Physiology - Cell Physiology* **295,** C1647-1657.

Ishikawa J, Ohga K, Yoshino T, Takezawa R, Ichikawa A, Kubota H & Yamada T. (2003). A pyrazole derivative, YM-58483, potently inhibits store-operated sustained Ca^{2+} influx and IL-2 production in T lymphocytes. *The Journal of Immunology* **170,** 4441-4449.

Jain J, McCaffrey PG, Miner Z, Kerppola TK, Lambert JN, Verdine GL, Curran T & Rao A. (1993). The T-cell transcription factor NFATp is a substrate for calcineurin and interacts with Fos and Jun. *Nature* **365,** 352-355.

Jardin I, Lopez JJ, Salido GM & Rosado JA. (2008). Orai1 mediates the interaction between STIM1 and hTRPC1 and regulates the mode of activation of hTRPC1-forming Ca^{2+} channels. *Journal of Biological Chemistry* **283,** 25296-25304.

Ji W, Xu P, Li Z, Lu J, Liu L, Zhan Y, Chen Y, Hille B, Xu T & Chen L. (2008). Functional stoichiometry of the unitary calcium-release-activated calcium channel. *Proceedings of the National Academy of Sciences USA* **105,** 13668-13673.

Johansen J, Harris A, Rychly D & Ergul A. (2005). Oxidative stress and the use of antioxidants in diabetes: Linking basic science to clinical practice. *Cardiovascular Diabetology* **4,** 5.

Junod A, Lambert AE, Orci L, Pictet R, Gonet AE & Renold AE. (1967). Studies of the diabetogenic action of streptozotocin. *Proceedings of the Society for Experimental Biology and Medicine* **126,** 201-205.

Junod A, Lambert AE, Stauffacher W & Renold AE. (1969). Diabetogenic action of streptozotocin: relationship of dose to metabolic response. *The Journal of Clinical Investigation* **48,** 2129-2139.

Kajimura M & Curry FE. (1999). Endothelial cell shrinkage increases permeability through a Ca^{2+}-dependent pathway in single frog mesenteric microvessels. *The Journal of Physiology* **518 (Pt 1),** 227-238.

Kayo T & Koizumi A. (1998). Mapping of murine diabetogenic gene mody on chromosome 7 at D7Mit258 and its involvement in pancreatic islet and beta cell development during the perinatal period. *The Journal of Clinical Investigation* **101,** 2112-2118.

Keaney JF, Larson MG, Vasan RS, Wilson PWF, Lipinska I, Corey D, Massaro JM, Sutherland P, Vita JA & Benjamin EJ. (2003). Obesity and systemic oxidative stress: clinical correlates of oxidative stress in the Framingham Study. *Arteriosclerosis, Thrombosis, and Vascular Biology* **23,** 434-439.

Kim CA & Bowie JU. (2003). SAM domains: uniform structure, diversity of function. *Trends in Biochemical Sciences* **28,** 625-628.

Kim MS, Zeng W, Yuan JP, Shin DM, Worley PF & Muallem S. (2009). Native store-operated Ca^{2+} influx requires the channel function of Orai1 and TRPC1. *The Journal of Biological Chemistry* **284,** 9733-9741.

Kimura C, Oike M & Ito Y. (1998a). Acute glucose overload abolishes Ca^{2+} oscillation in cultured endothelial cells from bovine aorta: a possible role of superoxide anion. *Circulation Research* **82,** 677-685.

Kimura C, Oike M, Kashiwagi S & Ito Y. (1998b). Effects of acute glucose overload on histamine H2 receptor-mediated Ca^{2+} mobilization in bovine cerebral endothelial cells. *Diabetes* **47,** 104-112.

Kirpichnikov D & Sowers JR. (2001). Diabetes mellitus and diabetes-associated vascular disease. *Trends in Endocrinology & Metabolism* **12,** 225-230.

Kitabchi AE, Umpierrez GE, Fisher JN, Murphy MB & Stentz FB. (2008). Thirty years of personal experience in hyperglycemic crises: diabetic ketoacidosis and hyperglycemic hyperosmolar state. *Journal of Clinical Endocrinology & Metabolism* **93,** 1541-1552.

Klee CB, Ren H & Wang X. (1998). Regulation of the calmodulin-stimulated protein phosphatase, calcineurin. *The Journal of Biological Chemistry* **273,** 13367-13370.

Kozak JA, Kerschbaum HH & Cahalan MD. (2002). Distinct properties of CRAC and MIC channels in RBL cells. *The Journal of General Physiology* **120,** 221-235.

Kronzon I & Tunick PA. (2006). Aortic atherosclerotic disease and stroke. *Circulation* **114,** 63-75.

Krumschnabel G, Gstir R, Manzl C, Prem C, Pafundo D & Schwarzbaum PJ. (2003). Metabolic and ionic responses of trout hepatocytes to anisosmotic exposure. *Journal of Experimental Biology* **206,** 1799-1808.

Kulkarni RN, Almind K, Goren HJ, Winnay JN, Ueki K, Okada T & Kahn CR. (2003). Impact of genetic background on development of hyperinsulinemia and diabetes in insulin receptor/insulin receptor substrate-1 double heterozygous mice. *Diabetes* **52,** 1528-1534.

Laakso M. (1999). Hyperglycemia and cardiovascular disease in type 2 diabetes. *Diabetes* **48,** 937-942.

Lam M, Dubyak G, Chen L, Nuñez G, Miesfeld RL & Distelhorst CW. (1994). Evidence that BCL-2 represses apoptosis by regulating endoplasmic reticulum-associated Ca^{2+} fluxes. *Proceedings of the National Academy of Sciences of the United States of America* **91,** 6569-6573.

Lang F, Busch GL, Ritter M, Volkl H, Waldegger S, Gulbins E & Haussinger D. (1998). Functional significance of cell volume regulatory mechanisms. *Physiological Reviews* **78,** 247-306.

Laporte R, Hui A & Laher I. (2004). Pharmacological modulation of sarcoplasmic reticulum function in smooth muscle. *Pharmacological Reviews* **56,** 439-513.

Le Deist F. (1995). A primary T-cell immunodeficiency associated with defective transmembrane calcium influx. *Blood* **85,** 1053-1062.

Le Deist F, Hivroz C, Partiseti M, Thomas C, Buc HA, Oleastro M, Belohradsky B, Choquet D & Fischer A. (1995). A primary T-cell immunodeficiency associated with defective transmembrane calcium influx. *Blood* **85,** 1053-1062.

Lee KP, Yuan JP, So I, Worley PF & Muallem S. (2010). STIM1-dependent and STIM1-independent function of transient receptor potential canonical (TRPC) channels tunes their store-operated mode. *The Journal of Biological Chemistry* **285,** 38666-38673.

Lee YJ, Galoforo SS, Berns CM, Chen JC, Davis BH, Sim JE, Corry PM & Spitz DR. (1998). Glucose deprivation-induced cytotoxicity and alterations in mitogen-activated protein kinase activation are mediated by oxidative stress in multidrug-resistant human breast carcinoma cells. *The Journal of Biological Chemistry* **273,** 5294-5299.

Leroux L, Desbois P, Lamotte L, Duvillie B, Cordonnier N, Jackerott M, Jami J, Bucchini D & Joshi RL. (2001). Compensatory responses in mice carrying a null mutation for Ins1 or Ins2. *Diabetes* **50 Suppl 1,** S150-153.

Lewis RS. (1999). Store-operated calcium channels. *Advances in Second Messenger and Phosphoprotein Research* **33,** 279-307.

Li J, Cubbon RM, Wilson LA, Amer MS, McKeown L, Hou B, Majeed Y, Tumova S, Seymour VAL, Taylor H, Stacey M, O'Regan D, Foster R, Porter KE, Kearney MT & Beech DJ. (2011). Orai1 and CRAC channel dependence of VEGF-activated Ca^{2+} entry and endothelial tube formation / novelty and significance. *Circulation Research* **108,** 1190-1198.

Li Z, Lu J, Xu P, Xie X, Chen L & Xu T. (2007). Mapping the interacting domains of STIM1 and Orai1 in Ca^{2+} release-activated Ca^{2+} channel activation. *The Journal of Biological Chemistry* **282,** 29448-29456.

Liang C-C, Park AY & Guan J-L. (2007). In vitro scratch assay: a convenient and inexpensive method for analysis of cell migration in vitro. *Nature Protocols* **2,** 329-333.

Liao Y, Erxleben C, Yildirim E, Abramowitz J, Armstrong DL & Birnbaumer L. (2007). Orai proteins interact with TRPC channels and confer responsiveness to store depletion. *Proceedings of the National Academy of Sciences USA* **104,** 4682-4687.

Liou J, Kim ML, Do Heo W, Jones JT, Myers JW, Ferrell JJE & Meyer T. (2005). STIM is a Ca^{2+} sensor essential for Ca^{2+}-store-depletion-triggered Ca^{2+} influx. *Current Biology* **15,** 1235-1241.

Lipinski B. (2001). Pathophysiology of oxidative stress in diabetes mellitus. *Journal of Diabetes and its Complications* **15,** 203-210.

Lis A, Peinelt C, Beck A, Parvez S, Monteilh-Zoller M, Fleig A & Penner R. (2007). CRACM1, CRACM2, and CRACM3 are store-operated Ca^{2+} channels with distinct functional properties. *Current Biology* **17,** 794-800.

Liu D, Maier A, Scholze A, Rauch U, Boltzen U, Zhao Z, Zhu Z & Tepel M. (2008). High glucose enhances transient receptor potential channel canonical type 6-dependent calcium influx in human platelets via phosphatidylinositol 3-kinase-dependent pathway. *Arteriosclerosis, Thrombosis, and Vascular Biology* **28,** 746-751.

Liu J, Farmer JD, Jr., Lane WS, Friedman J, Weissman I & Schreiber SL. (1991). Calcineurin is a common target of cyclophilin-cyclosporin A and FKBP-FK506 complexes. *Cell* **66,** 807-815.

Livak KJ & Schmittgen TD. (2001). Analysis of relative gene expression data using real-time quantitative PCR and the 2(-Delta Delta C(T)) method. *Methods* **25,** 402-408.

Locke EG, Bonilla M, Liang L, Takita Y & Cunningham KW. (2000). A homolog of voltage-gated Ca^{2+}channels stimulated by depletion of secretory Ca^{2+} in yeast. *Molecular and Cellular Biology* **20,** 6686-6694.

Loh C, Shaw KT, Carew J, Viola JP, Luo C, Perrino BA & Rao A. (1996). Calcineurin binds the transcription factor NFAT1 and reversibly regulates its activity. *The Journal of Biological Chemistry* **271,** 10884-10891.

Lounsbury KM, Hu Q & Ziegelstein RC. (2000). Calcium signaling and oxidant stress in the vasculature. *Free Radical Biology and Medicine* **28,** 1362-1369.

Low PA, Nickander KK & Tritschler HJ. (1997). The roles of oxidative stress and antioxidant treatment in experimental diabetic neuropathy. *Diabetes* **46 Suppl 2,** S38-42.

Luo B, Soesanto Y & McClain DA. (2008). Protein modification by O-linked GlcNAc reduces angiogenesis by inhibiting Akt activity in endothelial cells. *Arteriosclerosis, Thrombosis, and Vascular Biology* **28,** 651-657.

Ma Q. (2010). Transcriptional responses to oxidative stress: Pathological and toxicological implications. *Pharmacology & Therapeutics* **125,** 376-393.

Mancarella S, Wang Y, Deng X, Landesberg G, Scalia R, Panettieri RA, Mallilankaraman K, Tang XD, Madesh M & Gill DL. (2011a). Hypoxia-induced acidosis uncouples the STIM-Orai calcium signaling complex. *The Journal of Biological Chemistry* **286,** 44788-44798.

Mancarella S, Wang Y & Gill DL. (2011b). Signal transduction: STIM1 senses both Ca^{2+} and heat. *Nature Chemical Biology* **7,** 344-345.

Mangiagalli A, Samuele A, Armentero M-T, Bazzini E, Nappi G & Blandini F. (2004). Effects of homocysteine on apoptosis-related proteins and anti-oxidant systems in isolated human lymphocytes. *European Journal of Biochemistry* **271,** 1671-1676.

Manji SSM, Parker NJ, Williams RT, van Stekelenburg L, Pearson RB, Dziadek M & Smith PJ. (2000). STIM1: a novel phosphoprotein located at the cell surface. *Biochimica et Biophysica Acta (BBA) - Protein Structure and Molecular Enzymology* **1481,** 147-155.

Manolio TA, Collins FS, Cox NJ, Goldstein DB, Hindorff LA, Hunter DJ, McCarthy MI, Ramos EM, Cardon LR, Chakravarti A, Cho JH, Guttmacher AE, Kong A, Kruglyak L, Mardis E, Rotimi CN, Slatkin M, Valle D, Whittemore AS, Boehnke M, Clark AG, Eichler EE, Gibson G, Haines JL, Mackay TFC, McCarroll SA & Visscher PM. (2009). Finding the missing heritability of complex diseases. *Nature* **461,** 747-753.

Marchenko SM & Sage SO. (2000). Hyperosmotic but not hyposmotic stress evokes a rise in cytosolic Ca^{2+} concentration in endothelium of intact rat aorta. *Experimental Physiology* **85,** 151-157.

Maritim AC, Sanders RA & Watkins JB. (2003). Diabetes, oxidative stress, and antioxidants: A review. *Journal of Biochemical and Molecular Toxicology* **17,** 24-38.

Maruyama Y, Ogura T, Mio K, Kato K, Kaneko T, Kiyonaka S, Mori Y & Sato C. (2009). Tetrameric Orai1 is a teardrop-shaped molecule with a long, tapered cytoplasmic domain. *The Journal of Biological Chemistry* **284,** 13676-13685.

Mayer EL, Jacobsen DW & Robinson K. (1996). Homocysteine and coronary atherosclerosis. *Journal of the American College of Cardiology* **27,** 517-527.

McCarl C-A, Picard C, Khalil S, Kawasaki T, Rother J, Papolos A, Kutok J, Hivroz C, LeDeist F, Plogmann K, Ehl S, Notheis G, Albert MH, Belohradsky BH, Kirschner J, Rao A, Fischer A & Feske S. (2009). ORAI1 deficiency and lack of store-operated Ca^{2+} entry cause immunodeficiency, myopathy, and ectodermal dysplasia. *Journal of Allergy and Clinical Immunology* **124,** 1311-1318.e1317.

McLennan SV, Heffernan S, Wright L, Rae C, Fisher E, Yue DK & Turtle JR. (1991). Changes in hepatic glutathione metabolism in diabetes. *Diabetes* **40,** 344-348.

Mene P, Pugliese G, Pricci F, Di Mario U, Cinotti GA & Pugliese F. (1997). High glucose level inhibits capacitative Ca^{2+} influx in cultured rat mesangial cells by a protein kinase C-dependent mechanism. *Diabetologia* **40,** 521-527.

Mercer JC, DeHaven WI, Smyth JT, Wedel B, Boyles RR, Bird GS & Putney JW. (2006). Large store-operated calcium selective currents due to co-expression of Orai1 or Orai2 with the intracellular calcium sensor, Stim1. *The Journal of Biological Chemistry* **281,** 24979-24990.

Merritt JE, Armstrong WP, Benham CD, Hallam TJ, Jacob R, Jaxa-Chamiec A, Leigh BK, McCarthy SA, Moores KE & Rink TJ. (1990). SK&F 96365, a novel inhibitor of receptor-mediated calcium entry. *The Biochemical Journal* **271,** 515-522.

Mignen O, Thompson JL & Shuttleworth TJ. (2007). STIM1 regulates Ca^{2+} entry via arachidonate-regulated Ca^{2+}-selective (ARC) channels without store depletion or translocation to the plasma membrane. *The Journal of Physiology* **579,** 703-715.

Mignen O, Thompson JL & Shuttleworth TJ. (2008). Orai1 subunit stoichiometry of the mammalian CRAC channel pore. *The Journal of Physiology* **586,** 419-425.

Mita M, Ito K, Taira K, Nakagawa J, Walsh MP & Shoji M. (2010). Attenuation of store-operated Ca^{2+} entry and enhanced expression of TRPC channels in caudal artery smooth muscle from Type 2 diabetic Goto-Kakizaki rats. *Clinical and Experimental Pharmacology and Physiology* **37,** 670-678.

Montero M, Lobatón CD, Gutierrez-Fernández S, Moreno A & Alvarez J. (2004). Calcineurin-independent inhibition of mitochondrial Ca^{2+} uptake by cyclosporin A. *British Journal of Pharmacology* **141,** 263-268.

Morrish NJ, Wang SL, Stevens LK, Fuller JH & Keen H. (2001). Mortality and causes of death in the WHO Multinational Study of Vascular Disease in Diabetes. *Diabetologia* **44 Suppl 2,** S14-21.

Mortuza R, Chen S, Feng B, Sen S & Chakrabarti S. (2013). High glucose induced alteration of SIRTs in endothelial cells causes rapid aging in a p300 and FOXO regulated pathway. *PLoS ONE* **8,** e54514.

Motiani RK, Abdullaev IF & Trebak M. (2010). A novel native store-operated calcium channel encoded by Orai3. *The Journal of Biological Chemistry* **285,** 19173-19183.

Muik M, Fahrner M, Derler I, Schindl R, Bergsmann J, Frischauf I, Groschner K & Romanin C. (2009). A cytosolic homomerization and a modulatory domain within STIM1 C terminus determine coupling to ORAI1 channels. *The Journal of Biological Chemistry* **284,** 8421-8426.

Muraki K, Iwata Y, Katanosaka Y, Ito T, Ohya S, Shigekawa M & Imaizumi Y. (2003). TRPV2 is a component of osmotically sensitive cation channels in murine aortic myocytes. *Circulation Research* **93,** 829-838.

Nijenhuis T, Sloan AJ, Hoenderop JG, Flesche J, van Goor H, Kistler AD, Bakker M, Bindels RJ, de Boer RA, Moller CC, Hamming I, Navis G, Wetzels JF, Berden JH, Reiser J, Faul C & van der Vlag J. (2011). Angiotensin II contributes to podocyte injury by increasing TRPC6 expression via an

NFAT-mediated positive feedback signaling pathway. *The American Journal of Pathology* **179,** 1719-1732.

Nishikawa T, Edelstein D, Du XL, Yamagishi S-i, Matsumura T, Kaneda Y, Yorek MA, Beebe D, Oates PJ, Hammes H-P, Giardino I & Brownlee M. (2000). Normalizing mitochondrial superoxide production blocks three pathways of hyperglycaemic damage. *Nature* **404,** 787-790.

Ogawa A, Firth AL, Smith KA, Maliakal MV & Yuan JX. (2012). PDGF enhances store-operated Ca^{2+} entry by upregulating STIM1/Orai1 via activation of Akt/mTOR in human pulmonary arterial smooth muscle cells. *American Journal of Physiology - Cell Physiology* **302,** C405-411.

Ohba T, Watanabe H, Murakami M, Sato T, Ono K & Ito H. (2009). Essential role of STIM1 in the development of cardiomyocyte hypertrophy. *Biochemical and Biophysical Research Communications* **389,** 172-176.

Ohba T, Watanabe H, Murakami M, Takahashi Y, Iino K, Kuromitsu S, Mori Y, Ono K, Iijima T & Ito H. (2007). Upregulation of TRPC1 in the development of cardiac hypertrophy. *Journal of Molecular and Cellular Cardiology* **42,** 498-507.

Ong HL, Cheng KT, Liu X, Bandyopadhyay BC, Paria BC, Soboloff J, Pani B, Gwack Y, Srikanth S, Singh BB, Gill D & Ambudkar IS. (2007). Dynamic assembly of TRPC1-STIM1-Orai1 ternary complex is involved in store-operated calcium influx. *The Journal of Biological Chemistry* **282,** 9105-9116.

Oritani K & Kincade PW. (1996). Identification of stromal cell products that interact with pre-B cells. *The Journal of Cell Biology* **134,** 771-782.

Outinen PA, Sood SK, Pfeifer SI, Pamidi S, Podor TJ, Li J, Weitz JI & Austin RC. (1999). Homocysteine-induced endoplasmic reticulum stress and growth arrest leads to specific changes in gene expression in human vascular endothelial cells. *Blood* **94,** 959-967.

Paemeleire K, de Hemptinne A & Leybaert L. (1999). Chemically, mechanically, and hyperosmolarity-induced calcium responses of rat cortical capillary endothelial cells in culture. *Experimental Brain Research* **126,** 473-481.

Pani B, Ong HL, Brazer SC, Liu X, Rauser K, Singh BB & Ambudkar IS. (2009). Activation of TRPC1 by STIM1 in ER-PM microdomains involves release of the channel from its scaffold caveolin-1. *Proceedings of the National Academy of Sciences USA* **106,** 20087-20092.

Parekh AB. (2003). Store-operated Ca^{2+} entry: dynamic interplay between endoplasmic reticulum, mitochondria and plasma membrane. *The Journal of Physiology* **547,** 333-348.

Parekh AB & Penner R. (1995). Activation of store-operated calcium influx at resting InsP3 levels by sensitization of the InsP3 receptor in rat basophilic leukaemia cells. *The Journal of Physiology* **489 (Pt 2),** 377-382.

Parekh AB & Penner R. (1997). Store depletion and calcium influx. *Physiological Reviews* **77,** 901-930.

Parekh AB & Putney JW. (2005). Store-Operated Calcium Channels. *Physiological Reviews* **85,** 757-810.

Park CY, Hoover PJ, Mullins FM, Bachhawat P, Covington ED, Raunser S, Walz T, Garcia KC, Dolmetsch RE & Lewis RS. (2009). STIM1 clusters and activates CRAC channels via direct binding of a cytosolic domain to Orai1. *Cell* **136,** 876-890.

Partiseti M, Le Deist F, Hivroz C, Fischer A, Korn H & Choquet D. (1994). The calcium current activated by T cell receptor and store depletion in human lymphocytes is absent in a primary immunodeficiency. *The Journal of Biological Chemistry* **269,** 32327-32335.

Parvez S, Beck A, Peinelt C, Soboloff J, Lis A, Monteilh-Zoller M, Gill DL, Fleig A & Penner R. (2008). STIM2 protein mediates distinct store-dependent and store-independent modes of CRAC channel activation. *The FASEB Journal* **22,** 752-761.

Passaro A, Calzoni F, Volpato S, Nora ED, Pareschi PL, Zamboni PF, Fellin R & Solini A. (2003). Effect of metabolic control on homocysteine levels in type 2 diabetic patients: a 3-year follow-up. *Journal of Internal Medicine* **254,** 264-271.

Peinelt C, Lis A, Beck A, Fleig A & Penner R. (2008). 2-Aminoethoxydiphenyl borate directly facilitates and indirectly inhibits STIM1-dependent gating of CRAC channels. *The Journal of Physiology* **586,** 3061-3073.

Peinelt C, Vig M, Koomoa DL, Beck A, Nadler MJS, Koblan-Huberson M, Lis A, Fleig A, Penner R & Kinet J-P. (2006). Amplification of CRAC current by STIM1 and CRACM1 (Orai1). *Nature Cell Biology* **8,** 771-773.

Peiro C, Lafuente N, Matesanz N, Cercas E, Llergo JL, Vallejo S, Rodriguez-Manas L & Sanchez-Ferrer CF. (2001). High glucose induces cell death of cultured

human aortic smooth muscle cells through the formation of hydrogen peroxide. *British Journal of Pharmacology* **133,** 967-974.

Penna A, Demuro A, Yeromin AV, Zhang SL, Safrina O, Parker I & Cahalan MD. (2008). The CRAC channel consists of a tetramer formed by Stim-induced dimerization of Orai dimers. *Nature* **456,** 116-120.

Perez-Matute P, Zulet MA & Martinez JA. (2009). Reactive species and diabetes: counteracting oxidative stress to improve health. *Current Opinion in Pharmacology* **9,** 771-779.

Periasamy M & Kalyanasundaram A. (2007). SERCA pump isoforms: Their role in calcium transport and disease. *Muscle & Nerve* **35,** 430-442.

Philipson KD & Nicoll DA. (2000). Sodium-calcium exchange: a molecular perspective. *Annual Review of Physiology* **62,** 111-133.

Picard C, McCarl C-A, Papolos A, Khalil S, Lüthy K, Hivroz C, LeDeist F, Rieux-Laucat F, Rechavi G, Rao A, Fischer A & Feske S. (2009). STIM1 mutation associated with a syndrome of immunodeficiency and autoimmunity. *New England Journal of Medicine* **360,** 1971-1980.

Pieper GM & Dondlinger LA. (1998). Antioxidant pyrrolidine dithiocarbamate prevents defective bradykinin-stimulated calcium accumulation and nitric oxide activity following exposure of endothelial cells to elevated glucose concentration. *Diabetologia* **41,** 806-812.

Podrez EA, Abu-Soud HM & Hazen SL. (2000). Myeloperoxidase-generated oxidants and atherosclerosis. *Free Radical Biology & Medicine* **28,** 1717-1725.

Poteser M, Graziani A, Rosker C, Eder P, Derler I, Kahr H, Zhu MX, Romanin C & Groschner K. (2006). TRPC3 and TRPC4 associate to form a redox-sensitive cation channel. *The Journal of Biological Chemistry* **281,** 13588-13595.

Potier M, Gonzalez JC, Motiani RK, Abdullaev IF, Bisaillon JM, Singer HA & Trebak M. (2009). Evidence for STIM1- and Orai1-dependent store-operated calcium influx through I_{CRAC} in vascular smooth muscle cells: role in proliferation and migration. *The FASEB Journal* **23,** 2425-2437.

Pozzan T, Rizzuto R, Volpe P & Meldolesi J. (1994). Molecular and cellular physiology of intracellular calcium stores. *Physiological Reviews* **74,** 595-636.

Prakriya M, Feske S, Gwack Y, Srikanth S, Rao A & Hogan PG. (2006). Orai1 is an essential pore subunit of the CRAC channel. *Nature* **443,** 230-233.

Prakriya M & Lewis RS. (2002). Separation and characterization of currents through store-operated CRAC channels and Mg^{2+}-inhibited cation (MIC) channels. *The Journal of General Physiology* **119,** 487-507.

Prakriya M & Lewis RS. (2003). CRAC channels: activation, permeation, and the search for a molecular identity. *Cell Calcium* **33,** 311-321.

Putney J. (2005). Physiological mechanisms of TRPC activation. *Pflügers Archiv - European Journal of Physiology* **451,** 29-34.

Putney JW. (1986). A model for receptor-regulated calcium entry. *Cell Calcium* **7,** 1-12.

Putney JW. (2004). The enigmatic TRPCs: multifunctional cation channels. *Trends in Cell Biology* **14,** 282-286.

Putney JW. (2007). New molecular players in capacitative Ca^{2+} entry. *Journal of Cell Science* **120,** 1959-1965.

Putney JW Jr. (2001). Pharmacology of capacitative calcium entry. *Molecular Interventions* **1,** 84-94.

Pyorala K, Laakso M & Uusitupa M. (1987). Diabetes and atherosclerosis: an epidemiologic view. *Diabetes/Metabolism Reviews* **3,** 463-524.

Rakieten N, Rakieten ML & Nadkarni MV. (1963). Studies on the diabetogenic action of streptozotocin (NSC-37917). *Cancer Chemotherapy Reports* **29,** 91-98.

Rao G & Berk B. (1992). Active oxygen species stimulate vascular smooth muscle cell growth and proto-oncogene expression. *Circulation Research* **70,** 593-599.

Rerup CC. (1970). Drugs producing diabetes through damage of the insulin secreting cells. *Pharmacological reviews* **22,** 485-518.

Rieber AJ, Marr HS, Comer MB & Edgell CJ. (1993). Extent of differentiated gene expression in the human endothelium-derived EA.hy926 cell line. *Thrombosis and haemostasis* **69,** 476-480.

Robbins CS, Hilgendorf I, Weber GF, Theurl I, Iwamoto Y, Figueiredo J-L, Gorbatov R, Sukhova GK, Gerhardt LMS, Smyth D, Zavitz CCJ, Shikatani EA, Parsons M, van Rooijen N, Lin HY, Husain M, Libby P, Nahrendorf M,

Weissleder R & Swirski FK. (2013). Local proliferation dominates lesional macrophage accumulation in atherosclerosis. *Nature Medicine* **19,** 1166-1172.

Roberts-Thomson SJ, Peters AA, Grice DM & Monteith GR. (2010). ORAI-mediated calcium entry: mechanism and roles, diseases and pharmacology. *Pharmacology & Therapeutics* **127,** 121-130.

Roger VL, Go AS, Lloyd-Jones DM, Benjamin EJ, Berry JD, Borden WB, Bravata DM, Dai S, Ford ES, Fox CS, Fullerton HJ, Gillespie C, Hailpern SM, Heit JA, Howard VJ, Kissela BM, Kittner SJ, Lackland DT, Lichtman JH, Lisabeth LD, Makuc DM, Marcus GM, Marelli A, Matchar DB, Moy CS, Mozaffarian D, Mussolino ME, Nichol G, Paynter NP, Soliman EZ, Sorlie PD, Sotoodehnia N, Turan TN, Virani SS, Wong ND, Woo D & Turner MB. (2012). Heart disease and stroke statistics--2012 update: a report from the American Heart Association. *Circulation* **125,** e2-e220.

Roldan Palomo AR, Martin P, Rebolledo A, Enrique N, Flores LE & Milesi V. (2012). Human umbilical artery smooth muscle exhibits a 2-APB-sensitive capacitative contractile response evoked by vasoactive substances and expresses mRNAs for STIM, Orai and TRPC channels. *Biocell* **36,** 73-81.

Roos J, DiGregorio PJ, Yeromin AV, Ohlsen K, Lioudyno M, Zhang S, Safrina O, Kozak JA, Wagner SL, Cahalan MD, Velicelebi G & Stauderman KA. (2005). STIM1, an essential and conserved component of store-operated Ca^{2+} channel function. *The Journal of Cell Biology* **169,** 435-445.

Rosenkranz AC, Rauch BH, Doller A, Eberhardt W, Bohm A, Bretschneider E & Schror K. (2011). Regulation of human vascular protease-activated receptor-3 through mRNA stabilization and the transcription factor nuclear factor of activated T cells (NFAT). *Molecular Pharmacology* **80,** 337-344.

Ross K, Whitaker M & Reynolds NJ. (2007). Agonist-induced calcium entry correlates with STIM1 translocation. *Journal of Cellular Physiology* **211,** 569-576.

Saavedra FR, Redondo PC, Hernandez-Cruz JM, Salido GM, Pariente JA & Rosado JA. (2004). Store-operated Ca^{2+} entry and tyrosine kinase pp60src hyperactivity are modulated by hyperglycemia in platelets from patients with non insulin-dependent diabetes mellitus. *Archives of Biochemistry and Biophysics* **432,** 261-268.

Sabbioni S, Barbanti-Brodano G, Croce CM & Negrini M. (1997). GOK: A gene at 11p15 involved in rhabdomyosarcoma and rhabdoid tumor development. *Cancer Research* **57,** 4493-4497.

Salido GsM, Sage SO & Rosado JA. (2009). TRPC channels and store-operated Ca^{2+} entry. *Biochimica et Biophysica Acta - Molecular Cell Research* **1793,** 223-230.

Sanchez JC & Wilkins RJ. (2004). Changes in intracellular calcium concentration in response to hypertonicity in bovine articular chondrocytes. *Comparative Biochemistry and Physiology - Part A: Molecular & Integrative Physiology* **137,** 173-182.

Sauer H, Wartenberg M & Hescheler J. (2001). Reactive oxygen species as intracellular messengers during cell growth and differentiation. *Cellular Physiology and Biochemistry* **11,** 173-186.

Saxena AK, Srivastava P, Kale RK & Baquer NZ. (1993). Impaired antioxidant status in diabetic rat liver: Effect of vanadate. *Biochemical Pharmacology* **45,** 539-542.

Schach C, Xu M, Platoshyn O, Keller SH & Yuan JXJ. (2007). Thiol oxidation causes pulmonary vasodilation by activating K^+ channels and inhibiting store-operated Ca^{2+} channels. *American Journal of Physiology - Lung Cellular and Molecular Physiology* **292,** L685-L698.

Schindl R, Bergsmann J, Frischauf I, Derler I, Fahrner M, Muik M, Fritsch R, Groschner K & Romanin C. (2008). 2-Aminoethoxydiphenyl borate alters selectivity of Orai3 channels by increasing their pore size. *The Journal of Biological Chemistry* **283,** 20261-20267.

Schliess F, Reinehr R & Haussinger D. (2007). Osmosensing and signaling in the regulation of mammalian cell function. *The FEBS Journal* **274,** 5799-5803.

Schliess F, von Dahl S & Haussinger D. (2001). Insulin resistance induced by loop diuretics and hyperosmolarity in perfused rat liver. *Biological Chemistry* **382,** 1063-1069.

Serafini AT, Lewis RS, Clipstone NA, Bram RJ, Fanger C, Fiering S, Herzenberg LA & Crabtree GR. (1995). Isolation of mutant T lymphocytes with defects in capacitative calcium entry. *Immunity* **3,** 239-250.

Shaw JP, Utz PJ, Durand DB, Toole JJ, Emmel EA & Crabtree GR. (1988). Identification of a putative regulator of early T cell activation genes. *Science* **241,** 202-205.

Shigematsu S, Yamauchi K, Nakajima K, Iijima S, Aizawa T & Hashizume K. (1999). D-Glucose and insulin stimulate migration and tubular formation of human endothelial cells in vitro. *American Journal of Physiology* **277,** E433-438.

Shungu DC, Weiduschat N, Murrough JW, Mao X, Pillemer S, Dyke JP, Medow MS, Natelson BH, Stewart JM & Mathew SJ. (2012). Increased ventricular lactate in chronic fatigue syndrome. III. Relationships to cortical glutathione and clinical symptoms implicate oxidative stress in disorder pathophysiology. *NMR in Biomedicine* **25,** 1073-1087.

Siddharth M, Datta SK, Bansal S, Mustafa M, Banerjee BD, Kalra OP & Tripathi AK. (2012). Study on organochlorine pesticide levels in chronic kidney disease patients: association with estimated glomerular filtration rate and oxidative stress. *Journal of Biochemical & Molecular Toxicology* **26,** 241-247.

Smyth JT, Dehaven WI, Bird GS & Putney JW, Jr. (2008). Ca^{2+}-store-dependent and -independent reversal of Stim1 localization and function. *Journal of Cell Science* **121,** 762-772.

Soboloff J, Rothberg BS, Madesh M & Gill DL. (2012). STIM proteins: dynamic calcium signal transducers. *Nature Reviews Molecular Cell Biology* **13,** 549-565.

Soboloff J, Spassova MA, Dziadek MA & Gill DL. (2006a). Calcium signals mediated by STIM and Orai proteins-A new paradigm in inter-organelle communication. *Biochimica et Biophysica Acta - Molecular Cell Research* **1763,** 1161-1168.

Soboloff J, Spassova MA, Hewavitharana T, He L-P, Xu W, Johnstone LS, Dziadek MA & Gill DL. (2006b). STIM2 is an inhibitor of STIM1-mediated store-operated Ca^{2+} entry. *Current Biology* **16,** 1465-1470.

Soboloff J, Spassova MA, Tang XD, Hewavitharana T, Xu W & Gill DL. (2006c). Orai1 and STIM Reconstitute Store-operated Calcium Channel Function. *Journal of Biological Chemistry* **281,** 20661-20665.

Sorrentino V & Rizzuto R. (2001). Molecular genetics of Ca(2+) stores and intracellular Ca(2+) signalling. *Trends in Pharmacological Sciences* **22,** 459-464.

Spassova MA, Soboloff J, He L-P, Xu W, Dziadek MA & Gill DL. (2006). STIM1 has a plasma membrane role in the activation of store-operated Ca^{2+} channels. *Proceedings of the National Academy of Sciences USA* **103,** 4040-4045.

Stathopulos PB, Li G-Y, Plevin MJ, Ames JB & Ikura M. (2006). Stored Ca^{2+} depletion-induced oligomerization of stromal interaction molecule 1 (STIM1) via the EF-SAM region. *The Journal of Biological Chemistry* **281,** 35855-35862.

Stathopulos PB, Zheng L & Ikura M. (2009). Stromal interaction molecule (STIM) 1 and STIM2 calcium sensing regions exhibit distinct unfolding and oligomerization kinetics. *The Journal of Biological Chemistry* **284,** 728-732.

Stathopulos PB, Zheng L, Li G-Y, Plevin MJ & Ikura M. (2008). Structural and mechanistic insights into STIM1-mediated initiation of store-operated calcium entry. *Cell* **135,** 110-122.

Strotmann R, Harteneck C, Nunnenmacher K, Schultz G & Plant TD. (2000). OTRPC4, a nonselective cation channel that confers sensitivity to extracellular osmolarity. *Nature Cell Biology* **2,** 695-702.

Sweeney ZK, Minatti A, Button DC & Patrick S. (2009). Small-molecule inhibitors of store-operated calcium entry. *ChemMedChem* **4,** 706-718.

Takahashi Y, Murakami M, Watanabe H, Hasegawa H, Ohba T, Munehisa Y, Nobori K, Ono K, Iijima T & Ito H. (2007). Essential role of the N-terminus of murine Orai1 in store-operated Ca^{2+} entry. *Biochemical and Biophysical Research Communications* **356,** 45-52.

Takemura H, Hughes AR, Thastrup O & Putney JW. (1989). Activation of calcium entry by the tumor promoter thapsigargin in parotid acinar cells. Evidence that an intracellular calcium pool and not an inositol phosphate regulates calcium fluxes at the plasma membrane. *The Journal of Biological Chemistry* **264,** 12266-12271.

Takemura H & Putney JW, Jr. (1989). Capacitative calcium entry in parotid acinar cells. *The Biochemical Journal* **258,** 409-412.

Tamareille S, Mignen O, Capiod T, Rucker-Martin C & Feuvray D. (2006). High glucose-induced apoptosis through store-operated calcium entry and calcineurin in human umbilical vein endothelial cells. *Cell Calcium* **39,** 47-55.

Targosz-Korecka M, Brzezinka G, Malek K, Stepien E & Szymonski M. (2013). Stiffness memory of EA.hy926 endothelial cells in response to chronic hyperglycemia. *Cardiovascular Diabetology* **12,** 96.

The Diabetes Control and Complications Trial Research Group. (1993). The effect of intensive treatment of diabetes on the development and progression of long-term complications in insulin-dependent diabetes mellitus. *New England Journal of Medicine* **329,** 977-986.

Timmerman LA, Clipstone NA, Ho SN, Northrop JP & Crabtree GR. (1996). Rapid shuttling of NF-AT in discrimination of Ca^{2+} signals and immunosuppression. *Nature* **383,** 837-840.

Tintinger GR, Theron AJ, Potjo M & Anderson R. (2007). Reactive oxidants regulate membrane repolarization and store-operated uptake of calcium by formyl peptide-activated human neutrophils. *Free Radical Biology and Medicine* **42,** 1851-1857.

Tohyama Y, Takano T & Yamamura H. (2004). B cell responses to oxidative stress. *Current Pharmaceutical Design* **10,** 835-839.

Touyz RM & Schiffrin EL. (1999). Ang II-stimulated superoxide production is mediated via phospholipase D in human vascular smooth muscle cells. *Hypertension* **34,** 976-982.

Touyz RM & Schiffrin EL. (2000). Signal transduction mechanisms mediating the physiological and pathophysiological actions of angiotensin II in vascular smooth muscle cells. *Pharmacological Reviews* **52,** 639-672.

Trebak M, St. J. Bird G, McKay RR & Putney JW. (2002). Comparison of human TRPC3 channels in receptor-activated and store-operated modes. *The Journal of Biological Chemistry* **277,** 21617-21623.

Tretter L, Sipos I & Adam-Vizi V. (2004). Initiation of neuronal damage by complex I deficiency and oxidative stress in Parkinson's disease. *Neurochemical Research* **29,** 569-577.

Trevillyan JM, Chiou XG, Chen Y-W, Ballaron SJ, Sheets MP, Smith ML, Wiedeman PE, Warrior U, Wilkins J, Gubbins EJ, Gagne GD, Fagerland J, Carter GW, Luly JR, Mollison KW & Djuric SW. (2001). Potent inhibition of NFAT activation and T cell cytokine production by novel low molecular weight pyrazole compounds. *The Journal of Biological Chemistry* **276,** 48118-48126.

Turko IV, Marcondes S & Murad F. (2001). Diabetes-associated nitration of tyrosine and inactivation of succinyl-CoA:3-oxoacid CoA-transferase. *American Journal of Physiology - Heart and Circulatory Physiology* **281,** H2289-2294.

Tyagi N, Sedoris KC, Steed M, Ovechkin AV, Moshal KS & Tyagi SC. (2005). Mechanisms of homocysteine-induced oxidative stress. *American Journal of Physiology - Heart and Circulatory Physiology* **289,** H2649-2656.

UK Prospective Diabetes Study Group. (1998). Intensive blood-glucose control with sulphonylureas or insulin compared with conventional treatment and risk of complications in patients with type 2 diabetes (UKPDS 33). *Lancet* **352,** 837-853.

Valko M, Leibfritz D, Moncol J, Cronin MTD, Mazur M & Telser J. (2007). Free radicals and antioxidants in normal physiological functions and human disease. *Int J Biochem Cell Biol* **39,** 44-84.

van Gils JM, Derby MC, Fernandes LR, Ramkhelawon B, Ray TD, Rayner KJ, Parathath S, Distel E, Feig JL, Alvarez-Leite JI, Rayner AJ, McDonald TO, O'Brien KD, Stuart LM, Fisher EA, Lacy-Hulbert A & Moore KJ. (2012). The neuroimmune guidance cue netrin-1 promotes atherosclerosis by inhibiting the emigration of macrophages from plaques. *Nature Immunology* **13,** 136-143.

Varga-Szabo D, Authi KS, Braun A, Bender M, Ambily A, Hassock SR, Gudermann T, Dietrich A & Nieswandt B. (2008a). Store-operated Ca(2+) entry in platelets occurs independently of transient receptor potential (TRP) C1. *Pflügers Archiv - European Journal of Physiology* **457,** 377-387.

Varga-Szabo D, Braun A, Kleinschnitz C, Bender M, Pleines I, Pham M, Renne T, Stoll G & Nieswandt B. (2008b). The calcium sensor STIM1 is an essential mediator of arterial thrombosis and ischemic brain infarction. *The Journal of Experimental Medicine* **205,** 1583-1591.

Varnai P, Hunyady L & Balla T. (2009). STIM and Orai: the long-awaited constituents of store-operated calcium entry. *Trends in Pharmacological Sciences* **30,** 118-128.

Varnai P, Toth B, Toth DJ, Hunyady L & Balla T. (2007). Visualization and manipulation of plasma membrane-endoplasmic reticulum contact sites indicates the presence of additional molecular components within the STIM1-Orai1 complex. *The Journal of Biological Chemistry* **282,** 29678-29690.

Venkatachalam K, van Rossum DB, Patterson RL, Ma H-T & Gill DL. (2002). The cellular and molecular basis of store-operated calcium entry. *Nature Cell Biology* **4,** E263-E272.

Vig M, Peinelt C, Beck A, Koomoa DL, Rabah D, Koblan-Huberson M, Kraft S, Turner H, Fleig A, Penner R & Kinet J-P. (2006). CRACM1 is a plasma membrane protein essential for store-operated Ca^{2+} entry. *Science***, 312** 1220-1223.

Wang J, Takeuchi T, Tanaka S, Kubo SK, Kayo T, Lu D, Takata K, Koizumi A & Izumi T. (1999). A mutation in the insulin 2 gene induces diabetes with

severe pancreatic beta-cell dysfunction in the Mody mouse. *The Journal of Clinical Investigation* **103,** 27-37.

Wang M, Dhingra K, Hittelman WN, Liehr JG, de Andrade M & Li D. (1996). Lipid peroxidation-induced putative malondialdehyde-DNA adducts in human breast tissues. *Cancer Epidemiology Biomarkers & Prevention* **5,** 705-710.

Wang Y, Deng X, Mancarella S, Hendron E, Eguchi S, Soboloff J, Tang XD & Gill DL. (2010). The calcium store sensor, STIM1, reciprocally controls Orai and CaV1.2 channels. *Science* **330,** 105-109.

Wang Y, Deshpande M & Payne R. (2002). 2-Aminoethoxydiphenyl borate inhibits phototransduction and blocks voltage-gated potassium channels in Limulus ventral photoreceptors. *Cell Calcium* **32,** 209-216.

Weiss DL, Hural J, Tara D, Timmerman LA, Henkel G & Brown MA. (1996). Nuclear factor of activated T cells is associated with a mast cell interleukin 4 transcription complex. *Molecular and Cellular Biology* **16,** 228-235.

Williams RT, Manji SS, Parker NJ, Hancock MS, Van Stekelenburg L, Eid JP, Senior PV, Kazenwadel JS, Shandala T, Saint R, Smith PJ & Dziadek MA. (2001). Identification and characterization of the STIM (stromal interaction molecule) gene family: coding for a novel class of transmembrane proteins. *The Biochemical Journal* **357,** 673-685.

Williams RT, Senior PV, Van Stekelenburg L, Layton JE, Smith PJ & Dziadek MA. (2002). Stromal interaction molecule 1 (STIM1), a transmembrane protein with growth suppressor activity, contains an extracellular SAM domain modified by N-linked glycosylation. *Biochimica et Biophysica Acta* **1596,** 131-137.

Williamson DF, Thompson TJ, Thun M, Flanders D, Pamuk E & Byers T. (2000). Intentional weight loss and mortality among overweight individuals with diabetes. *Diabetes Care* **23,** 1499-1504.

Winslow MM, Neilson JR & Crabtree GR. (2003). Calcium signalling in lymphocytes. *Current Opinion in Immunology* **15,** 299-307.

Wissenbach U, Philipp SE, Gross SA, Cavalie A & Flockerzi V. (2007). Primary structure, chromosomal localization and expression in immune cells of the murine ORAI and STIM genes. *Cell Calcium* **42,** 439-446.

Worley PF, Zeng W, Huang GN, Yuan JP, Kim JY, Lee MG & Muallem S. (2007). TRPC channels as STIM1-regulated store-operated channels. *Cell Calcium* **42,** 205-211.

Wu X, Zagranichnaya TK, Gurda GT, Eves EM & Villereal ML. (2004). A TRPC1/TRPC3-mediated increase in store-operated calcium entry is required for differentiation of H19-7 hippocampal neuronal cells. *The Journal of Biological Chemistry* **279,** 43392-43402.

Wuensch T, Thilo F, Krueger K, Scholze A, Ristow M & Tepel M. (2010). High glucose-induced oxidative stress increases transient receptor potential channel expression in human monocytes. *Diabetes* **59,** 844-849.

Xiao B, Coste B, Mathur J & Patapoutian A. (2011). Temperature-dependent STIM1 activation induces Ca^{2+} influx and modulates gene expression. *Nature Chemical Biology* **7,** 351-358.

Xu SZ & Beech DJ. (2001). TrpC1 is a membrane-spanning subunit of store-operated Ca^{2+} channels in native vascular smooth muscle cells. *Circulation Research* **88,** 84-87.

Xu SZ, Boulay G, Flemming R & Beech DJ. (2006a). E3-targeted anti-TRPC5 antibody inhibits store-operated calcium entry in freshly isolated pial arterioles. *American Journal of Physiology - Heart and Circulatory Physiology* **291,** H2653-2659.

Xu SZ, Muraki K, Zeng F, Li J, Sukumar P, Shah S, Dedman AM, Flemming PK, McHugh D, Naylor J, Cheong A, Bateson AN, Munsch CM, Porter KE & Beech DJ. (2006b). A sphingosine-1-phosphate-activated calcium channel controlling vascular smooth muscle cell motility. *Circulation Research* **98,** 1381-1389.

Xu SZ, Sukumar P, Zeng F, Li J, Jairaman A, English A, Naylor J, Ciurtin C, Majeed Y, Milligan CJ, Bahnasi YM, Al-Shawaf E, Porter KE, Jiang L-H, Emery P, Sivaprasadarao A & Beech DJ. (2008a). TRPC channel activation by extracellular thioredoxin. *Nature* **451,** 69-72.

Xu SZ, Zeng B, Daskoulidou N, Chen GL, Atkin SL & Lukhele B. (2012). Activation of TRPC cationic channels by mercurial compounds confers the cytotoxicity of mercury exposure. *Toxicological Sciences* **125,** 56-68.

Xu SZ, Zeng F, Boulay G, Grimm C, Harteneck C & Beech DJ. (2005). Block of TRPC5 channels by 2-aminoethoxydiphenyl borate: a differential, extracellular and voltage-dependent effect. *British Journal of Pharmacology* **145,** 405-414.

Xu SZ, Zhong W, Ghavideldarestani M, Saurabh R, Lindow SW & Atkin SL. (2009). Multiple mechanisms of soy isoflavones against oxidative stress-

induced endothelium injury. *Free Radical Biology and Medicine* **47,** 167-175.

Xu SZ, Zhong W, Watson NM, Dickerson E, Wake JD, Lindow SW, Newton CJ & Atkin SL. (2008b). Fluvastatin reduces oxidative damage in human vascular endothelial cells by upregulating Bcl-2. *The Journal of Thrombosis and Haemostasis* **6,** 692-700.

Yan Y, Wei C-l, Zhang W-r, Cheng H-p & Liu J. (2006). Cross-talk between calcium and reactive oxygen species signaling. *Acta Pharmacologica Sinica* **27,** 821-826.

Yang S, Zhang JJ & Huang XY. (2009). Orai1 and STIM1 are critical for breast tumor cell migration and metastasis. *Cancer Cell* **15,** 124-134.

Yeromin AV, Zhang SL, Jiang W, Yu Y, Safrina O & Cahalan MD. (2006). Molecular identification of the CRAC channel by altered ion selectivity in a mutant of Orai. *Nature* **443,** 226-229.

Yoshioka M, Kayo T, Ikeda T & Koizumi A. (1997). A novel locus, Mody4, distal to D7Mit189 on chromosome 7 determines early-onset NIDDM in nonobese C57BL/6 (Akita) mutant mice. *Diabetes* **46,** 887-894.

Young IS, Tate S, Lightbody JH, McMaster D & Trimble ER. (1995). The effects of desferrioxamine and ascorbate on oxidative stress in the streptozotocin diabetic rat. *Free Radical Biology and Medicine* **18,** 833-840.

Yuan JP, Kim MS, Zeng W, Shin DM, Huang G, Worley PF & Muallem S. (2009a). TRPC channels as STIM1-regulated SOCs. *Channels* **3,** 221-225.

Yuan JP, Zeng W, Dorwart MR, Choi Y-J, Worley PF & Muallem S. (2009b). SOAR and the polybasic STIM1 domains gate and regulate Orai channels. *Nature Cell Biology* **11,** 337-343.

Zafari AM, Ushio-Fukai M, Akers M, Yin Q, Shah A, Harrison DG, Taylor WR & Griendling KK. (1998). Role of NADH/NADPH oxidase–derived H_2O_2 in angiotensin II–induced vascular hypertrophy. *Hypertension* **32,** 488-495.

Zakharov SI, Smani T, Dobrydneva Y, Monje F, Fichandler C, Blackmore PF & Bolotina VM. (2004). Diethylstilbestrol is a potent inhibitor of store-operated channels and capacitative Ca(2+) influx. *Molecular Pharmacology* **66,** 702-707.

Zbidi H, Lopez JJ, Amor NB, Bartegi A, Salido GM & Rosado JA. (2009). Enhanced expression of STIM1/Orai1 and TRPC3 in platelets from patients with type 2 diabetes mellitus. *Blood Cells, Molecules and Diseases* **43,** 211-213.

Zeggini E, Scott LJ, Saxena R, Voight BF, Marchini JL, Hu T, de Bakker PIW, Abecasis GR, Almgren P, Andersen G, Ardlie K, Bostrom KB, Bergman RN, Bonnycastle LL, Borch-Johnsen K, Burtt NP, Chen H, Chines PS, Daly MJ, Deodhar P, Ding C-J, Doney ASF, Duren WL, Elliott KS, Erdos MR, Frayling TM, Freathy RM, Gianniny L, Grallert H, Grarup N, Groves CJ, Guiducci C, Hansen T, Herder C, Hitman GA, Hughes TE, Isomaa B, Jackson AU, Jorgensen T, Kong A, Kubalanza K, Kuruvilla FG, Kuusisto J, Langenberg C, Lango H, Lauritzen T, Li Y, Lindgren CM, Lyssenko V, Marvelle AF, Meisinger C, Midthjell K, Mohlke KL, Morken MA, Morris AD, Narisu N, Nilsson P, Owen KR, Palmer CNA, Payne F, Perry JRB, Pettersen E, Platou C, Prokopenko I, Qi L, Qin L, Rayner NW, Rees M, Roix JJ, Sandbaek A, Shields B, Sjogren M, Steinthorsdottir V, Stringham HM, Swift AJ, Thorleifsson G, Thorsteinsdottir U, Timpson NJ, Tuomi T, Tuomilehto J, Walker M, Watanabe RM, Weedon MN, Willer CJ, Illig T,

Hveem K, Hu FB, Laakso M, Stefansson K, Pedersen O, Wareham NJ, Barroso I, Hattersley AT, Collins FS, Groop L, McCarthy MI, Boehnke M & Altshuler D. (2008). Meta-analysis of genome-wide association data and large-scale replication identifies additional susceptibility loci for type 2 diabetes. *Nature Genetics* **40,** 638-645.

Zeng B, Chen GL & Xu SZ. (2012). Store-independent pathways for cytosolic STIM1 clustering in the regulation of store-operated Ca^{2+} influx. *Biochemical Pharmacology* **84,** 1024-1035.

Zeng W, Yuan JP, Kim MS, Choi YJ, Huang GN, Worley PF & Muallem S. (2008). STIM1 gates TRPC Channels, but not Orai1, by electrostatic interaction. *Molecular Cell* **32,** 439-448.

Zhang C, Cai Y, Adachi MT, Oshiro S, Aso T, Kaufman RJ & Kitajima S. (2001). Homocysteine induces programmed cell death in human vascular endothelial cells through activation of the unfolded protein response. *The Journal of Biological Chemistry* **276,** 35867-35874.

Zhang H-S, Xiao J-H, Cao E-H & Qin J-F. (2005). Homocysteine inhibits store-mediated calcium entry in human endothelial cells: Evidence for involvement of membrane potential and actin cytoskeleton. *Molecular and Cellular Biochemistry* **269,** 37-47.

Zhang SL. (2005). STIM1 is a Ca^{2+} sensor that activates CRAC channels and migrates from the Ca^{2+} store to the plasma membrane. *Nature* **437,** 902-905.

Zhang SL, Yeromin AV, Zhang XH-F, Yu Y, Safrina O, Penna A, Roos J, Stauderman KA & Cahalan MD. (2006). Genome-wide RNAi screen of Ca^{2+} influx identifies genes that regulate Ca^{2+} release-activated Ca^{2+} channel

activity. *Proceedings of the National Academy of Sciences USA* **103,** 9357-9362.

Zhang W, Meng H, Li Z-H, Shu Z, Ma X & Zhang B-X. (2007). Regulation of STIM1, store-operated Ca^{2+} influx, and nitric oxide generation by retinoic acid in rat mesangial cells. *American Journal of Physiology - Renal Physiology* **292,** F1054-1064.

Zhang XY, Chen da C, Xiu MH, Yang FD, Tan YL, He S, Kosten TA & Kosten TR. (2013). Thioredoxin, a novel oxidative stress marker and cognitive performance in chronic and medicated schizophrenia versus healthy controls. *Schizophrenia Research* **143,** 301-306.

Zheng L, Stathopulos PB, Li G-Y & Ikura M. (2008). Biophysical characterization of the EF-hand and SAM domain containing Ca^{2+} sensory region of STIM1 and STIM2. *Biochemical and Biophysical Research Communications* **369,** 240-246.

Zhou Y, Mancarella S, Wang Y, Yue C, Ritchie M, Gill DL & Soboloff J. (2009). The short N-terminal domains of STIM1 and STIM2 control the activation kinetics of Orai1 channels. *The Journal of Biological Chemistry* **284,** 19164-19168.

Zhu JH, Chen JZ, Wang XX, Xie XD, Sun J & Zhang FR. (2006). Homocysteine accelerates senescence and reduces proliferation of endothelial progenitor cells. *Journal of Molecular and Cellular Cardiology* **40,** 648-652.

Zipper H, Brunner H, Bernhagen Jr & Vitzthum F. (2004). Investigations on DNA intercalation and surface binding by SYBR Green I, its structure determination and methodological implications. *Nucleic Acids Research* **32,** e103.

Zitt C, Strauss B, Schwarz EC, Spaeth N, Rast G, Hatzelmann A & Hoth M. (2004). Potent inhibition of Ca^{2+} release-activated Ca^{2+} channels and T-lymphocyte activation by the pyrazole derivative BTP2. *The Journal of Biological Chemistry* **279,** 12427-12437.

List of Publications

Published articles

Jiang HN, Zeng B, Zhang Y, **Daskoulidou N**, Fan H, Qu JM & Xu SZ. (2013). Involvement of TRPC channels in lung cancer cell differentiation and the correlation analysis in human non-small cell lung cancer. *PLoS ONE* **8,** e67637.

Xu SZ, Zeng B, **Daskoulidou N**, Chen GL, Atkin SL & Lukhele B. (2012). Activation of TRPC cationic channels by mercurial compounds confers the cytotoxicity of mercury exposure. *Toxicological Sciences* **125,** 56-68.

Submitted manuscripts

Daskoulidou N, Zeng B, Berglund L, Jiang H, Chen GL, Kotova O, Bhandari S, Griffin S, Gomez MF, Atkin SL, Xu SZ. (2013). High glucose enhances store-operated calcium entry by upregulation of ORAI and STIM via calcineurin/NFAT signalling in human vascular endothelial cells. *Diabetes*

Zeng B, Chen GL, **Daskoulidou N**, Xu SZ. (2013). Ryanodine receptor agonist 4-chloro-3-ethylphenol blocks ORAI store-operated channels. *British Journal of Pharmacology*

Chen GL, Gomez MF, **Daskoulidou N**, Zeng B, Jiang H, Atkin SL, Xu SZ. (2013). ORAI store-operated Ca^{2+} channels are associated with proximal renal tubule dysfunction in diabetic nephropathy. *Journal of Clinical Investigation*

Conference proceedings-oral presentation

Daskoulidou N, Atkin SL and Xu SZ. (2012). Store-operated Ca^{2+} channel ORAI and STIM regulated by high glucose. *Experimental Biology 2012*, San Diego Convention Centre, April 21-25, San Diego, California, USA, pp. 85.

Conference proceedings-poster presentations

Daskoulidou N, Atkin SL and Xu SZ. (2012). Store-operated Ca^{2+} channel ORAI and STIM regulated by high glucose. *Experimental Biology 2012*, San Diego Convention Centre, April 21-25, San Diego, California, USA, pp. 85.

Daskoulidou N, Atkin SL and Xu SZ. (2012). Store-operated Ca^{2+} channel ORAI and STIM regulated by high glucose. *HYMS Postgraduate Research Conference*, University of York, June 1, York, UK.

Green A, Bhandari S, Atkin S, Ayoola J, **Daskoulidou N**, Zeng B, Xu SZ. (2011). Expression and localisation of ORAI channels in normal and diabetic nephropathy human kidney. *BRS/RA Conference 2011*, Birmingham, UK, pp.54.

Daskoulidou N, Atkin SL, Xu SZ. (2011). Regulation of store-operated Ca^{2+} channel molecules ORAI and STIM by high glucose. *Northern Cardiovascular Research Group 20th Anniversary meeting*, University of Hull, Hull, UK.

Xu SZ, Lukhele B, Atkin SL, **Daskoulidou N**. (2010). Involvement of TRPC cationic channel in the cytotoxicity of mercury poisoning. *New horizons in calcium signalling*, Board 37, October 10-13, Beijing, China, pp91.

Daskoulidou N, Atkin SL, Xu SZ. (2010). Expression of ORAI and STIM in vascular smooth muscle cells and the regulation by high glucose. *Physiology 2010*, Abstracts, June 30 - July 2, University of Manchester, UK, pp139.

Appendix I pcDNA4/TO vector map

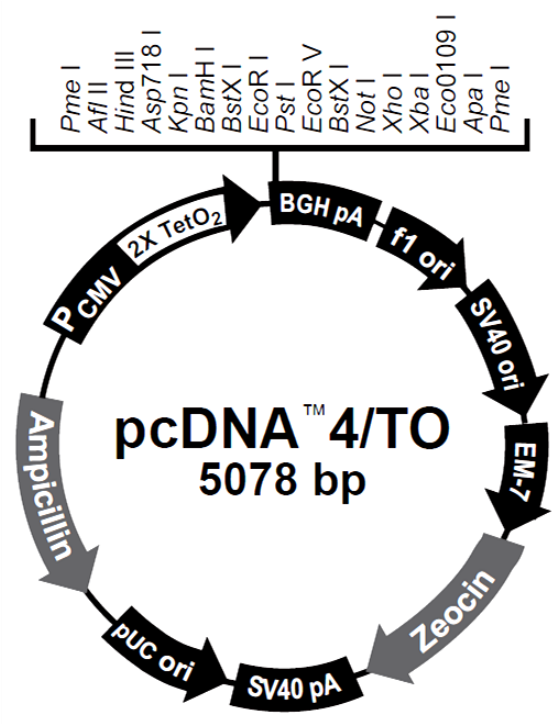

Appendix II Example sequencing for full length ORAI2

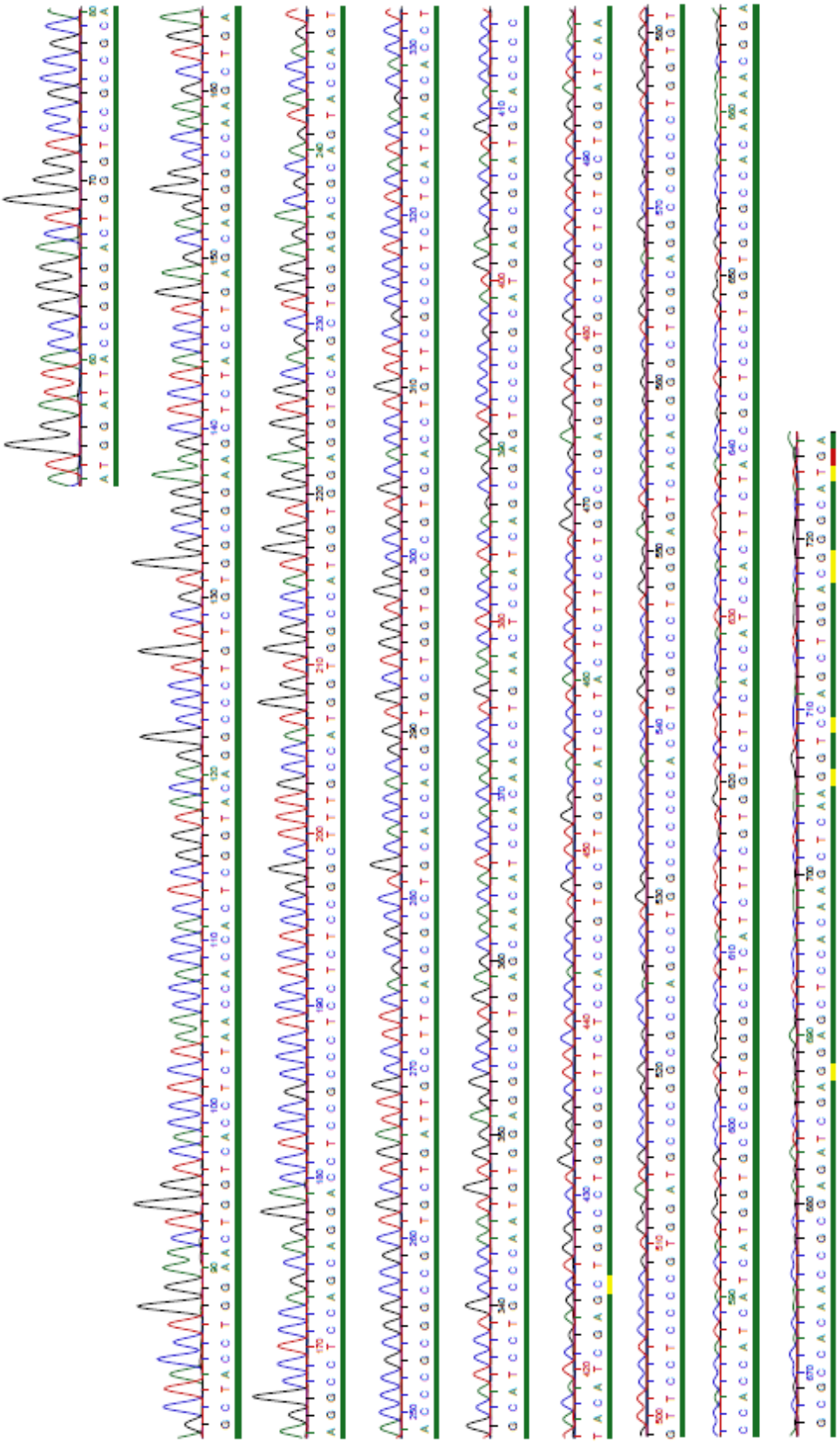

Appendix III Alignment of ORAI1 to the plasmid mCherry-ORAI1 sequence

ORAI1 NM_032790- ----------GCCGCCCGGGGGCTTTTG
ORAI1 plasmid- AGTGTGCTGGAATTCGGCACGAGG GCCGCCCGGGGGCTTTTG

CCAGCGGCGCCGCGGGCCTGCGTGCTGGGGCAGCGGGCACTTCTTCGACCTCGTCCTCCT
CCAGCGGCGCCGCGGGCCTGCGTGCTGGGGCAGCGGGCACTTCTTCGACCTCGTCCTCCT

CGTCCTGTGCGGCCGGCCGGGTGAGGCCGGGCCCGCGTAGGGGGCAGTCGGCGGCTGCCT
CGTCCTGTGCGGCCGGCCGGGTGAGGCCGGGCCCGCGTAGGGGGCAGTCGGCGGCTGCCT

CCGGCGGAGGTGCCTCGCGGCGCCCGGGCCGGCCCGCGCCTCGGCGGCGTGCTCCATGCA
CCGGCGGAGGTGCCTCGCGGCGCCCGGGCCGGCCCGCGCCTCGGCGGCGTGCTCCATGCA

TCCGGAGCCCGCCCCGCCCCCGAGCCGCAGCAGTCCCGAGCTTCCCCCAAGCGGCGGCAG
TCCGGAGCCCGCCCCGCCCCCGAGCCGCAGCAGTCCCGAGCTTCCCCCAAGCGGCGGCAG

CACCACCAGCGGCAGCCGCCGGAGCCGCCGCCGCAGCGGGGACGGGGAGCCCCCGGGGGC
CACCACCAGCGGCAGCCGCCGGAGCCGCCGCCGCAGCGGGGACGGGGAGCCCCCGGGGGC

CCCGCCACCGCCGCCGTCCGCCGTCACCTACCCGGACTGGATCGGCCAGAGTTACTCCGA
CCCGCCACCGCCGCCGTCCGCCGTCACCTACCCGGACTGGATCGGCCAGAGTTACTCCGA

GGTGATGAGCCTCAACGAGCACTCCATGCAGGCGCTGTCCTGGCGCAAGCTCTACTTGAG
GGTGATGAGCCTCAACGAGCACTCCATGCAGGCGCTGTCCTGGCGCAAGCTCTACTTGAG

CCGCGCCAAGCTTAAAGCCTCCAGCCGGACCTCGGCTCTGCTCTCCGGCTTCGCCATGGT
CCGCGCCAAGCTTAAAGCCTCCAGCCGGACCTCGGCTCTGCTCTCCGGCTTCGCCATGGT

GGCAATGGTGGAGGTGCAGCTGGACGCTGACCACGACTACCCACCGGGGCTGCTCATCGC
GGCAATGGTGGAGGTGCAGCTGGACGCTGACCACGACTACCCACCGGGGCTGCTCATCGC

CTTCAGTGCCTGCACCACAGTGCTGGTGGCTGTGCACCTGTTTGCGCTCATGATCAGCAC
CTTCAGTGCCTGCACCACAGTGCTGGTGGCTGTGCACCTGTTTGCGCTCATGATCAGCAC

CTGCATCCTGCCCAACATCGAGGCGGTGAGCAACGTGCACAATCTCAACTCGGTCAAGGA
CTGCATCCTGCCCAACATCGAGGCGGTGAGCAACGTGCACAATCTCAACTCGGTCAAGGA

GTCCCCCCATGAGCGCATGCACCGCCACATCGAGCTGGCCTGGGCCTTCTCCACCGTCAT
GTCCCCCCATGAGCGCATGCACCGCCACATCGAGCTGGCCTGGGCCTTCTCCACCGTCAT

CGGCACGCTGCTCTTCCTAGCTGAGGTGGTGCTGCTCTGCTGGGTCAAGTTCTTGCCCCT
CGGCACGCTGCTCTTCCTAGCTGAGGTGGTGCTGCTCTGCTGGGTCAAGTTCTTGCCCCT

CAAGAAGCAGCCAGGCCAGCCAAGGCCCACCAGCAAGCCCCCCGCCAGTGGCGCAGCAGC
CAAGAAGCAGCCAGGCCAGCCAAGGCCCACCAGCAAGCCCCCCGCCAGTGGCGCAGCAGC

CAACGTCAGCACCAGCGGCATCACCCCGGGCCAGGCAGCTGCCATCGCCTCGACCACCAT
CAACGTCAGCACCAGCGGCATCACCCCGGGCCAGGCAGCTGCCATCGCCTCGACCACCAT

CATGGTGCCCTTCGGCCTGATCTTTATCGTCTTCGCCGTCCACTTCTACCGCTCACTGGT
CATGGTGCCCTTCGG----------